

POLYTECHNIQUE MONTRÉAL
affiliée à l'Université de Montréal

Application de l'optimisation conique au problème d'écoulement de puissance optimal

CHRISTIAN BINGANE
Département de mathématiques et de génie industriel

Thèse présentée en vue de l'obtention du diplôme de *Philosophiæ Doctor*
Mathématiques de l'ingénieur

Mai 2019

POLYTECHNIQUE MONTRÉAL
affiliée à l'Université de Montréal

Cette thèse intitulée :

Application de l'optimisation conique au problème d'écoulement de puissance optimal

présentée par **Christian BINGANE**
en vue de l'obtention du diplôme de *Philosophiae Doctor*
a été dûment acceptée par le jury d'examen constitué de :

Dominique ORBAN, président

Miguel F. ANJOS, membre et directeur de recherche

Sébastien LE DIGABEL, membre et codirecteur de recherche

Matthias TAKOUDA, membre

Joshua A. TAYLOR, membre externe

DÉDICACE

*À mon père Muhindo, ma mère Muderhwa,
mes sœurs Nabintu, Namasale, Namburho et Bulonza,
et mes frères Ngabo, Muhindo, Bwimana et Maheshe.*

REMERCIEMENTS

Cette thèse est un rêve dont la réalisation ne serait possible sans l'apport de plusieurs personnes. Je profite de cette occasion pour remercier quelques personnes qui ont contribué indirectement ou directement à l'aboutissement de cette aventure.

Tout d'abord, je souhaite remercier les professeurs Miguel F. Anjos et Sébastien Le Digabel d'avoir accepté d'assurer la direction de cette thèse. Qu'ils trouvent ici les sentiments de toute ma reconnaissance pour l'aide précieuse et les conseils éclairés qu'ils ont bien voulu m'accorder afin de mener ce travail à son terme. J'ai apprécié leur supervision, leur disponibilité, leur patience et leurs remarques qui ont facilité largement l'accomplissement de cette thèse.

Merci également à la Chaire de recherche industrielle CRSNG–Hydro-Québec–Schneider Electric pour le support financier. Les échanges lors de rencontres techniques organisées par la Chaire, avec notamment Laurent Lenoir et Stéphane Alarie de l'IREQ, Claudio Rimada et Jesus Vargas de Schneider Electric, ont aussi été d'une grande aide dans la réalisation de cette thèse.

Un remerciement spécial à ma famille : mon père, ma mère, mes sœurs et mes frères pour leur affection inestimable et leur soutien inconditionnel depuis toujours. Koko bwenene !

Enfin, je remercie les amis de mon pays natal, les camarades du GERAD et les amis de mon pays d'accueil. Je n'oublie pas mes enseignants du Groupe scolaire du Mont Amba qui, les premiers, m'ont poussé à donner le meilleur de moi-même. Chacun d'entre eux a contribué à sa façon à l'aboutissement de cette longue aventure et qu'ils trouvent eux aussi ici ma plus profonde gratitude.

RÉSUMÉ

Le problème d'écoulement de puissance optimal consiste à déterminer, sur les bases des consommations et productions prévues, un plan de fonctionnement d'un réseau électrique qui optimise un certain objectif tout en respectant les contraintes physiques et sécuritaires. Sa formulation classique est un problème d'optimisation non convexe et très difficile à résoudre. Récemment, quelques relaxations convexes telles que la relaxation semidéfinie, la relaxation conique du second ordre, la relaxation quadratique convexe, ont montré un intérêt significatif dans la communauté scientifique. La relaxation semidéfinie est plus forte que la plupart d'entre elles et il existe des applications numériques où elle est exacte. Toutefois, sa résolution s'avère trop coûteuse comparativement à celle de la relaxation conique du second ordre pour un réseau de grande taille. Dans ce travail, nous proposons une nouvelle relaxation conique qui s'avère être un bon compromis entre la relaxation semidéfinie et la relaxation conique du second ordre pour des réseaux de grande taille en termes de gap d'optimalité et de temps de résolution. En effet, des résultats numériques sur des réseaux comportant jusqu'à 6515 nœuds montrent que la nouvelle relaxation est plus forte que la relaxation conique du second ordre et que sa résolution est beaucoup moins coûteuse que celle de la relaxation semidéfinie.

Ensuite, nous considérons le problème de répartition optimale de puissance réactive. Ce problème est en fait un problème d'écoulement de puissance optimal où les composants qui permettent de contrôler le flux de puissance réactive dans le réseau, tels que les condensateurs shunts, les transformateurs, sont pris en compte. Le problème de répartition optimale de puissance réactive est un problème mixte en nombres entiers, donc plus complexe que le problème classique. Pour le résoudre, nous utilisons la technique de l'arrondi combinée à une relaxation conique. Cette approche appliquée à des réseaux avec jusqu'à 3375 nœuds donne des meilleurs résultats que si l'on avait considéré une simple relaxation continue du problème, qui est non convexe. En effet, les solutions optimales obtenues sont quasi globales.

En pratique, le problème d'écoulement de puissance optimal est un problème multi-période à cause, notamment, de la variation horaire de la consommation. D'autre part, le temps de résolution et la qualité de la solution représentent un besoin clé pour des algorithmes du problème d'écoulement de puissance optimal. En réalité, ce dernier est résolu toutes les 5-10 minutes afin de répondre aux besoins horaires des consommateurs. Dans la dernière partie de ce travail, nous montrons que la relaxation développée dans la première partie peut être exacte. Par la suite, nous l'extrapolons au problème multi-période et les résultats numériques sur des réseaux ayant jusqu'à 500 nœuds montrent que la relaxation multi-période est prometteuse pour des applications réelles.

ABSTRACT

The classical alternating current optimal power flow (ACOPF) problem is highly nonconvex and generally hard to solve. Convex relaxations, in particular semidefinite, second-order cone, convex quadratic, and linear relaxations, have recently attracted significant interest. The semidefinite relaxation is the strongest among them and is exact for many cases. However, the computational efficiency for solving large-scale semidefinite optimization is lower than for second-order cone optimization. In this work, we first propose a conic relaxation obtained by combining semidefinite optimization with the reformulation-linearization technique, commonly known as RLT. The proposed relaxation, called tight-and-cheap relaxation (TCR), is stronger than the second-order cone relaxation and nearly as tight as the standard semidefinite relaxation. Computational experiments using standard test cases with up to 6515 buses show that the time to solve the new conic relaxation is up to one order of magnitude lower than for the chordal relaxation, a semidefinite relaxation technique that exploits the sparsity of power networks.

In the second part of this work, we consider the optimal reactive power dispatch (ORPD) problem, which is an ACOPF problem where discrete control devices for regulating the reactive power, such as shunt elements and tap changers, are considered. The ORPD problem is modelled as a mixed-integer nonlinear optimization problem and its complexity is increased compared to the ACOPF problem. We show that a round-off technique applied with a tight conic relaxation of the ORPD problem leads to near-global optimal solutions with very small guaranteed optimality gaps, unlike with the nonconvex continuous relaxation. We report computational results on selected MATPOWER test cases with up to 3375 buses.

Many power system applications that require solving an OPF problem are multi-period because of several reasons such as the evolution of market prices or the behavior of the demand. On the other hand, computational speed and global optimality are a key need for practical OPF algorithms. In fact, in real-time applications, an OPF problem is run every few minutes to meet the daily requirements optimally in every hour. In the last part of this work, we show that TCR can be exact and can provide a global optimal solution for the ACOPF problem, theoretically and numerically. Thereafter, we propose a multi-period TCR for the multi-period ACOPF problem and computational experiments using MATPOWER test cases with up to 500 buses show that this new relaxation is promising for real-life applications.

TABLE DES MATIÈRES

| | |
|---|----------|
| DÉDICACE | iii |
| REMERCIEMENTS | iv |
| RÉSUMÉ | v |
| ABSTRACT | vi |
| TABLE DES MATIÈRES | vii |
| LISTE DES TABLEAUX | x |
| LISTE DES FIGURES | xi |
| LISTE DES SIGLES ET ABRÉVIATIONS | xii |
| CHAPITRE 1 INTRODUCTION | 1 |
| 1.1 Définitions et concepts de base | 1 |
| 1.1.1 Optimisation mathématique | 1 |
| 1.1.2 Relaxation | 2 |
| 1.2 Éléments de la problématique | 3 |
| 1.3 Objectifs de recherche | 4 |
| CHAPITRE 2 REVUE DE LITTÉRATURE | 5 |
| 2.1 Optimisation semidéfinie | 5 |
| 2.1.1 Ensemble convexe, fonction convexe | 5 |
| 2.1.2 Optimisation convexe | 7 |
| 2.1.3 Optimisation conique | 8 |
| 2.1.4 Optimisation semidéfinie | 8 |
| 2.2 Écoulement de puissance : équations d'équilibre | 9 |
| 2.3 Problème d'écoulement de puissance optimal | 13 |
| 2.3.1 Formulation générale et méthodes de résolution | 13 |
| 2.3.2 Formulation classique et relaxations semidéfinies | 13 |
| 2.3.3 Traitement de variables entières : technique de l'arrondi | 19 |
| 2.3.4 Problème multi-période | 20 |

| | | |
|------------|--|----|
| CHAPITRE 3 | ORGANISATION DE LA THÈSE | 22 |
| CHAPITRE 4 | ARTICLE 1: TIGHT-AND-CHEAP CONIC RELAXATION FOR THE AC OPTIMAL POWER FLOW PROBLEM | 23 |
| 4.1 | Nomenclature | 23 |
| 4.1.1 | Notations | 23 |
| 4.1.2 | Operators | 23 |
| 4.1.3 | Input data | 24 |
| 4.1.4 | Variables | 24 |
| 4.2 | Introduction | 24 |
| 4.3 | ACOPF: Formulation | 25 |
| 4.4 | ACOPF: Conic relaxations | 27 |
| 4.4.1 | Semidefinite relaxation | 27 |
| 4.4.2 | Chordal relaxation | 28 |
| 4.4.3 | Second-order cone relaxation | 29 |
| 4.5 | New conic relaxation | 30 |
| 4.5.1 | Tight-and-cheap relaxation | 30 |
| 4.5.2 | Strengthening | 33 |
| 4.6 | Computational results | 34 |
| 4.7 | Conclusion | 35 |
| CHAPITRE 5 | ARTICLE 2: TIGHT-AND-CHEAP CONIC RELAXATION FOR THE OP- TIMAL REACTIVE POWER DISPATCH PROBLEM | 38 |
| 5.1 | Nomenclature | 38 |
| 5.1.1 | Notations | 38 |
| 5.1.2 | Operators | 38 |
| 5.1.3 | Input data | 39 |
| 5.1.4 | Variables | 39 |
| 5.2 | Introduction | 39 |
| 5.3 | ORPD: Formulation | 41 |
| 5.4 | ORPD: Convexification | 43 |
| 5.4.1 | Semidefinite relaxation 1 (SDR1) | 43 |
| 5.4.2 | Semidefinite relaxation 2 (SDR2) | 46 |
| 5.5 | ORPD: Solution approach | 49 |
| 5.6 | Computational results | 50 |
| 5.7 | Conclusion | 52 |

| | | |
|------------|---|----|
| CHAPITRE 6 | ARTICLE 3: CONICOPF: A TIGHT-AND-CHEAP CONIC RELAXATION WITH ACCURACY METRICS FOR SINGLE-PERIOD AND MULTI-PERIOD ACOPF PROBLEMS | 57 |
| 6.1 | Nomenclature | 57 |
| 6.1.1 | Notations | 57 |
| 6.1.2 | Operators | 57 |
| 6.1.3 | Input data | 58 |
| 6.1.4 | Variables | 58 |
| 6.2 | Introduction | 58 |
| 6.3 | ACOPF: Tight-and-cheap relaxation | 60 |
| 6.4 | MP-ACOPF: Multi-period TCR | 63 |
| 6.5 | Computational results | 65 |
| 6.5.1 | Exactness of TCR | 65 |
| 6.5.2 | MP-TCR | 68 |
| 6.6 | Conclusion | 69 |
| CHAPITRE 7 | DISCUSSION GÉNÉRALE | 71 |
| 7.1 | Synthèse des travaux | 71 |
| 7.2 | Limitations de la solution proposée | 71 |
| CHAPITRE 8 | CONCLUSION ET RECOMMANDATIONS | 73 |
| RÉFÉRENCES | | 74 |

LISTE DES TABLEAUX

| | | |
|-----------|--|----|
| Table 4.1 | Cost minimization | 36 |
| Table 4.2 | Loss minimization | 37 |
| Table 5.1 | Dimensions of test instances | 51 |
| Table 5.2 | Cost minimization: Normalized optimal values | 54 |
| Table 5.3 | Loss minimization: Normalized optimal values | 55 |
| Table 5.4 | Cost minimization: Optimality gaps and computation times | 56 |
| Table 5.5 | Loss minimization: Optimality gaps and computation times | 56 |
| Table 6.1 | Exactness of TCR: Cost minimization | 67 |
| Table 6.2 | Exactness of TCR: Loss minimization | 67 |
| Table 6.3 | MP-TCR : Cost minimization | 70 |
| Table 6.4 | MP-TCR : Loss minimization | 70 |

LISTE DES FIGURES

| | | |
|------------|--|----|
| Figure 2.1 | Ensemble convexe | 5 |
| Figure 2.2 | Fonction convexe | 6 |
| Figure 2.3 | Réseau de puissance | 10 |
| Figure 2.4 | Graphe, clique, cycle et corde | 16 |
| Figure 2.5 | Graphe et extension cordale | 16 |
| Figure 6.1 | Time varying demand profile | 68 |
| Figure 6.2 | Cost minimization of <code>case14</code> instance: Optimal active and reactive outputs of each generator | 69 |
| Figure 6.3 | Cost minimization of <code>case14</code> instance: Voltage magnitudes of each bus | 70 |

LISTE DES SIGLES ET ABRÉVIATIONS

| | |
|-------------------------------------|---|
| AC | Alternating current |
| OPF | Optimal power flow |
| ACOPF | Alternating current optimal power flow |
| MP-OPF | Multi-period optimal power flow |
| MP-ACOPF | Multi-period alternating current optimal power flow |
| ORPD | Optimal reactive power dispatch |
| PSD | Positive semidefinite |
| SDP | Semidefinite programming |
| SOCP | Second-order cone programming |
| SDR | Semidefinite relaxation |
| CHR | Chordal relaxation |
| SOCR | Second-order cone relaxaion |
| TCR | Tight-and-cheap relaxation |
| STCR | Strong tight-and-cheap relaxation |
| MP-TCR | Multi-period tight-and-cheap relaxation |
| NP | Nondeterministic polynomial time |
| NLP | Nonlinear programming |
| MINLP | Mixed-integer nonlinear programming |
| RLT | Reformulation-linearization technique |
| s. c. | Sous les contraintes |
| s. t. | Subject to |
| \mathbb{R}/\mathbb{C} | Ensemble des nombres réels/complexes |
| \mathbb{H}^n | Ensemble des matrices hermitiennes |
| $j = \sqrt{-1}$ | Unité imaginaire |
| a/a | Nombre réel/complexe |
| \mathbf{a}/\mathbf{a} | Vecteur réel/complexe |
| A/A | Matrice réelle/complexe |
| $\text{Re}(\cdot)/\text{Im}(\cdot)$ | Opérateur partie réelle/imaginaire |
| $(\cdot)^*$ | Opérateur conjugué |
| $ \cdot $ | Opérateur amplitude ou cardinalité |
| $\angle(\cdot)$ | Opérateur phase |
| $(\cdot)^H$ | Opérateur transconjugué |
| $\text{rank}(\cdot)$ | Opérateur rang |

CHAPITRE 1 INTRODUCTION

Exploiter un réseau électrique est à la fois un défi technique et économique. En tout temps, il est soumis à des contraintes physiques et sécuritaires très strictes qui, si elles ne sont pas respectées, peuvent entraîner son effondrement total. En fonction des capacités de production, les opérateurs du réseau doivent couvrir la demande en énergie et assurer sa stabilité avec un coût relativement moindre.

Ces dernières années, l'industrie électro-énergétique a connu un essor très important : la demande d'électricité est devenue de plus en plus accrue et les technologies utilisées de plus en plus sophistiquées. Cet accroissement de la demande entraîne une concurrence féroce sur les marchés d'électricité entre différents producteurs. D'autre part, le développement des infrastructures permettant de faire face à l'obsolescence technique et économique de celles en fonctionnement n'arrive pas à suivre l'accroissement exponentiel de la consommation. D'où le besoin des fournisseurs de recourir à une répartition économique optimale des charges dans les différentes centrales en fonctionnement qui leur permettra non seulement d'optimiser leur production mais aussi d'offrir des prix concurrentiels sur les marchés.

Le problème d'écoulement de puissance optimal consiste à déterminer, sur les bases des consommations et productions prévues, un plan de fonctionnement (tensions, puissance active et réactive, etc.) d'un réseau électrique qui minimise, par exemple, les coûts de production tout en respectant les contraintes physiques et sécuritaires : lois de Kirchhoff, limites de tensions, limites de puissances, etc. Sa formulation classique est un problème d'optimisation continu, non convexe et très difficile à résoudre. Parmi les méthodes de résolution existantes, aucune d'entre elles ne garantit l'atteinte d'un optimum global. Or, pour les raisons économiques évoquées plus haut, la recherche d'un optimal global peut s'avérer cruciale.

1.1 Définitions et concepts de base

1.1.1 Optimisation mathématique

Soit un ensemble fermé $\Omega \subseteq \mathbb{R}^n$ et soit une fonction $f: \Omega \rightarrow \mathbb{R}$. Un problème d'optimisation mathématique est un problème de la forme

$$\hat{v} = \min\{f(\mathbf{x}) \mid \mathbf{x} \in \Omega\}, \quad (1.1)$$

où Ω est appelé *ensemble réalisable* ou *ensemble des contraintes*, f est la *fonction objectif* et \hat{v} est la *valeur optimale*. Il consiste à trouver une solution \mathbf{x} qui minimise une fonction f tout en respectant un ensemble de contraintes Ω . Dépendamment de l'ensemble Ω et de la fonction f , on dit que le problème (1.1) est

- linéaire : Ω est défini par des contraintes linéaires et f est une fonction linéaire,
- quadratique : Ω est défini par des contraintes linéaires et f est une fonction quadratique,
- quadratique à contraintes quadratiques : Ω est défini par des contraintes quadratiques et f est une fonction quadratique,
- convexe : Ω est un ensemble convexe et f est une fonction convexe,
- conique : Ω est un cône convexe et f est une fonction linéaire,
- en nombres entiers : $\Omega \subseteq \mathbb{Z}^n$, i.e., *toutes* les variables sont contraintes à ne prendre que des valeurs entières,
- mixte en nombres entiers : $\Omega \subseteq \mathbb{R}^k \times \mathbb{Z}^{n-k}$, i.e., *certaines* variables sont contraintes à ne prendre que des valeurs entières, etc.

Lorsque Ω est vide, le problème (1.1) est dit *non réalisable* et, par convention, $\hat{v} = +\infty$. Si pour tout $v \in \mathbb{R}$, il existe un point réalisable $\mathbf{x} \in \Omega$ tel que $f(\mathbf{x}) < v$, alors le problème (1.1) est dit *non borné* et on écrit $\hat{v} = -\infty$. Pour un problème réalisable, on dit qu'une solution $\hat{\mathbf{x}} \in \Omega$ est un

- *minimum global* si pour tout $\mathbf{x} \in \Omega$, $f(\hat{\mathbf{x}}) \leq f(\mathbf{x})$,
- *minimum local* s'il existe $\varepsilon > 0$ tel que pour tout $\mathbf{x} \in \Omega$ et $\|\mathbf{x} - \hat{\mathbf{x}}\| < \varepsilon$, $f(\hat{\mathbf{x}}) \leq f(\mathbf{x})$.

Tandis qu'un minimum global représente la meilleure solution dans tout l'ensemble Ω , un minimum local ne l'est que dans son voisinage. Tout minimum global est donc local, cependant la réciproque n'est vraie que pour un problème convexe.

En général, lorsque le problème (1.1) est non convexe, il peut exister plusieurs minima locaux et trouver un minimum global peut s'avérer très ardu. En effet, il existe plusieurs méthodes qui permettent de trouver un minimum local au problème (1.1) aussi bien théoriquement que pratiquement. Cependant, ces méthodes ne peuvent garantir si le minimum local trouvé est aussi global.

1.1.2 Relaxation

On dit qu'un problème

$$\underline{v} = \min\{\underline{f}(\mathbf{x}) \mid \mathbf{x} \in \bar{\Omega}\}, \quad (1.2)$$

où $\bar{\Omega} \subseteq \mathbb{R}^n$ et $\underline{f}: \bar{\Omega} \rightarrow \mathbb{R}$, est une *relaxation* du problème (1.1) si $\Omega \subseteq \bar{\Omega}$ et $\underline{f}(\mathbf{x}) \leq f(\mathbf{x})$ pour tout $\mathbf{x} \in \Omega$. La valeur optimale \underline{v} du problème relaxé (1.2) est une borne inférieure à la valeur

optimale \hat{v} du problème original (1.1) et on peut montrer que si $\underline{f}(x) = f(x)$ pour tout $x \in \Omega$ et que le minimum global du problème relaxé est réalisable pour le problème original, alors il est aussi global pour ce dernier.

Relaxer un problème d'optimisation consiste à étendre son ensemble réalisable et/ou à sous-estimer sa fonction objectif afin d'obtenir un problème plus facile à résoudre. Cette technique combinée aux méthodes de Branch-and-Bound, Branch-and-Cut, Cutting-Plane. . . est celle qu'on utilise généralement pour trouver un minimum global d'un problème non convexe.

1.2 Éléments de la problématique

Le projet de recherche rejoint le problème soumis dans [1] par l'Institut de recherche d'Hydro-Québec (IREQ).

TransÉnergie est une division d'Hydro-Québec qui exploite le réseau de transport d'électricité le plus vaste d'Amérique du Nord. Le réseau de transport comprend un peu plus de 500 postes et 34 272 km de lignes à différentes tensions. Ces lignes transportent l'énergie produite par les alternateurs vers les zones de charge et vers les réseaux de transport hors Québec (Ontario, Nouveau-Brunswick, Nord-Est des États-Unis). Les zones de charge elles-mêmes disposent de leurs propres réseaux, exploités par la division Hydro-Québec Distribution.

La production active disponible dans le réseau de transport est en général supérieure aux charges et exportations. L'engagement des alternateurs peut donc être fonction d'objectifs variés : minimisation des coûts de production, respect des limites des quantités électriques avant et après défaillances, maximisation de la capacité de transit, réduction des pertes de transport, etc. Nous nous intéressons seulement à la réduction des pertes.

Les pertes actives dans le réseau sont fonction de la résistance électrique des équipements de transport d'énergie, essentiellement les lignes et transformateurs et des courants qui y circulent. Ces courants variant au cours de la journée, on souhaite revoir la réduction des pertes une fois par heure.

Pour un transit de puissance active donné entre deux nœuds du réseau, réduire les pertes revient à réduire le courant en ajustant les tensions des nœuds. Ces tensions sont particulièrement sensibles à la circulation de puissance réactive. Le contrôle de cette dernière peut se faire à l'aide de nombreux dispositifs disséminés dans le réseau : condensateurs shunts, inducteurs shunts, compensateurs statiques et compensateurs synchrones. D'un autre côté, les tensions peuvent être directement contrôlées par des transformateurs à rapport variable, voire par des manœuvres de lignes. Toutefois, le contrôle de la tension est soumis à des contraintes opérationnelles, qui ne sont pas prises en compte par les produits commerciaux :

- seul un petit nombre de réglages peut être exécuté par le personnel du centre de conduite du réseau, compte tenu du temps disponible et des délais de réglage ;
- les réglages sont séquentiels et non instantanés ;
- après chaque réglage, les quantités électriques doivent respecter leurs limites à court terme (plus étendues que les limites en régime permanent).

Le problème soumis se résume ainsi : minimiser les pertes actives du réseau de transport, sur un horizon de 24 heures, tout en respectant

- l'écoulement de puissance dans le réseau (décrit par un système d'équations),
- les limites des moyens de contrôle,
- les limites en régime permanent des quantités électriques (tensions, puissances actives et réactives) et
- les contraintes opérationnelles.

1.3 Objectifs de recherche

Le problème formulé ci-haut est communément connu sous le nom de problème d'écoulement de puissance optimal. L'objectif principal de notre projet de recherche est de proposer un modèle qui garantit l'atteinte d'un optimal global et dont le temps de résolution est relativement moindre. Nous le subdivisons en 3 sous-objectifs :

1. développer un modèle continu de minimisation des pertes pour une période donnée (1 heure) ;
2. intégrer les composants de contrôle de la puissance réactive dans le modèle précédent ;
3. extrapoler les 2 premiers objectifs à une planification à long terme (24 heures).

CHAPITRE 2 REVUE DE LITTÉRATURE

Ce chapitre résume la revue de littérature nécessaire à la réalisation du projet de doctorat. Il est subdivisé en deux parties :

- l'optimisation semidéfinie et
- le problème d'écoulement de puissance optimal.

Pour chaque partie, nous donnons une brève description qui permet d'avoir une compréhension globale du sujet. Pour approfondir sur les deux sujets, nous suggérons au lecteur les références suivantes : [2] sur l'optimisation convexe, [3,4] sur l'optimisation semidéfinie et [5,6] sur l'optimisation dans les réseaux électriques.

2.1 Optimisation semidéfinie

2.1.1 Ensemble convexe, fonction convexe

Ensemble convexe

Définition 1. Un ensemble $\Omega \subseteq \mathbb{R}^n$ est dit *convexe* si

$$\forall \mathbf{x}, \mathbf{y} \in \Omega, \forall \alpha \in [0, 1], (1 - \alpha)\mathbf{x} + \alpha\mathbf{y} \in \Omega.$$

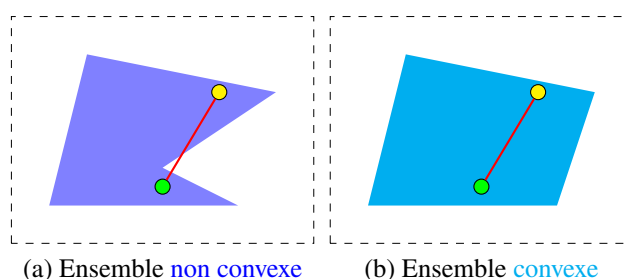


Figure 2.1 Ensemble convexe

La définition ci-dessus est équivalente à celle-ci : un ensemble $\Omega \subseteq \mathbb{R}^n$ est dit convexe si pour tout $\mathbf{x}_1, \mathbf{x}_2, \dots, \mathbf{x}_p \in \Omega$, pour tout $\alpha_1, \alpha_2, \dots, \alpha_p \geq 0$, $\sum_{i=1}^p \alpha_i = 1$ et $\sum_{i=1}^p \alpha_i \mathbf{x}_i \in \Omega$.

Un vecteur $\mathbf{x} \in \mathbb{R}^n$ est une *combinaison convexe* de p vecteurs $\mathbf{x}_1, \mathbf{x}_2, \dots, \mathbf{x}_p \in \mathbb{R}^n$ s'il existe $\alpha_1, \alpha_2, \dots, \alpha_p \geq 0$ tels que $\sum_{i=1}^p \alpha_i = 1$ et $\mathbf{x} = \sum_{i=1}^p \alpha_i \mathbf{x}_i$. L'ensemble de toutes les combinaisons

convexes des points d'un ensemble $\Omega \subseteq \mathbb{R}^n$, qu'on note $\text{conv}(\Omega)$, est appelé *enveloppe convexe* de Ω .

THÉORÈME 1. Soit $\Omega \subseteq \mathbb{R}^n$. L'enveloppe convexe $\text{conv}(\Omega)$ est le plus petit ensemble convexe qui contient Ω .

Démonstration. Soit $\Omega \subseteq \mathbb{R}^n$. Supposons qu'il existe un ensemble convexe $\bar{\Omega} \subseteq \mathbb{R}^n$ tel que $\Omega \subseteq \bar{\Omega} \subset \text{conv}(\Omega)$. Alors il existe $\mathbf{x} \in \text{conv}(\Omega)$ tel que $\mathbf{x} \notin \bar{\Omega}$.

Par définition, si $\mathbf{x} \in \text{conv}(\Omega)$, alors il existe p vecteurs $\mathbf{x}_1, \mathbf{x}_2, \dots, \mathbf{x}_p \in \Omega$ et p scalaires $\alpha_1, \alpha_2, \dots, \alpha_p \geq 0$ tels que $\sum_{i=1}^p \alpha_i = 1$ et $\mathbf{x} = \sum_{i=1}^p \alpha_i \mathbf{x}_i$. D'autre part, comme $\Omega \subseteq \bar{\Omega}$, alors $\mathbf{x}_1, \mathbf{x}_2, \dots, \mathbf{x}_p \in \bar{\Omega}$ et par convexité de $\bar{\Omega}$, $\mathbf{x} = \sum_{i=1}^p \alpha_i \mathbf{x}_i \in \bar{\Omega}$. Ceci contredit le fait que $\mathbf{x} \notin \bar{\Omega}$. D'où $\text{conv}(\Omega)$ est le plus petit ensemble convexe qui contient Ω . \square

Fonction convexe

Définition 2. Soit $\Omega \subseteq \mathbb{R}^n$ un ensemble *convexe*. Une fonction $f: \Omega \rightarrow \mathbb{R}$ est dite *convexe* sur Ω si

$$\forall \mathbf{x}, \mathbf{y} \in \Omega, \forall \alpha \in [0, 1], f((1 - \alpha)\mathbf{x} + \alpha\mathbf{y}) \leq (1 - \alpha)f(\mathbf{x}) + \alpha f(\mathbf{y}).$$

La fonction f est dite *concave* si $-f$ est convexe.

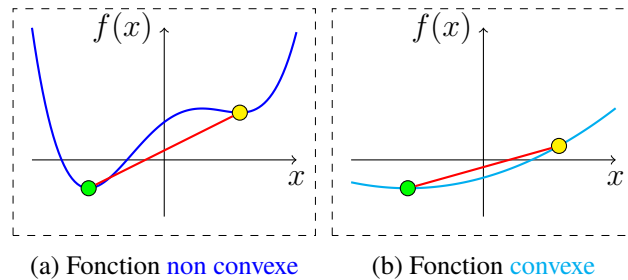


Figure 2.2 Fonction convexe

Définition 3. Soit $\Omega \subseteq \mathbb{R}^n$ un ensemble *convexe*. Soit une fonction $f: \Omega \rightarrow \mathbb{R}$.

1. Un *sous-estimateur convexe* de f sur Ω est une fonction convexe $g: \Omega \rightarrow \mathbb{R}$ telle que $g(\mathbf{x}) \leq f(\mathbf{x})$ pour tout $\mathbf{x} \in \Omega$. Le plus grand sous-estimateur est appelé *enveloppe convexe* de f sur Ω .
2. Un *sur-estimateur concave* de f sur Ω est une fonction concave $h: \Omega \rightarrow \mathbb{R}$ telle que $h(\mathbf{x}) \geq f(\mathbf{x})$ pour tout $\mathbf{x} \in \Omega$. Le plus petit sur-estimateur est appelé *enveloppe concave* de f sur Ω .

2.1.2 Optimisation convexe

Définition 4. Un problème $\min\{f(\mathbf{x}) \mid \mathbf{x} \in \Omega\}$, où $\Omega \subseteq \mathbb{R}^n$ et $f: \Omega \rightarrow \mathbb{R}$, est dit *convexe* si l'ensemble réalisable Ω est convexe et la fonction objectif f est convexe sur Ω .

THÉORÈME 2. Soit un problème convexe $\min\{f(\mathbf{x}) \mid \mathbf{x} \in \Omega \subseteq \mathbb{R}^n\}$. Si $\hat{\mathbf{x}}$ est un minimum local du problème, alors $\hat{\mathbf{x}}$ est un minimum global.

Démonstration. Si $\hat{\mathbf{x}}$ est un minimum local, alors il existe $\varepsilon > 0$ tel que pour tout $\mathbf{x} \in \Omega$ et $\|\mathbf{x} - \hat{\mathbf{x}}\| < \varepsilon$, $f(\hat{\mathbf{x}}) \leq f(\mathbf{x})$.

Supposons que $\hat{\mathbf{x}}$ n'est pas un minimum global. Alors il existe $\mathbf{y} \in \Omega$ tel que $\|\mathbf{y} - \hat{\mathbf{x}}\| \geq \varepsilon$ et $f(\mathbf{y}) < f(\hat{\mathbf{x}})$. Comme Ω est convexe, pour tout $0 < \alpha < 1$, $(1 - \alpha)\hat{\mathbf{x}} + \alpha\mathbf{y} \in \Omega$. En particulier, si $\alpha = \frac{\varepsilon}{2\|\mathbf{y} - \hat{\mathbf{x}}\|}$, on a $\mathbf{z} = (1 - \alpha)\hat{\mathbf{x}} + \alpha\mathbf{y} \in \Omega$, $\|\mathbf{z} - \hat{\mathbf{x}}\| = \frac{\varepsilon}{2} < \varepsilon$ et par la suite, $f(\hat{\mathbf{x}}) \leq f(\mathbf{z})$.

D'autre part, la fonction objectif f étant convexe sur Ω , on a $f(\mathbf{z}) \leq (1 - \alpha)f(\hat{\mathbf{x}}) + \alpha f(\mathbf{y}) < f(\hat{\mathbf{x}})$. Ceci contredit le fait que $\hat{\mathbf{x}}$ est un minimum local. D'où $\hat{\mathbf{x}}$ est un minimum global. \square

THÉORÈME 3. Soit $\Omega \subseteq \mathbb{R}^n$ un ensemble non vide et soit $\mathbf{c} \in \mathbb{R}^n$ un vecteur non nul. Soit $\hat{v} = \inf\{\mathbf{c}^T \mathbf{x} \mid \mathbf{x} \in \Omega\}$ que l'on suppose fini. Alors $\inf\{\mathbf{c}^T \mathbf{x} \mid \mathbf{x} \in \text{conv}(\Omega)\} = \hat{v}$.

Démonstration. Comme $\Omega \subseteq \text{conv}(\Omega)$, on a $\inf\{\mathbf{c}^T \mathbf{x} \mid \mathbf{x} \in \text{conv}(\Omega)\} \leq \hat{v}$. D'autre part, pour tout $\mathbf{x} \in \text{conv}(\Omega)$, il existe p vecteurs $\mathbf{x}_1, \mathbf{x}_2, \dots, \mathbf{x}_p \in \Omega$ et p scalaires $\alpha_1, \alpha_2, \dots, \alpha_p \geq 0$ tels que $\sum_{i=1}^p \alpha_i = 1$ et $\mathbf{x} = \sum_{i=1}^p \alpha_i \mathbf{x}_i$. Par la suite, $\mathbf{c}^T \mathbf{x} = \sum_{i=1}^p \alpha_i \mathbf{c}^T \mathbf{x}_i \geq \sum_{i=1}^p \alpha_i \hat{v} = \hat{v}$. D'où $\inf\{\mathbf{c}^T \mathbf{x} \mid \mathbf{x} \in \text{conv}(\Omega)\} = \hat{v}$. \square

THÉORÈME 4. Soit $\Omega \subseteq \mathbb{R}^n$ un ensemble convexe non vide et soit une fonction $f: \Omega \rightarrow \mathbb{R}$. Soit $\hat{v} = \inf\{f(\mathbf{x}) \mid \mathbf{x} \in \Omega\}$ que l'on suppose fini. Si \underline{f} est l'enveloppe convexe de f sur Ω , alors $\inf\{\underline{f}(\mathbf{x}) \mid \mathbf{x} \in \Omega\} = \hat{v}$.

Démonstration. Comme \underline{f} est un sous-estimateur de f sur Ω , on a $\inf\{\underline{f}(\mathbf{x}) \mid \mathbf{x} \in \Omega\} \leq \hat{v}$. D'autre part, la fonction $g(\mathbf{x}) = \hat{v}$ est un sous-estimateur convexe de f sur Ω . Par définition de \underline{f} , on a $\inf\{\underline{f}(\mathbf{x}) \mid \mathbf{x} \in \Omega\} \geq \hat{v}$. D'où $\inf\{\underline{f}(\mathbf{x}) \mid \mathbf{x} \in \Omega\} = \hat{v}$. \square

D'après le théorème 2, tout minimum local d'un problème convexe est aussi global. Les théorèmes 3 et 4 stipulent qu'il est possible de construire une relaxation convexe exacte d'un problème non convexe. Nous devons tout de même souligner que construire l'enveloppe convexe d'un ensemble ou d'une fonction quelconques est très difficile. Une discussion plus approfondie sur l'optimisation globale et les techniques de relaxation convexe peut être trouvée dans [7].

2.1.3 Optimisation conique

Définition 5. Soit \mathcal{V} un \mathbb{R} -espace vectoriel. Un sous-ensemble $\mathcal{K} \subseteq \mathcal{V}$ est un *cône* si pour tout $\mathbf{x} \in \mathcal{K}$ et pour tout $\alpha > 0$, $\alpha\mathbf{x} \in \mathcal{K}$.

On dit qu'un cône $\mathcal{K} \subseteq \mathbb{R}^n$ est

- *pointé* s'il ne contient aucune droite ;
- *solide* si son intérieur est non vide ;
- *propre* s'il est à la fois convexe, fermé, solide et pointé.

Comme exemples de cône propre, on peut citer

- l'orthant positif $\mathbb{R}_+^n = \{\mathbf{x} \in \mathbb{R}^n \mid x_i \geq 0, i = 1, 2, \dots, n\}$ et
- le cône du second ordre $\mathbb{R}_\nabla^{n+1} = \{(\mathbf{x}, t) \in \mathbb{R}^n \times \mathbb{R} \mid \|\mathbf{x}\|_2 \leq t\}$.

Un problème d'optimisation conique est un problème convexe qui consiste à optimiser une fonction linéaire sur l'intersection d'un sous-espace affine et d'un cône propre. Dans l'espace vectoriel $\mathcal{V} = \mathbb{R}^n$, on peut le formuler comme suit :

$$\begin{aligned} \min_{\mathbf{x} \in \mathbb{R}^n} \quad & \mathbf{a}_0^T \mathbf{x} \\ \text{s. c.} \quad & \mathbf{a}_i^T \mathbf{x} = b_i, \quad i = 1, 2, \dots, m, \\ & \mathbf{x} \in \mathcal{K}, \end{aligned}$$

où $\mathbf{a}_0, \mathbf{a}_1, \dots, \mathbf{a}_m \in \mathbb{R}^n$, $b_1, b_2, \dots, b_m \in \mathbb{R}$ et $\mathcal{K} \subseteq \mathbb{R}^n$ est un cône propre.

2.1.4 Optimisation semidéfinie

Définition 6. Une matrice $A \in \mathbb{C}^{n \times n}$ est dite hermitienne si et seulement si $A^H = A$, où A^H est la transconjugée de A .

L'ensemble \mathbb{H}^n des matrices hermitiennes d'ordre n est un \mathbb{R} -espace vectoriel de dimension n^2 . Pour tout $A, B \in \mathbb{H}^n$, on définit le produit scalaire de A par B , noté $\langle A, B \rangle$, par

$$\langle A, B \rangle = \text{tr}(AB) = \sum_{1 \leq i, j \leq n} A_{ij}^* B_{ij},$$

où $\text{tr}(\cdot)$ est l'opérateur trace.

Définition 7. Une matrice $A \in \mathbb{H}^n$ est dite

- *semidéfinie positive*, noté $A \succeq 0$, si $\mathbf{x}^H A \mathbf{x} \geq 0$ pour tout $\mathbf{x} \in \mathbb{C}^n$;

— *définie positive*, noté $A \succ 0$, si $\mathbf{x}^H A \mathbf{x} > 0$ pour tout $\mathbf{x} \in \mathbb{C}^n \setminus \{0\}$.

On peut montrer que l'ensemble \mathbb{H}_+^n des matrices semidéfinies positives est un cône propre de même dimension que \mathbb{H}^n et que son intérieur est l'ensemble \mathbb{H}_{++}^n des matrices définies positives.

Un problème d'optimisation semidéfinie est un problème conique défini sur le cône des matrices semidéfinies positives. Sa formulation standard est donnée par

$$\begin{aligned} \min_{X \in \mathbb{H}^n} \quad & \text{tr}(A_0 X) \\ \text{s. c.} \quad & \text{tr}(A_i X) = b_i, \quad i = 1, 2, \dots, m, \\ & X \succeq 0, \end{aligned}$$

où $A_0, A_1, \dots, A_m \in \mathbb{H}^n$ et $b_1, b_2, \dots, b_m \in \mathbb{R}$.

L'optimisation semidéfinie a connu un engouement sans précédent à partir des années 1990 suite, d'une part, aux résultats de Goemans et Williamson [8] sur l'approximation du problème de coupe maximum et d'autre part, aux progrès réalisés par Nesterov et Nemirovskii [9] dans le domaine des algorithmes de point intérieur. Elle trouve des applications dans divers domaines tels que l'optimisation combinatoire, la théorie de contrôle, pour ne citer que ceux-là. Grâce aux méthodes de point intérieur, plusieurs de ces applications peuvent être aujourd'hui résolues efficacement aussi bien en théorie qu'en pratique [10–13].

2.2 Écoulement de puissance : équations d'équilibre

Dans ce qui suit, nous utilisons les notations suivantes :

- $\mathcal{P} = (\mathcal{N}, \mathcal{L})$: réseau de puissance,
- \mathcal{N} : ensemble des nœuds,
- \mathcal{L} : Ensemble des branches,
- $j = \sqrt{-1}$: unité imaginaire,
- $s_{Gk} = p_{Gk} + jq_{Gk}$: puissance générée par le nœud k ,
- $s_{Dk} = p_{Dk} + jq_{Dk}$: puissance consommée par le nœud k ,
- $y'_k = g'_k + jb'_k$: admittance du compensateur shunt branché au nœud k ,
- $v_k = v_k \angle \delta_k$: tension au nœud k ,
- $y_\ell^{-1} = r_\ell + jx_\ell$: impédance série de la branche ℓ ,
- b'_ℓ : susceptance de la branche ℓ et
- t_ℓ : rapport de transformation de la branche ℓ .

Soit $\mathcal{P} = (\mathcal{N}, \mathcal{L})$ un réseau de puissance, où $\mathcal{N} = \{1, 2, \dots, n\}$ est l'ensemble des nœuds et $\mathcal{L} \subseteq \mathcal{N} \times \mathcal{N}$ est l'ensemble des branches. Chaque branche $\ell \in \mathcal{L}$ a un nœud de départ k et un nœud d'arrivée m et on note $\ell = (k, m)$. Un réseau de puissance peut être considéré comme un graphe simple et connexe comme le montre la figure 2.3a.

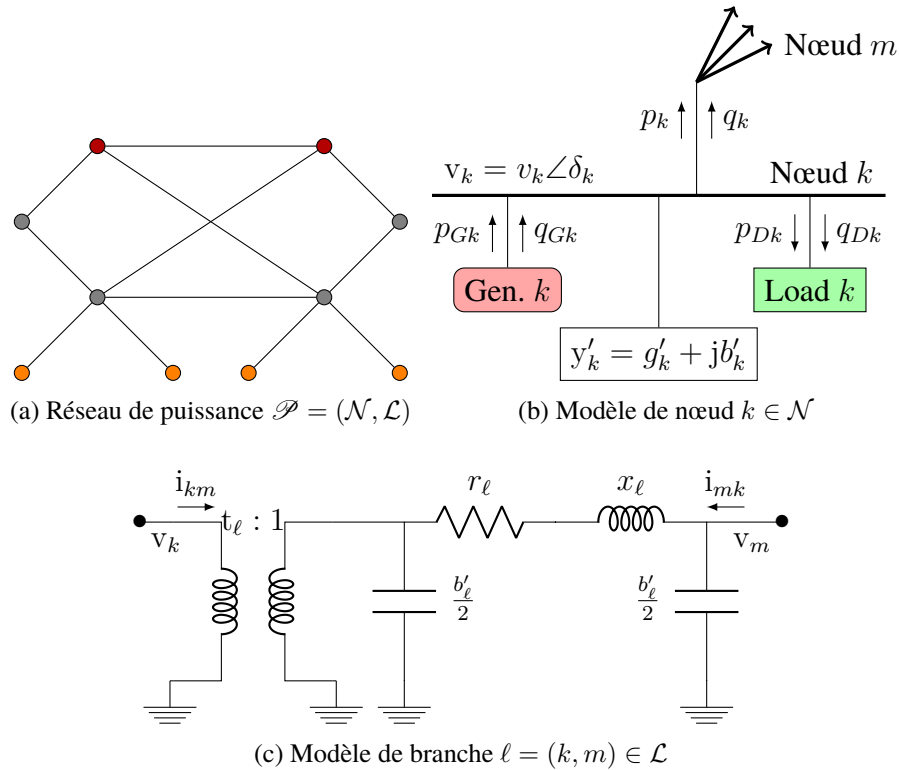


Figure 2.3 Réseau de puissance

À un nœud $k \in \mathcal{N}$ peuvent être connectés

- un générateur qui produit une puissance $s_{Gk} = p_{Gk} + jq_{Gk}$,
- une charge qui consomme une puissance $s_{Dk} = p_{Dk} + jq_{Dk}$ ou
- un compensateur shunt d'admittance $y'_k = g'_k + jb'_k$

comme illustré sur la figure 2.3b. Le nœud k est soumis à une tension complexe v_k d'amplitude v_k et de phase δ_k .

Une branche $\ell \in \mathcal{L}$, modélisée sur la figure 2.3c, peut représenter

- une ligne de transmission ou
- un transformateur ou bien
- un déphaseur

dépendamment du rapport de transformation t_ℓ .

Les courants i_{km} et i_{mk} injectés par les nœuds k et m respectivement dans la branche $\ell = (k, m) \in \mathcal{L}$ sont donnés par

$$\begin{bmatrix} i_{km} \\ i_{mk} \end{bmatrix} = \begin{bmatrix} \frac{1}{|t_\ell|^2} \left(j \frac{b'_\ell}{2} + y_\ell \right) & -\frac{y_\ell}{t_\ell^*} \\ -\frac{y_\ell}{t_\ell} & j \frac{b'_\ell}{2} + y_\ell \end{bmatrix} \begin{bmatrix} v_k \\ v_m \end{bmatrix},$$

où $y_\ell = (r_\ell + jx_\ell)^{-1}$ est l'admittance série de la branche. Alors le courant $i_k = \sum_{(k,m) \in \mathcal{L}} i_{km} + \sum_{(m,k) \in \mathcal{L}} i_{mk}$ injecté par chaque nœud $k = 1, 2, \dots, n$ à ses branches adjacentes est donné par l'équation matricielle

$$\mathbf{i} = \mathbf{Y} \mathbf{v}, \quad (2.1)$$

où $\mathbf{Y} \in \mathbb{C}^{n \times n}$ est appelée *matrice d'admittances* et $\mathbf{v} \in \mathbb{C}^n$ est le vecteur de tensions aux nœuds. La matrice d'admittances \mathbf{Y} est déterminée comme suit :

$$\begin{aligned} Y_{kk} &= \sum_{\ell=(k,m) \in \mathcal{L}} \frac{1}{|t_\ell|^2} \left(j \frac{b'_\ell}{2} + y_\ell \right) + \sum_{\ell=(m,k) \in \mathcal{L}} \left(j \frac{b'_\ell}{2} + y_\ell \right) \quad \forall k = 1, 2, \dots, n, \\ Y_{km} &= \begin{cases} -\frac{y_\ell}{t_\ell^*} & \text{si } \ell = (k, m) \in \mathcal{L}, \\ -\frac{y_\ell}{t_\ell} & \text{si } \ell = (m, k) \in \mathcal{L}, \\ 0 & \text{sinon.} \end{cases} \end{aligned}$$

On déduit que la puissance s_k injectée par le nœud $k = 1, 2, \dots, n$ à ses branches adjacentes est

$$s_k = v_k i_k^* = v_k \left(\sum_{m=1}^n Y_{km} v_m \right)^* = \sum_{m=1}^n Y_{km}^* v_k v_m^* = \mathbf{v}^H \mathbf{Y}_k^H \mathbf{v}, \quad (2.2)$$

où $\mathbf{Y}_k = \mathbf{e}_k \mathbf{e}_k^T \mathbf{Y}$ avec \mathbf{e}_k , le k -ième vecteur de la base canonique de \mathbb{R}^n .

D'autre part, d'après la loi (de courant) de Kirchhoff, la puissance injectée s_k par un nœud $k = 1, 2, \dots, n$ vaut la puissance générée moins la puissance consommée par ce nœud, i.e.,

$$s_k = s_{Gk} - s_{Dk} - (y'_k)^* |v_k|^2. \quad (2.3)$$

De (2.2) et (2.3), il suit que nous devons avoir

$$(y'_k)^* |v_k|^2 + \mathbf{v}^H \mathbf{Y}_k^H \mathbf{v} = s_{Gk} - s_{Dk} \quad (2.4)$$

pour tout $k = 1, 2, \dots, n$. Supposons que $v_k = v_k \angle \delta_k$ pour tout $k = 1, 2, \dots, n$ et que la matrice

d'admittances Y peut s'écrire $Y = G + jB$, où $G = \text{Re } Y$ et $B = \text{Im } Y$, alors (2.4) devient

$$(g'_k + G_{kk})v_k^2 + \sum_{m=1}^n [G_{km}v_kv_m \cos(\delta_k - \delta_m) + B_{km}v_kv_m \sin(\delta_k - \delta_m)] = p_{Gk} - p_{Dk}, \quad (2.5a)$$

$$-(b'_k + B_{kk})v_k^2 - \sum_{m=1}^n [B_{km}v_kv_m \cos(\delta_k - \delta_m) - G_{km}v_kv_m \sin(\delta_k - \delta_m)] = q_{Gk} - q_{Dk} \quad (2.5b)$$

pour tout $k = 1, 2, \dots, n$. Les équations (2.5) sont les *équations réelles d'équilibre* d'écoulement de puissance sous forme polaire.

Si pour tout $k = 1, 2, \dots, n$, les puissances p_{Gk} , q_{Gk} et p_{Dk} , q_{Dk} sont connues, alors les équations (2.5) forment un système de $2n$ équations à $2n$ inconnues : $\delta_1, \delta_2, \dots, \delta_n$ et v_1, v_2, \dots, v_n . Le problème consistant à résoudre ce système est appelé *problème d'écoulement de puissance*.

Les équations (2.5) étant non linéaires, les méthodes les plus utilisées pour résoudre le problème d'écoulement de puissance sont *la méthode de Gauss-Seidel*, *la méthode de Newton-Raphson* et *la méthode de découplage*. La méthode de Gauss-Seidel est beaucoup moins performante que la méthode de Newton-Raphson et, aujourd'hui, elle n'est utilisée que pour de réseaux de petite taille ou pour obtenir une solution initiale à l'algorithme de Newton-Raphson appliqué aux réseaux de très grande taille. La méthode du découplage est une version modifiée de la méthode de Newton-Raphson et converge plus rapidement que celle-ci. On peut trouver plus de détails dans [14].

Si $\mathcal{P} = (\mathcal{N}, \mathcal{L})$ est un réseau de transport, on observe ce qui suit :

1. $r_\ell \ll x_\ell$ pour tout $\ell \in \mathcal{L}$,
2. $\delta_k - \delta_m \approx 0$ pour tout $\ell = (k, m) \in \mathcal{L}$ et
3. $v_k \approx 1.0$ pour tout $k \in \mathcal{N}$.

À la lumière de ces observations, on peut supposer dans (2.5) que :

1. $G_{km} \approx 0$ pour tout $\{k, m\}$,
2. $\cos(\delta_k - \delta_m) \approx 1$, $\sin(\delta_k - \delta_m) \approx \delta_k - \delta_m$ pour tout $\{k, m\}$ et
3. $v_k \approx 1$ pour tout $k = 1, 2, \dots, n$

et les équations (2.5) se réduisent à :

$$\sum_{m=1}^n B_{km}(\delta_k - \delta_m) = p_{Gk} - p_{Dk} \quad (2.6)$$

pour tout $k = 1, 2, \dots, n$. Les équations (2.6) sont appelées *équations linéarisées d'écoulement de puissance*. Nous verrons plus tard que ces équations sont celles utilisées dans la formulation linéaire du problème d'écoulement de puissance optimal.

2.3 Problème d'écoulement de puissance optimal

2.3.1 Formulation générale et méthodes de résolution

De façon générale, le problème d'écoulement de puissance optimal peut se formuler comme suit

$$\min_{\mathbf{u}, \mathbf{x}} f(\mathbf{u}, \mathbf{x}) \quad (2.7a)$$

$$\text{s. c. } \mathbf{g}(\mathbf{u}, \mathbf{x}) = \mathbf{0}, \quad (2.7b)$$

$$\mathbf{h}(\mathbf{u}, \mathbf{x}) \leq \mathbf{0}, \quad (2.7c)$$

où \mathbf{u} représente les variables de contrôle (puissances active et réactive produites, régulateurs de tension, etc.) et \mathbf{x} représente les variables d'état (amplitudes et phases de tensions aux nœuds, courants de branches, etc.). Les variables de contrôle peuvent être discrètes ou continues tandis que celles d'état sont toujours continues. Les contraintes d'égalité $\mathbf{g}(\mathbf{u}, \mathbf{x}) = \mathbf{0}$ décrivent les équations d'équilibre d'écoulement de puissance et les contraintes d'inégalités $\mathbf{h}(\mathbf{u}, \mathbf{x}) \leq \mathbf{0}$ sont les contraintes limites de variables. La fonction objectif $f(\mathbf{u}, \mathbf{x})$ peut représenter le coût total de production, la perte totale de puissance active dans le réseau, etc.

À cause des équations d'équilibre d'écoulement de puissance (2.5), le problème (2.7) est non convexe et généralement très difficile à résoudre à l'optimalité globale. En pratique, pour les réseaux de transport, on remplace les équations (2.5) par leurs approximations linéaires (2.6) pour obtenir une formulation linéaire qu'on peut résoudre efficacement. Bien évidemment, cette formulation n'est pas rigoureusement fiable : sa solution optimale n'est pas nécessairement réalisable pour le problème original.

Dans [15, 16] sont listées les méthodes déterministes, non déterministes et hybrides qui sont utilisées pour résoudre le problème (2.7). Cependant, aucune d'entre elles ne garantit l'atteinte d'un optimum global. Au cours de la dernière décennie, des relaxations semidéfinies ont été développées dans [17, 18] et il a été montré qu'elles permettent d'atteindre un optimum global pour quelques réseaux tests de la littérature. Ces relaxations découlent de la formulation (2.4) des équations d'équilibre d'écoulement de puissance.

2.3.2 Formulation classique et relaxations semidéfinies

La formulation classique du problème d'écoulement de puissance optimal peut être considérée comme un problème d'optimisation quadratique à contraintes quadratiques. Des équations (2.4) et

sans perte de généralité, on peut l'énoncer comme suit

$$\min_{\mathbf{v} \in \mathbb{C}^n} \mathbf{v}^H \mathbf{M}_0 \mathbf{v} \quad (2.8a)$$

$$\text{s. c. } \underline{p}_k \leq \mathbf{v}^H \mathbf{M}_k \mathbf{v} \leq \bar{p}_k, \quad k = 1, 2, \dots, n, \quad (2.8b)$$

$$\underline{q}_k \leq \mathbf{v}^H \mathbf{N}_k \mathbf{v} \leq \bar{q}_k, \quad k = 1, 2, \dots, n, \quad (2.8c)$$

$$\underline{v}_k \leq |\mathbf{v}_k| \leq \bar{v}_k, \quad k = 1, 2, \dots, n, \quad (2.8d)$$

où $\mathbf{v} \in \mathbb{C}^n$ représente le vecteur des tensions aux nœuds et $\underline{v}_k > 0$ pour tout $k = 1, 2, \dots, n$.

Une matrice $\mathbf{A} \in \mathbb{C}^{n \times n}$ définie sur le réseau $\mathcal{P} = (\mathcal{N}, \mathcal{L})$ est une matrice telle que $A_{km} = A_{mk} = 0$ s'il n'existe aucune branche (k, m) ni (m, k) dans $\mathcal{P} = (\mathcal{N}, \mathcal{L})$. Notons que les matrices $\mathbf{M}_0, \mathbf{M}_1, \dots, \mathbf{M}_n$ et $\mathbf{N}_1, \mathbf{N}_2, \dots, \mathbf{N}_n$ dans (2.8) sont toutes hermitiennes et définies sur le réseau de puissance $\mathcal{P} = (\mathcal{N}, \mathcal{L})$.

Relaxation semidéfinie

Pour toute matrice $\mathbf{A} \in \mathbb{H}^n$ et tout vecteur $\mathbf{v} \in \mathbb{C}^n$, on peut écrire $\mathbf{v}^H \mathbf{A} \mathbf{v} = \text{tr}(\mathbf{A} \mathbf{v} \mathbf{v}^H)$. Si on pose $\mathbf{V} := \mathbf{v} \mathbf{v}^H$, alors le problème (2.8) devient

$$\begin{aligned} \min_{\mathbf{V} \in \mathbb{H}^n} \quad & \text{tr}(\mathbf{M}_0 \mathbf{V}) \\ \text{s. c.} \quad & \underline{p}_k \leq \text{tr}(\mathbf{M}_k \mathbf{V}) \leq \bar{p}_k, \quad k = 1, 2, \dots, n, \\ & \underline{q}_k \leq \text{tr}(\mathbf{N}_k \mathbf{V}) \leq \bar{q}_k, \quad k = 1, 2, \dots, n, \\ & \underline{v}_k^2 \leq V_{kk} \leq \bar{v}_k^2, \quad k = 1, 2, \dots, n, \\ & \mathbf{V} = \mathbf{v} \mathbf{v}^H. \end{aligned}$$

Dans cette formulation, seule la contrainte $\mathbf{V} = \mathbf{v} \mathbf{v}^H$ n'est pas convexe. Par contre, on peut montrer qu'elle équivaut à $\mathbf{V} \succeq 0$ et $\text{rang } \mathbf{V} = 1$. En omettant la contrainte non convexe du rang, on obtient la relaxation semidéfinie ci-dessous proposée pour la première fois en 2008 dans [18] :

$$\min_{\mathbf{V} \in \mathbb{H}^n} \quad \text{tr}(\mathbf{M}_0 \mathbf{V}) \quad (2.9a)$$

$$\text{s. c. } \underline{p}_k \leq \text{tr}(\mathbf{M}_k \mathbf{V}) \leq \bar{p}_k, \quad k = 1, 2, \dots, n, \quad (2.9b)$$

$$\underline{q}_k \leq \text{tr}(\mathbf{N}_k \mathbf{V}) \leq \bar{q}_k, \quad k = 1, 2, \dots, n, \quad (2.9c)$$

$$\underline{v}_k^2 \leq V_{kk} \leq \bar{v}_k^2, \quad k = 1, 2, \dots, n, \quad (2.9d)$$

$$\mathbf{V} \succeq 0. \quad (2.9e)$$

Si la solution optimale $\hat{\mathbf{V}}$ du problème relaxé (2.9) est de rang 1, on peut toujours construire une

solution optimale globale au problème original (2.8) \hat{v} tel que $\hat{V} = \hat{v}\hat{v}^H$. Dans ce cas, on dit que la relaxation est exacte. D'un autre côté, dans le cas où la solution optimale \hat{V} du problème relaxé (2.9) est de rang au moins deux, il est difficile d'y trouver une interprétation physique et, par la suite, de retrouver une solution réalisable v du problème original.

L'inconvénient avec la relaxation (2.9) est qu'en pratique, sa résolution directe est trop coûteuse pour un réseau de grande taille. Le coût de sa résolution est directement lié à la taille n^2 de la matrice V , où n est le nombre des nœuds dans le réseau. Par ailleurs, on peut remarquer que seules les entrées $V_{kk} := |v_k|^2$ et $V_{km} := v_k v_m^*$ correspondant aux nœuds et branches du réseau respectivement sont impliquées dans le problème d'optimisation (2.9). Sachant que les réseaux de puissance sont relativement creux ou moins denses, c'est-à-dire le nombre des branches dans un réseau est très proche du nombre des nœuds, on voit que la résolution de la relaxation semidéfinie prend en compte beaucoup trop de variables qui ne sont pas nécessaires.

Relaxation cordale

Afin d'augmenter la vitesse de résolution de la relaxation semidéfinie (2.9), on propose en 2012 dans [19] d'exploiter la caractéristique creuse de réseaux de puissance en remplaçant la contrainte $V \succeq 0$ par des contraintes semidéfinies de taille moindre.

Associons au réseau de puissance $\mathcal{P} = (\mathcal{N}, \mathcal{L})$, le graphe simple, connexe et non orienté $\mathcal{G} = (\mathcal{N}, \mathcal{E})$, où $\mathcal{N} = \{1, 2, \dots, n\}$ et $\mathcal{E} = \{\{k, m\} \mid (k, m) \text{ ou } (m, k) \in \mathcal{L}\}$ sont respectivement l'ensemble des sommets et l'ensemble des arêtes. Un sous-ensemble des sommets $\mathcal{K} \subseteq \mathcal{N}$ est une clique si tous ses sommets sont adjacents dans \mathcal{G} . On dit que la clique \mathcal{K} est *maximale* si elle n'est contenue dans aucune autre clique de plus grande taille. Un cycle est un γ -uplet $(k_1, k_2, \dots, k_\gamma)$ de sommets distincts de \mathcal{N} tel que $\{k_1, k_2\}, \{k_2, k_3\}, \dots, \{k_{\gamma-1}, k_\gamma\}, \{k_\gamma, k_1\} \in \mathcal{E}$; le nombre $\gamma \geq 3$ est la taille du cycle. Une corde d'un cycle $(k_1, k_2, \dots, k_\gamma)$ est une arête $\{k_i, k_j\} \in \mathcal{E}$ telle que $1 \leq i < j \leq \gamma$ et $2 \leq j - i \leq \gamma - 2$. Une illustration de ces concepts est donnée dans la figure 2.4.

On dit qu'un graphe $\mathcal{G} = (\mathcal{N}, \mathcal{E})$ est cordal ou triangulé si tout cycle d'au moins 4 sommets contient une corde. Une extension cordale de \mathcal{G} est un graphe cordal $\mathcal{G}' = (\mathcal{N}, \mathcal{E}')$ qui contient \mathcal{G} , i.e., $\mathcal{E} \subseteq \mathcal{E}'$. Comme le montre la figure 2.5, un graphe $\mathcal{G} = (\mathcal{N}, \mathcal{E})$ non cordal peut avoir plusieurs extensions cordales. En général, trouver l'extension cordale nécessitant le moins d'ajout d'arêtes est un problème NP-difficile.

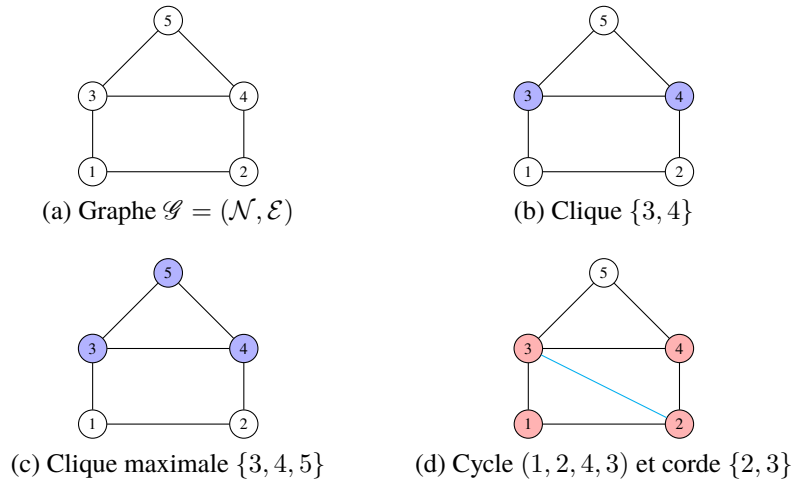


Figure 2.4 Graphe, clique, cycle et corde

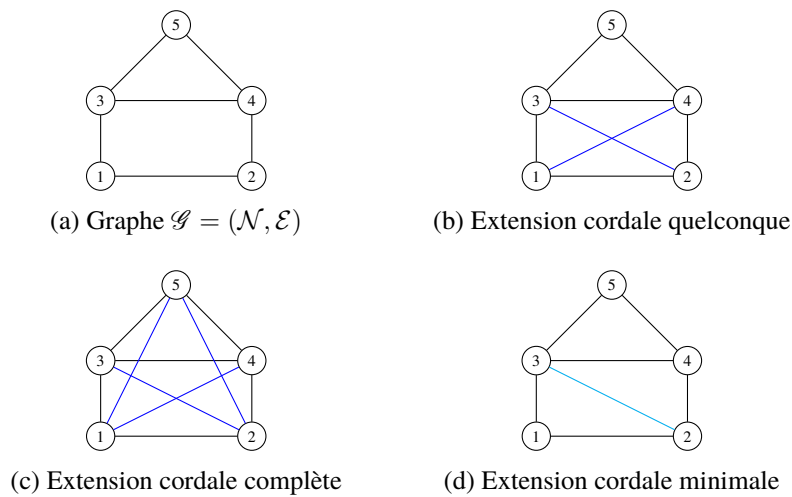


Figure 2.5 Graphe et extension cordale

Considérons, à présent, la matrice partielle suivante

$$V_{\mathcal{G}} := \{V_{kk} \in \mathbb{R} \forall k \in \mathcal{N}, V_{km} \in \mathbb{C}, V_{mk} = V_{km}^* \forall \{k, m\} \in \mathcal{E}\}$$

qui ne prend en compte que les entrées de la matrice V impliquées directement au problème d'optimisation (2.9). Par exemple, pour le graphe de la figure 2.4a, on peut représenter la matrice

partielle $V_{\mathcal{G}}$ comme suit

$$V_{\mathcal{G}} := \begin{bmatrix} V_{11} & V_{12} & V_{13} & & & & \\ V_{12}^* & V_{22} & & & & & \\ V_{13}^* & & V_{33} & V_{34} & V_{35} & & \\ & & & V_{24} & & & \\ & & & & V_{24}^* & V_{34}^* & V_{44} & V_{45} \\ & & & & & & & V_{45}^* & V_{55} \end{bmatrix} \quad (2.10)$$

Notons que la taille de la matrice partielle $V_{\mathcal{G}}$ est $n + 2|\mathcal{E}|$, inférieure à la taille n^2 de la matrice complète V . D'autre part, la matrice V peut être vue comme une complétion de la matrice partielle $V_{\mathcal{G}}$.

On dit que la matrice partielle $V_{\mathcal{G}}$ est semidéfinie positive, qu'on note $V_{\mathcal{G}} \succeq 0$, si toutes les sous-matrices $V_{\mathcal{K}}$ correspondant aux cliques maximales \mathcal{K} de \mathcal{G} sont semidéfinies positives. Par exemple, pour le graphe de la figure 2.4a, on a

$$V_{\mathcal{G}} := \begin{bmatrix} V_{11} & V_{12} & V_{13} & & & & \\ V_{12}^* & V_{22} & & & & & \\ V_{13}^* & & V_{33} & V_{34} & V_{35} & & \\ & & & V_{24} & & & \\ & & & & V_{24}^* & V_{34}^* & V_{44} & V_{45} \\ & & & & & & & V_{45}^* & V_{55} \end{bmatrix} \succeq 0 \Leftrightarrow \begin{cases} V_{\{1,2\}} := \begin{bmatrix} V_{11} & V_{12} \\ V_{12}^* & V_{22} \end{bmatrix} \succeq 0 \\ V_{\{1,3\}} := \begin{bmatrix} V_{11} & V_{13} \\ V_{13}^* & V_{33} \end{bmatrix} \succeq 0, \\ V_{\{2,4\}} := \begin{bmatrix} V_{22} & V_{24} \\ V_{24}^* & V_{44} \end{bmatrix} \succeq 0, \\ V_{\{3,4,5\}} := \begin{bmatrix} V_{33} & V_{34} & V_{35} \\ V_{34}^* & V_{44} & V_{45} \\ V_{35}^* & V_{45}^* & V_{55} \end{bmatrix} \succeq 0. \end{cases}$$

Par définition, une matrice est semidéfinie positive si toutes ses sous-matrices principales sont aussi semidéfinies positives. Il suit que si une complétion V de la matrice partielle $V_{\mathcal{G}}$ est semidéfinie positive, alors la matrice partielle $V_{\mathcal{G}}$ l'est aussi. Cependant, si la matrice partielle $V_{\mathcal{G}}$ est semidéfinie positive, il existe une complétion V semidéfinie positive si et seulement si le graphe \mathcal{G} est cordal [20].

Soit $V_{\mathcal{G}'}$ la matrice partielle d'une extension cordale $\mathcal{G}' = (\mathcal{N}, \mathcal{E}')$ de $\mathcal{G} = (\mathcal{N}, \mathcal{E})$. Si $V_{\mathcal{G}'}$ est semidéfinie positive, alors il existe une complétion V semidéfinie positive. Par exemple, pour le

graphe de la figure 2.4a et l'extension cordale de la figure 2.5b, si

$$V_{\mathcal{G}'} := \begin{bmatrix} V_{11} & V_{12} & V_{13} & V_{14} & & \\ V_{12}^* & V_{22} & V_{23} & V_{24} & & \\ V_{13}^* & V_{23}^* & V_{33} & V_{34} & V_{35} & \\ V_{14}^* & V_{24}^* & V_{34}^* & V_{44} & V_{45} & \\ & & V_{35}^* & V_{45}^* & V_{55} & \end{bmatrix} \succeq 0 \Leftrightarrow \begin{cases} V_{\{1,2,3,4\}} := \begin{bmatrix} V_{11} & V_{12} & V_{13} & V_{14} \\ V_{12}^* & V_{22} & V_{23} & V_{24} \\ V_{13}^* & V_{23}^* & V_{33} & V_{34} \\ V_{14}^* & V_{24}^* & V_{34}^* & V_{44} \end{bmatrix} \succeq 0, \\ V_{\{3,4,5\}} := \begin{bmatrix} V_{33} & V_{34} & V_{35} \\ V_{34}^* & V_{44} & V_{45} \\ V_{35}^* & V_{45}^* & V_{55} \end{bmatrix} \succeq 0, \end{cases}$$

alors, il existe $V_{15}, V_{25} \in \mathbb{C}$ tels que

$$V = \begin{bmatrix} V_{11} & V_{12} & V_{13} & V_{14} & V_{15} \\ V_{12}^* & V_{22} & V_{23} & V_{24} & V_{25} \\ V_{13}^* & V_{23}^* & V_{33} & V_{34} & V_{35} \\ V_{14}^* & V_{24}^* & V_{34}^* & V_{44} & V_{45} \\ V_{15}^* & V_{25}^* & V_{35}^* & V_{45}^* & V_{55} \end{bmatrix} \succeq 0.$$

On peut donc remplacer la contrainte $V \succeq 0$ dans la relaxation semidéfinie (2.9) par les contraintes $V_{\mathcal{K}} \succeq 0$ correspondantes à toutes les cliques maximales \mathcal{K} d'une extension cordale $\mathcal{G}' = (\mathcal{N}, \mathcal{E}')$ du graphe $\mathcal{G} = (\mathcal{N}, \mathcal{E})$ associé au réseau de puissance $\mathcal{P} = (\mathcal{N}, \mathcal{L})$. La relaxation obtenue est appelée *relaxation cordale*; elle est moins coûteuse que la relaxation semidéfinie et lui est équivalente. Soulignons tout de même que le coût de sa résolution dépend de la taille des cliques maximales de l'extension cordale considérée.

Relaxation conique du second ordre

Si on remplace la contrainte $V \succeq 0$ dans (2.9) par les contraintes suivantes

$$V_{\{k,m\}} := \begin{bmatrix} V_{kk} & V_{km} \\ V_{km}^* & V_{mm} \end{bmatrix} \succeq 0 \quad \forall (k, m) \in \mathcal{L}, \quad (2.11)$$

on obtient la relaxation conique du second ordre. Pour toute branche $(k, m) \in \mathcal{L}$ du réseau, on peut montrer que (2.11) équivaut à

$$\sqrt{4[\operatorname{Re}(V_{km})]^2 + 4[\operatorname{Im}(V_{km})]^2 + (V_{kk} - V_{mm})^2} \leq V_{kk} + V_{mm},$$

ce qui correspond à un cône elliptique du second ordre dans \mathbb{R}^4 avec comme variables $\text{Re}(V_{km})$, $\text{Im}(V_{km})$, V_{kk} et V_{mm} .

La relaxation conique du second ordre a été proposée pour la première fois en 2006 dans [17]. Elle est, en termes de résolution, beaucoup moins coûteuse que la relaxation semidéfinie et équivaut à cette dernière pour un réseau radial, c'est-à-dire le graphe correspondant au réseau est un arbre. Cependant, la relaxation semidéfinie demeure plus forte pour les réseaux maillés.

2.3.3 Traitement de variables entières : technique de l'arrondi

En général, le problème d'écoulement de puissance optimal est un problème non linéaire mixte en nombres entiers qu'on peut formuler comme suit :

$$\hat{v} = \min f_0(\mathbf{x}, \mathbf{y}) \quad (2.12a)$$

$$\text{s. c. } f_i(\mathbf{x}, \mathbf{y}) \leq 0, \quad i = 1, 2, \dots, m, \quad (2.12b)$$

$$(\mathbf{x}, \mathbf{y}) \in \mathbb{R}^{n_1} \times \mathbb{Z}^{n_2}, \quad (2.12c)$$

où $f_i: \mathbb{R}^{n_1} \times \mathbb{Z}^{n_2} \rightarrow \mathbb{R}$ pour tout $i = 0, 1, \dots, m$. Les variables entières $\mathbf{y} \in \mathbb{Z}^{n_2}$ peuvent représenter de composants du réseau qui permettent par exemple de contrôler la puissance réactive tels que les transformateurs à rapport variable, les condensateurs shunts, etc.

Un problème d'optimisation non linéaire mixte en nombres entiers est un problème dont, d'une part, la fonction objectif et les contraintes sont décrites par des fonctions non linéaires et, d'autre part, certaines variables sont contraintes à ne prendre que de valeurs entières [21]. De façon stricte, un problème non linéaire mixte en nombres entiers est un problème non convexe. Cependant il est dit *convexe* si sa relaxation continue est un problème convexe, c'est-à-dire que les fonctions f_0, f_1, \dots, f_m dans (2.12) sont toutes convexes. Les problèmes non linéaires mixtes en nombres entiers sont une généralisation des problèmes linéaires mixtes en nombres entiers et des problèmes non linéaires et héritent de la difficulté de ces deux classes de problèmes. En effet, il existe des exemples de problèmes non linéaires mixtes en nombres entiers et non convexes qui sont non seulement NP-difficiles, mais aussi *indécidables*. Plus de détails peuvent être trouvés dans [22, 23].

La méthode la plus utilisée pour résoudre un problème d'écoulement de puissance optimal avec variables entières est la technique de l'arrondi qui marche comme suit :

1. résoudre la relaxation continue du problème non linéaire mixte en nombres entiers (2.12),
2. ensuite, arrondir les solutions optimales correspondant aux variables entières \mathbf{y} aux valeurs entières les plus proches,
3. enfin, fixer les variables entières \mathbf{y} à ces valeurs et résoudre le sous-problème obtenu.

En effet, en fixant toutes les variables entières, i.e., $\mathbf{y} = \tilde{\mathbf{y}} \in \mathbb{Z}^{n_2}$, on obtient le sous-problème de (2.12) suivant

$$\hat{v}_{SP} = \min_{\tilde{\mathbf{y}} \in \mathbb{Z}^{n_2}} f_0(\mathbf{x}, \tilde{\mathbf{y}}) \quad (2.13a)$$

$$\text{s. c. } f_i(\mathbf{x}, \tilde{\mathbf{y}}) \leq 0, \quad i = 1, 2, \dots, m, \quad (2.13b)$$

$$\mathbf{x} \in \mathbb{R}^{n_1}. \quad (2.13c)$$

et le problème (2.12) se réécrit

$$\hat{v} = \min_{\tilde{\mathbf{y}} \in \mathbb{Z}^{n_2}} \left\{ \min_{\mathbf{x} \in \mathbb{R}^{n_1}} \{f_0(\mathbf{x}, \tilde{\mathbf{y}}) \mid f_i(\mathbf{x}, \tilde{\mathbf{y}}) \leq 0, i = 1, 2, \dots, m\} \right\}.$$

Si le sous-problème (2.13) est réalisable, alors sa valeur optimale \hat{v}_{SP} est une borne supérieure pour la valeur optimale \hat{v} du problème (2.12) et sa solution optimale $(\hat{\mathbf{x}}_{SP}, \tilde{\mathbf{y}})$ est appelée *solution sous-optimale* du problème (2.12). Le sous-problème (2.13) peut ne pas être convexe et trouver sa solution globale peut alors devenir difficile. Dans ce cas, toute valeur optimale locale \bar{v}_{SP} de (2.13) peut toutefois être considérée comme une borne supérieure de \hat{v} .

Considérons à présent une relaxation continue de (2.12) :

$$\hat{v}_R = \min_{\mathbf{x}, \mathbf{y}} \underline{f}_0(\mathbf{x}, \mathbf{y}) \quad (2.14a)$$

$$\text{s. c. } (\mathbf{x}, \mathbf{y}) \in \bar{\Omega} \subseteq \mathbb{R}^{n_1} \times \mathbb{R}^{n_2}, \quad (2.14b)$$

où $\bar{\Omega}$ contient l'ensemble réalisable de (2.12) et \underline{f}_0 sous-estime f_0 pour toute solution réalisable de (2.12). La qualité de la solution sous-optimale $(\hat{\mathbf{x}}_{SP}, \tilde{\mathbf{y}})$ du sous-problème (2.13) dépend fortement de la solution $\tilde{\mathbf{y}}$ obtenue après avoir arrondi la solution optimale de la relaxation continue (2.14). Comme la relaxation (2.14) est en général non convexe et qu'on a aucune garantie sur la globalité de sa solution obtenue avec un solveur local, la solution sous-optimale obtenue par la suite est dans la plupart des cas de mauvaise qualité ou non réalisable pour le problème original.

2.3.4 Problème multi-période

La plupart des applications réelles qui nécessitent la résolution du problème d'écoulement de puissance sont multi-périodes à cause de la variation horaire de la consommation dans une journée, des conditions météorologiques, des limites opérationnelles d'équipements de contrôle ou d'autres contraintes temporelles et mécaniques. Un modèle multi-période est alors judicieux pour prendre en compte toutes ces considérations.

Considérons l'ensemble de périodes de temps $\{1, 2, \dots, \bar{\tau}\}$. Un problème d'écoulement de puis-

sance optimal multi-période peut être donné par

$$\min_{\mathbf{x}^1, \mathbf{x}^2, \dots, \mathbf{x}^{\bar{\tau}}} \sum_{\tau=1}^{\bar{\tau}} f^{\tau}(\mathbf{x}^{\tau}) \quad (2.15a)$$

$$\text{s. c. } \mathbf{g}^{\tau}(\mathbf{x}^{\tau}) \leq \mathbf{0}, \quad \tau = 1, 2, \dots, \bar{\tau}, \quad (2.15b)$$

$$\mathbf{h}^{\tau}(\mathbf{x}^{\tau}, \mathbf{x}^{\tau+1}) \leq \mathbf{0}, \quad \tau = 1, 2, \dots, \bar{\tau} - 1, \quad (2.15c)$$

où (2.15b) représente les contraintes habituelles d'un problème d'écoulement de puissance optimal sur une période et (2.15c) représente les contraintes de couplage entre deux périodes consécutives. Ces dernières délimitent par exemple la variation abrupte de production d'une période à une autre ou régulent le stockage en énergie entre différentes périodes.

Au delà des contraintes que l'on peut considérer dans le modèle, la préoccupation majeure du problème (2.15) est plutôt sa taille qui équivaut à $\bar{\tau}$ fois la taille d'un problème d'écoulement de puissance optimal sur une seule période [6]. Par exemple, appliquer directement la relaxation semidéfinie à ce problème est inapproprié, bien qu'elle pourrait donner de bons résultats.

CHAPITRE 3 ORGANISATION DE LA THÈSE

La thèse est rédigée par articles qui sont au nombre de trois, reportés dans les chapitres 4, 5 et 6, respectivement.

Dans le chapitre 4, nous proposons une nouvelle relaxation du problème classique d'écoulement de puissance optimal. Les travaux réalisés dans ce chapitre ont été publiés dans la revue *IEEE Transactions on Power Systems* [24]. Ensuite, dans le chapitre 5, nous considérons le problème de répartition optimale de puissance réactive, qui est une des versions mixtes en nombres entiers du problème d'écoulement de puissance optimal. Nous proposons de résoudre ce problème avec la technique de l'arrondi combinée avec une relaxation conique du problème plutôt que sa relaxation continue non convexe. Les travaux du chapitre 5 ont été publiés dans la revue *IEEE Transactions on Power Systems* [25]. Finalement, dans le chapitre 6, nous montrons que la nouvelle relaxation développée dans le chapitre 4 peut être exacte et nous l'extrapolons au problème multi-période d'écoulement de puissance optimal. Ce chapitre a été soumis pour publication dans la revue *Mathematical Programming Computation* [26]. Une discussion générale sur la contribution des trois articles est donnée dans le chapitre 7.

Le reste de la thèse est organisé comme suit. Le chapitre 2 présente une revue critique de la littérature et situe notre contribution par rapport à ce qui a déjà été fait et le chapitre 8 conclue cette thèse en proposant quelques améliorations futures.

CHAPITRE 4 ARTICLE 1: TIGHT-AND-CHEAP CONIC RELAXATION FOR THE AC OPTIMAL POWER FLOW PROBLEM

Christian Bingane, Miguel F. Anjos, and Sébastien Le Digabel. Tight-and-cheap conic relaxation for the AC optimal power flow problem. *IEEE Transactions on Power Systems*, 33(6): 7181-7188, 2018.

Abstract: The classical alternating current optimal power flow problem is highly nonconvex and generally hard to solve. Convex relaxations, in particular semidefinite, second-order cone, convex quadratic, and linear relaxations, have recently attracted significant interest. The semidefinite relaxation is the strongest among them and is exact for many cases. However, the computational efficiency for solving large-scale semidefinite optimization is lower than for second-order cone optimization. We propose a conic relaxation obtained by combining semidefinite optimization with the reformulation-linearization technique, commonly known as RLT. The proposed relaxation is stronger than the second-order cone relaxation and nearly as tight as the standard semidefinite relaxation. Computational experiments using standard test cases with up to 6515 buses show that the time to solve the new conic relaxation is up to one order of magnitude lower than for the chordal relaxation, a semidefinite relaxation technique that exploits the sparsity of power networks.

Keywords: Conic optimization, optimal power flow, power systems, semidefinite programming.

4.1 Nomenclature

4.1.1 Notations

| | |
|-------------------------|---|
| \mathbb{R}/\mathbb{C} | Set of real/complex numbers, |
| \mathbb{H}^n | Set of $n \times n$ Hermitian matrices, |
| j | Imaginary unit, |
| a/a | Real/complex number, |
| \mathbf{a}/\mathbf{a} | Real/complex vector, |
| A/A | Real/complex matrix. |

4.1.2 Operators

| | |
|-------------------------------------|-------------------------------|
| $\text{Re}(\cdot)/\text{Im}(\cdot)$ | Real/imaginary part operator, |
| $(\cdot)^*$ | Conjugate operator, |

| | |
|----------------------|--|
| $ \cdot $ | Magnitude or cardinality set operator, |
| $\angle(\cdot)$ | Phase operator, |
| $(\cdot)^T$ | Transpose operator, |
| $(\cdot)^H$ | Conjugate transpose operator, |
| $\text{rank}(\cdot)$ | Rank operator. |

4.1.3 Input data

| | |
|---|---|
| $\mathcal{P} = (\mathcal{N}, \mathcal{L})$ | Power network, |
| \mathcal{N} | Set of buses, |
| $\mathcal{G} = \bigcup_{k \in \mathcal{N}} \mathcal{G}_k$ | Set of generators, |
| \mathcal{G}_k | Set of generators connected to bus k , |
| \mathcal{L} | Set of branches, |
| p_{Dk}/q_{Dk} | Active/reactive power demand at bus k , |
| g'_k/b'_k | Conductance/susceptance of shunt element at bus k , |
| c_{g2}, c_{g1}, c_{g0} | Generation cost coefficients of generator g , |
| $y_\ell^{-1} = r_\ell + jx_\ell$ | Series impedance of branch ℓ , |
| b'_ℓ | Total shunt susceptance of branch ℓ , |
| t_ℓ | Turns ratio of branch ℓ . |

4.1.4 Variables

| | |
|-----------------------|---|
| p_{Gg}/q_{Gg} | Active/reactive power generation by generator g , |
| v_k | Complex (phasor) voltage at bus k , |
| $p_{f\ell}/q_{f\ell}$ | Active/reactive power flow injected along branch ℓ by its <i>from</i> end, |
| $p_{t\ell}/q_{t\ell}$ | Active/reactive power flow injected along branch ℓ by its <i>to</i> end. |

4.2 Introduction

The optimal power flow (OPF) problem, introduced by Carpentier in 1962 [27], seeks to find a network operating point that optimizes an objective function such as generation cost subject to power flow equations and other operational constraints. A broad survey of the history of the problem and the related optimization methods appears in [15, 16, 28].

According to [15], the general OPF problem may be modelled using linear, mixed-integer linear, nonlinear, or mixed integer nonlinear optimization. We focus on the nonlinear version, also called alternating current optimal power flow (ACOPF) problem. The ACOPF problem is nonconvex and NP-hard [29, 30]. One way to tackle it is to use convex relaxations of the nonconvex constraints.

A conic optimization problem is a class of convex optimization problem that consists in optimizing a linear function over the intersection of an affine subspace and a convex cone. When the cone is the nonnegative orthant, the second-order cone, or the positive semidefinite matrices set, the conic optimization problem is a linear, a second-order cone or a semidefinite program respectively. A large theory can be found in [2] on convex optimization or in [3] on semidefinite optimization.

Since the ACOPF problem can be cast as a quadratically constrained quadratic program (QCQP), two principal conic relaxations have been proposed in the last decade: the second-order cone programming (SOCP) relaxation [17] and the semidefinite programming (SDP) relaxation [18]. These two relaxations offer several advantages. First, they can lead to global optimality. Second, because they are relaxations, they provide a bound on the global optimal value of the ACOPF problem. Third, if one of them is infeasible, then the ACOPF problem is infeasible.

We should note that the SDP relaxation is stronger than the SOCP relaxation but requires heavier computation. Therefore, a chordal relaxation was proposed in [31] in order to exploit the fact that power networks are not densely connected, thus reducing data storage and increasing computation speed. A full literature review on these three relaxations can be found in [32, 33]. Other convex relaxations have been developed in [34–38].

For radial networks, the SOCP relaxation is tantamount to the SDP relaxation. In this case, one would normally solve the first one rather than the second one due to the difference in computation time. For general meshed networks, it would be interesting to develop a relaxation as fast as the SOCP relaxation and as strong as the SDP relaxation. For example, three strong SOCP relaxations were developed in [39] that are very close in quality to the SDP relaxation and are faster to solve.

In this paper, we present a new conic relaxation that offers a favourable trade-off between the SOCP and the SDP relaxations for large-scale instances of ACOPF in terms of optimality gap and computation time. This relaxation is obtained through a combination of semidefinite optimization and the reformulation-linearization technique, known as RLT.

The remainder of this paper is organized as follows. In Section 4.3, we define the mathematical model of the ACOPF problem (without loss of generality). In Section 4.4, we describe principal conic relaxations of the ACOPF problem, especially semidefinite and second-order cone relaxations. In Section 4.5, we present the new conic relaxation, and we present computational results in Section 4.6. Section 4.7 concludes the paper.

4.3 ACOPF: Formulation

Consider a typical power network $\mathcal{P} = (\mathcal{N}, \mathcal{L})$ where $\mathcal{N} = \{1, \dots, n\}$ and $\mathcal{L} \subseteq \mathcal{N} \times \mathcal{N}$ denote respectively the set of buses and the set of branches (transmission lines, transformers and phase

shifters). Each branch $\ell \in \mathcal{L}$ has a *from* end k (on the *tap side*) and a *to* end m as modeled in [40]. We note $\ell = (k, m)$. The ACOPF problem is given as:

$$\min \sum_{g \in \mathcal{G}} c_{g2} p_{Gg}^2 + c_{g1} p_{Gg} + c_{g0} \quad (4.1a)$$

over variables $\mathbf{p}_G, \mathbf{q}_G \in \mathbb{R}^{|\mathcal{G}|}$, $\mathbf{p}_f, \mathbf{q}_f, \mathbf{p}_t, \mathbf{q}_t \in \mathbb{R}^{|\mathcal{L}|}$, and $\mathbf{v} \in \mathbb{C}^{|\mathcal{N}|}$, subject to

— Power balance equations:

$$\sum_{g \in \mathcal{G}_k} p_{Gg} - p_{Dk} - g'_k |v_k|^2 = \sum_{\ell=(k,m) \in \mathcal{L}} p_{f\ell} + \sum_{\ell=(m,k) \in \mathcal{L}} p_{t\ell} \quad \forall k \in \mathcal{N}, \quad (4.1b)$$

$$\sum_{g \in \mathcal{G}_k} q_{Gg} - q_{Dk} + b'_k |v_k|^2 = \sum_{\ell=(k,m) \in \mathcal{L}} q_{f\ell} + \sum_{\ell=(m,k) \in \mathcal{L}} q_{t\ell} \quad \forall k \in \mathcal{N}, \quad (4.1c)$$

— Line flow equations:

$$p_{f\ell} + jq_{f\ell} = \frac{v_k}{t_\ell} \left[\left(j \frac{b'_\ell}{2} + y_\ell \right) \frac{v_k}{t_\ell} - y_\ell v_m \right]^* \quad \forall \ell = (k, m) \in \mathcal{L}, \quad (4.1d)$$

$$p_{t\ell} + jq_{t\ell} = v_m \left[-y_\ell \frac{v_k}{t_\ell} + \left(j \frac{b'_\ell}{2} + y_\ell \right) v_m \right]^* \quad \forall \ell = (k, m) \in \mathcal{L}, \quad (4.1e)$$

— Generator power capacities:

$$\underline{p}_{Gg} \leq p_{Gg} \leq \bar{p}_{Gg}, \quad \underline{q}_{Gg} \leq q_{Gg} \leq \bar{q}_{Gg} \quad \forall g \in \mathcal{G}, \quad (4.1f)$$

— Line thermal limits:

$$|p_{f\ell} + jq_{f\ell}| \leq \bar{s}_\ell, \quad |p_{t\ell} + jq_{t\ell}| \leq \bar{s}_\ell \quad \forall \ell \in \mathcal{L}, \quad (4.1g)$$

— Voltage magnitude limits:

$$\underline{v}_k \leq |v_k| \leq \bar{v}_k \quad \forall k \in \mathcal{N}, \quad (4.1h)$$

— Reference bus constraint:

$$\angle v_1 = 0. \quad (4.1i)$$

The objective function (4.1a) is the cost of conventional generation as commonly used in the literature. Constraints (4.1b)–(4.1e) are derived from Kirchhoff's laws and represent power flows in the network. Constraint (4.1i) specifies bus $k = 1$ as the reference bus. We assume that $\underline{v}_k > 0$ for all $k \in \mathcal{N}$ in (4.1h), and that generation cost $c_{g2} p_{Gg}^2 + c_{g1} p_{Gg} + c_{g0}$ is a convex function for all $g \in \mathcal{G}$.

Due to the nonconvex constraints (4.1d)–(4.1e), (4.1) is highly nonconvex and NP-hard [29, 30].

Applying local methods to this problem provides no guarantee on the optimality of any solution found. Moreover, it is intractable to solve to global optimality for large-scale instances.

4.4 ACOPF: Conic relaxations

4.4.1 Semidefinite relaxation

With $V := \mathbf{v}\mathbf{v}^H$, the ACOPF problem (4.1) can be reformulated as follows

minimize (4.1a)

subject to (4.1f), (4.1g), (4.1i),

$$\sum_{g \in \mathcal{G}_k} p_{Gg} - p_{Dk} - g'_k V_{kk} = \sum_{\ell=(k,m) \in \mathcal{L}} p_{f\ell} + \sum_{\ell=(m,k) \in \mathcal{L}} p_{t\ell} \quad \forall k \in \mathcal{N}, \quad (4.2a)$$

$$\sum_{g \in \mathcal{G}_k} q_{Gg} - q_{Dk} + b'_k V_{kk} = \sum_{\ell=(k,m) \in \mathcal{L}} q_{f\ell} + \sum_{\ell=(m,k) \in \mathcal{L}} q_{t\ell} \quad \forall k \in \mathcal{N}, \quad (4.2b)$$

$$p_{f\ell} + j q_{f\ell} = \frac{1}{|t_\ell|^2} \left(-j \frac{b'_\ell}{2} + y_\ell^* \right) V_{kk} - \frac{y_\ell^*}{t_\ell} V_{km} \quad \forall \ell = (k, m) \in \mathcal{L}, \quad (4.2c)$$

$$p_{t\ell} + j q_{t\ell} = -\frac{y_\ell^*}{t_\ell} V_{mk} + \left(-j \frac{b'_\ell}{2} + y_\ell^* \right) V_{mm} \quad \forall \ell = (k, m) \in \mathcal{L}, \quad (4.2d)$$

$$\underline{v}_k^2 \leq V_{kk} \leq \bar{v}_k^2 \quad \forall k \in \mathcal{N}, \quad (4.2e)$$

$$V = \mathbf{v}\mathbf{v}^H. \quad (4.2f)$$

The nonconvexity of (4.2) is captured by the constraint (4.2f). We can show that $V = \mathbf{v}\mathbf{v}^H$ if and only if $V \succeq 0$ and $\text{rank}(V) = 1$. The *semidefinite relaxation* (SDR) in Model 1 is obtained by dropping the rank constraint. It was first introduced in [18] and later, a dual relaxation was developed in [41].

Model 1 Semidefinite relaxation (SDR)

Variables:

$$\mathbf{p}_G, \mathbf{q}_G \in \mathbb{R}^{|\mathcal{G}|}, \quad (4.3a)$$

$$\mathbf{p}_f, \mathbf{q}_f, \mathbf{p}_t, \mathbf{q}_t \in \mathbb{R}^{|\mathcal{L}|}, \quad (4.3b)$$

$$V \in \mathbb{H}^{|\mathcal{N}|}. \quad (4.3c)$$

Minimize: (4.1a)

Subject to: (4.1f), (4.1g), (4.2a)–(4.2e), $V \succeq 0$.

If the optimal solution \hat{V} of SDR is a rank-one matrix, then there exists a complex vector \hat{v} , global optimal solution of (4.1). In the literature, there are numerous examples where SDR is exact. However, its exactness is only guaranteed for a few classes of problems under some assumptions [33]. On the other hand, solving SDR for large-scale power systems (more than a thousand of buses) is computationally very expensive. In order to reduce data storage and increase computational speed, [31] proposes to exploit in SDR the sparsity of the OPF problem. This methodology, as we explain in Section 4.4.2, suggests to replace the positive semidefinite matrix V by less-sized positive semidefinite submatrices defined on a chordal extension of the power network [31, 32, 39].

4.4.2 Chordal relaxation

Let us interpret the network $\mathcal{P} = (\mathcal{N}, \mathcal{L})$ as a connected, simple and undirected graph $\mathcal{G} = (\mathcal{N}, \mathcal{E})$ where $\mathcal{N} = \{1, \dots, n\}$ represents the set of vertices and $\mathcal{E} = \{\{k, m\} : (k, m) \text{ or } (m, k) \in \mathcal{L}\}$, the set of edges. The power flow equations (4.1b)–(4.1e) in (4.1) depend only on $V_{kk} := |v_k|^2$, $k \in \mathcal{N}$, and $V_{km} := v_k v_m^*$, $\{k, m\} \in \mathcal{E}$. In other words, except for the constraint $V \succeq 0$, SDR depends only on a *partial matrix* $V_{\mathcal{G}}$. A partial matrix means a matrix in which only some of the entries are specified [20, 32].

A subset $\mathcal{K} \subseteq \mathcal{N}$ is a *clique* if every two distinct vertices in \mathcal{K} are adjacent in \mathcal{G} . A clique \mathcal{K} is *maximal* in \mathcal{G} if it is not a subset of a larger clique \mathcal{K}' . A *cycle* is a sequence $k_1 - k_2 - \dots - k_\gamma - k_1$ of γ distinct vertices such that $\{k_1, k_2\}, \{k_2, k_3\}, \dots, \{k_{\gamma-1}, k_\gamma\}, \{k_\gamma, k_1\} \in \mathcal{E}$, where $\gamma \geq 3$ is the length of the cycle. A *chord* of a cycle $k_1 - k_2 - \dots - k_\gamma - k_1$ is an edge $\{k_i, k_j\} \in \mathcal{E}$ such that $1 \leq i < j \leq \gamma$ and $2 \leq j - i \leq \gamma - 2$.

\mathcal{G} is *chordal* if every cycle of 4 and more vertices has a chord. A *chordal extension* of \mathcal{G} is a chordal graph $\mathcal{G}' = (\mathcal{N}, \mathcal{E}')$ that contains \mathcal{G} , i.e., $\mathcal{E} \subseteq \mathcal{E}'$. It was proved in [20] that the constraint $V \succeq 0$ in SDR is equivalent to $V_{\mathcal{K}} \succeq 0$ for every maximal clique \mathcal{K} of a chordal extension \mathcal{G}' of \mathcal{G} . $V_{\mathcal{K}}$ is the submatrix of V in which the set of row indices that remain and the set of column indices that remain are both \mathcal{K} . Thus, the *chordal relaxation* (CHR) is given in Model 2.

The optimal value \hat{v}_{CHR} of CHR is not affected by the choice of the chordal extension \mathcal{G}' . However, the optimal choice that minimizes the complexity of CHR is NP-hard to compute. Given a positive definite real matrix A of size n such that $A_{km} = 0$ if $\{k, m\} \notin \mathcal{E}$, let $A = LL^T$ be its Cholesky decomposition, where L is a lower triangular matrix. A chordal extension $\mathcal{G}' = (\mathcal{N}, \mathcal{E}')$ of $\mathcal{G} = (\mathcal{N}, \mathcal{E})$ is defined by $\mathcal{E}' = \{\{k, m\} : L_{km} + L_{mk} \neq 0, k \neq m\}$. The fill-in in the Cholesky decomposition depends on the ordering of the nodes $k \in \mathcal{N}$. The problem of finding the ordering that corresponds to the minimum fill-in is known to be NP-complete. See [32, 42, 43] for more details. Besides, [31, 44–46] have developed effective techniques to solve the chordal relaxation of

Model 2 Chordal relaxation (CHR)

Initialization: $\mathcal{G} = (\mathcal{N}, \mathcal{E})$, graph corresponding to $\mathcal{P} = (\mathcal{N}, \mathcal{L})$. Consider $A = L_{\mathcal{G}} + I_{|\mathcal{N}|} \succ 0$, where $L_{\mathcal{G}}$ is the Laplacian matrix of \mathcal{G} and $I_{|\mathcal{N}|}$ is the identity matrix of size $|\mathcal{N}|$.

Chordal extension:

1. Order nodes with heuristic algorithm “*approximate minimum degree*” provided by MATLAB-function `amd`.
2. Compute Cholesky decomposition LL^T of A . The sparsity pattern of L defines a chordal extension \mathcal{G}' of \mathcal{G} .
3. Identify $\{\mathcal{K}_1, \mathcal{K}_2, \dots, \mathcal{K}_\kappa\}$, family of maximal cliques of \mathcal{G}' .

Variables: (4.3).

Minimize: (4.1a)

Subject to: (4.1f), (4.1g), (4.2a)–(4.2e), $V_{\mathcal{K}_i} \succeq 0, i = 1, 2, \dots, \kappa$.

the ACOFP problem and we observe a significant speed-up factor computationally for large-scale power systems compared to the standard SDP relaxation.

4.4.3 Second-order cone relaxation

If we relax the constraint $V \succeq 0$ in SDR by $|\mathcal{L}|$ constraints of the form

$$V_{\{k,m\}} := \begin{bmatrix} V_{kk} & V_{km} \\ V_{km}^* & V_{mm} \end{bmatrix} \succeq 0 \quad \forall (k, m) \in \mathcal{L}, \quad (4.4)$$

we obtain the standard *second-order cone relaxation* (SOCR) in Model 3. In fact, (4.4) represents a rotated second-order cone constraint in the $(\text{Re}(V_{km}), \text{Im}(V_{km}), V_{kk}, V_{mm})$ -space for each branch $(k, m) \in \mathcal{L}$.

Model 3 Second-order cone relaxation (SOCR)

Variables: (4.3).

Minimize: (4.1a)

Subject to: (4.1f), (4.1g), (4.2a)–(4.2e), (4.4).

Proposition 1 ([32]). *Let $\hat{v}, \hat{v}_{SDR}, \hat{v}_{CHR}, \hat{v}_{SOCR}$ be the optimal values of ACOFP Problem (4.1), SDR, CHR and SOCR. Then $\hat{v}_{SOCR} \leq \hat{v}_{CHR} = \hat{v}_{SDR} \leq \hat{v}$. Moreover, for radial networks, $\hat{v}_{SOCR} = \hat{v}_{CHR} = \hat{v}_{SDR} \leq \hat{v}$.*

SOCR is of significant interest because it is computationally more efficient than SDR, and is thus

more amenable for large-scale instances. It was first proposed in [17] for radial networks, and was extended in [47] to meshed networks by including a trigonometric functional constraint for the voltage angle spread on each line in the network. Later, [39] proposed three strong SOCP relaxations and showed their computational advantages over SDR.

4.5 New conic relaxation

For two real variables x, y such that $\underline{x} \leq x \leq \bar{x}, \underline{y} \leq y \leq \bar{y}$ where $\underline{x}, \bar{x}, \underline{y}, \bar{y} \in \mathbb{R}$ and $\underline{x} < \bar{x}, \underline{y} < \bar{y}$, if $z = xy$ then

$$z \leq \underline{x}\underline{y} + \bar{x}\bar{y} - \bar{x}\underline{y}, \quad (4.5a)$$

$$z \leq \underline{x}\bar{y} + \bar{x}\underline{y} - \underline{x}\bar{y}, \quad (4.5b)$$

$$z \geq \underline{x}\underline{y} + \bar{x}\bar{y} - \bar{x}\underline{y}, \quad (4.5c)$$

$$z \geq \underline{x}\bar{y} + \bar{x}\underline{y} - \underline{x}\bar{y}. \quad (4.5d)$$

Inequalities (4.5) are called reformulation-linearization technique (RLT) inequalities. They describe the convex hull of $\{(x, y, z) \in \mathbb{R}^3: \underline{x} \leq x \leq \bar{x}, \underline{y} \leq y \leq \bar{y}, z = xy\}$ [48]. For a general nonconvex QCQP with bounded real variables, it has been shown in [49] that the use of SDP and RLT constraints together can produce better optimal bounds than either technique used alone. Earlier, it has been proven in [50] that the convex hull of $\{(\mathbf{x}, X) \in \mathbb{R}^2 \times \mathbb{H}^2: X = \mathbf{x}\mathbf{x}^T, \underline{\mathbf{x}} \leq \mathbf{x} \leq \bar{\mathbf{x}}\}$ is given by the SDP constraint $X \succeq \mathbf{x}\mathbf{x}^T$ together with the RLT inequalities on X_{11}, X_{12}, X_{22} . Hence, one might be tempted to transform ACOPF Problem (4.1) with complex variables \mathbf{v} into a problem with real variables $\mathbf{v}^r := \text{Re}(\mathbf{v}), \mathbf{v}^i := \text{Im}(\mathbf{v})$ and consider a relaxation based on SDP and RLT. Such a relaxation would not be as effective as might be expected due to nonrectangular bounds on \mathbf{v} [51].

On the other hand, it has been shown in [52] that relaxing nonconvex constraints of the ACOPF problem before converting from complex to real variables is more advantageous than doing the operations in opposite order. Thus, assuming $|\angle v_k - \angle v_m| \leq \pi/2$ for every branch $(k, m) \in \mathcal{L}$ in the network, equivalent valid inequalities have been proposed in [51, 53] to strengthen the SDP relaxation.

4.5.1 Tight-and-cheap relaxation

For all $(k, m) \in \mathcal{L}$, we have $V_{km} = v_k v_m^*$ from (4.2f), therefore $|V_{km}| = |v_k| |v_m|$. Considering $x = |v_k|, y = |v_m|, z = |V_{km}|$, and applying (4.5), we obtain

$$|V_{km}| \leq |v_k| \underline{v}_m + \bar{v}_k |v_m| - \bar{v}_k \underline{v}_m, \quad (4.6a)$$

$$|V_{km}| \leq |v_k|\bar{v}_m + \underline{v}_k|v_m| - \underline{v}_k\bar{v}_m, \quad (4.6b)$$

$$|V_{km}| \geq |v_k|\underline{v}_m + \underline{v}_k|v_m| - \underline{v}_k\underline{v}_m, \quad (4.6c)$$

$$|V_{km}| \geq |v_k|\bar{v}_m + \bar{v}_k|v_m| - \bar{v}_k\bar{v}_m, \quad (4.6d)$$

since $\bar{v}_k \leq |v_k| \leq \bar{v}_k$ for all $k \in \mathcal{N}$. Moreover for all $k \in \mathcal{N}$, $V_{kk} := |v_k|^2$, and thus we also have

$$V_{kk} \leq (\underline{v}_k + \bar{v}_k)|v_k| - \underline{v}_k\bar{v}_k \quad (4.6e)$$

All RLT inequalities (4.6) are nonconvex, except the constraint (4.6e) corresponding to the reference bus $k = 1$:

$$\operatorname{Re}(v_1) \geq \frac{V_{11} + \underline{v}_1\bar{v}_1}{\underline{v}_1 + \bar{v}_1}, \quad (4.7a)$$

$$\operatorname{Im}(v_1) = 0. \quad (4.7b)$$

Therefore, we define a new formulation of the SDP relaxation in Model 4. We denote nSDR. To the best of our knowledge, it is the first time that nSDR with $V \succeq \mathbf{v}\mathbf{v}^H$ is proposed for the ACOFF problem.

Model 4 New semidefinite relaxation (nSDR)

Variables: (4.3), $\mathbf{v} \in \mathbb{C}^{|\mathcal{N}|}$.

Minimize: (4.1a)

Subject to: (4.1f), (4.1g), (4.2a)–(4.2e), (4.7), $V \succeq \mathbf{v}\mathbf{v}^H$.

Lemma 1. *Let $y \in \mathbb{R}$ such that $\ell \leq y \leq u$, where $0 \leq \ell < u < +\infty$. If $x = \sqrt{y}$, then $x \geq \frac{y + \sqrt{\ell}\sqrt{u}}{\sqrt{\ell} + \sqrt{u}}$.*

Proof. Let $g(y) = \sqrt{y}$ a concave function on its domain. For all $0 \leq \ell < u < +\infty$, $\alpha \in [0, 1]$,

$$g((1 - \alpha)\ell + \alpha u) \geq (1 - \alpha)g(\ell) + \alpha g(u) = (1 - \alpha)\sqrt{\ell} + \alpha\sqrt{u}.$$

In particular, when $\alpha = \frac{y - \ell}{u - \ell}$, $\ell \leq y \leq u$, we have

$$\sqrt{y} = x \geq \frac{y + \sqrt{\ell}\sqrt{u}}{\sqrt{\ell} + \sqrt{u}}.$$

□

Lemma 2. *Let $A \in \mathbb{H}^m$, $B \in \mathbb{C}^{m \times n}$. If $A \succeq 0$, then $B^H A B \succeq 0$.*

Proof. Let $\mathbf{x} \in \mathbb{C}^n$ and $\mathbf{y} = \mathbf{B}\mathbf{x} \in \mathbb{C}^m$. Therefore, $\mathbf{x}^H \mathbf{B}^H \mathbf{A} \mathbf{B} \mathbf{x} = \mathbf{y}^H \mathbf{A} \mathbf{y} \geq 0$. \square

Proposition 2. *nSDR is equivalent to SDR.*

Proof. Every feasible solution V of nSDR is also feasible for SDR because $V \succeq \mathbf{v}\mathbf{v}^H \succeq 0$. It remains to prove that for every feasible solution V of SDR, there exists $\mathbf{v} \in \mathbb{C}^n$ such that (\mathbf{v}, V) is feasible for nSDR.

Given V feasible solution of SDR, let $\mathbf{v} = \frac{1}{\sqrt{V_{11}}} V \mathbf{e}_1$ where \mathbf{e}_1 is the n -dimensional vector with 1 in the first entry and 0 elsewhere. For all $k \in \mathcal{N}$, $v_k = \frac{1}{\sqrt{V_{11}}} V_{k1}$. In particular, $v_1 = \sqrt{V_{11}} \in \mathbb{R}$ and from Lemma 1,

$$\operatorname{Re}(v_1) = \sqrt{V_{11}} \geq \frac{V_{11} + \underline{v}_1 \bar{v}_1}{\underline{v}_1 + \bar{v}_1}.$$

Now, let $B = \begin{bmatrix} \frac{\mathbf{e}_1}{\sqrt{V_{11}}} & I_n \end{bmatrix} \in \mathbb{R}^{n \times (n+1)}$, where I_n is the identity matrix of size n . From Lemma 2,

$$B^T V B = \begin{bmatrix} 1 & \mathbf{v}^H \\ \mathbf{v} & V \end{bmatrix} \succeq 0 \Leftrightarrow V \succeq \mathbf{v}\mathbf{v}^H.$$

\square

Recall that SOCR is obtained from SDR by replacing the constraint $V \succeq 0$ in SDR by $|\mathcal{L}|$ smaller positive semidefiniteness constraints, each one corresponding to a branch of the network. Now we replace the constraint $V \succeq \mathbf{v}\mathbf{v}^H$ in Model 4 by $|\mathcal{L}|$ constraints of the form

$$\begin{bmatrix} 1 & v_k^* & v_m^* \\ v_k & V_{kk} & V_{km} \\ v_m & V_{km}^* & V_{mm} \end{bmatrix} \succeq 0 \quad \forall (k, m) \in \mathcal{L}. \quad (4.8)$$

to obtain the relaxation given in Model 5. We will refer to this relaxation as “*tight-and-cheap relaxation*” (TCR). Clearly TCR dominates SOCR and is dominated by SDR.

Model 5 Tight-and-cheap relaxation (TCR)

Variables: (4.3), $\mathbf{v} \in \mathbb{C}^{|\mathcal{N}|}$.

Minimize: (4.1a)

Subject to: (4.1f), (4.1g), (4.2a)–(4.2e), (4.7), (4.8).

4.5.2 Strengthening

Considering $k = 1$ as the reference bus, if the constraint $V \succeq 0$ in SDR holds, then

$$V_{\{1,k,m\}} := \begin{bmatrix} V_{11} & V_{1k} & V_{1m} \\ V_{1k}^* & V_{kk} & V_{km} \\ V_{1m}^* & V_{km}^* & V_{mm} \end{bmatrix} \succeq 0 \quad \forall (k, m) \in \mathcal{L}. \quad (4.9)$$

We define another relaxation given in Model 6. We call this relaxation “*strong tight-and-cheap relaxation*” (STCR). Like TCR, STCR dominates SOCR and is dominated by SDR.

Model 6 Strong tight-and-cheap relaxation (STCR)

Variables: (4.3).

Minimize: (4.1a)

Subject to: (4.1f), (4.1g), (4.2a)–(4.2e), (4.9).

Proposition 3. *STCR is stronger than TCR.*

Proof. We show that for every V feasible solution of STCR, there exists $\mathbf{v} \in \mathbb{C}^n$ such that (\mathbf{v}, V) is feasible for TCR. For all $k \in \mathcal{N}$, let $v_k = \frac{1}{\sqrt{V_{11}}} V_{k1}$. In particular, $v_1 = \sqrt{V_{11}} \in \mathbb{R}$ and from Lemma 1,

$$\operatorname{Re}(v_1) = \sqrt{V_{11}} \geq \frac{V_{11} + v_1 \bar{v}_1}{v_1 + \bar{v}_1}.$$

Now, for all $(k, m) \in \mathcal{L}$, if (4.9) holds, then by Lemma 2,

$$\begin{bmatrix} \frac{1}{\sqrt{V_{11}}} & \mathbf{0}^T \\ \mathbf{0} & I_2 \end{bmatrix} V_{\{1,k,m\}} \begin{bmatrix} \frac{1}{\sqrt{V_{11}}} & \mathbf{0}^T \\ \mathbf{0} & I_2 \end{bmatrix} = \begin{bmatrix} 1 & v_k^* & v_m^* \\ v_k & V_{kk} & V_{km} \\ v_m & V_{km}^* & V_{mm} \end{bmatrix} \succeq 0.$$

□

Proposition 4. *Let $\mathcal{G} = (\mathcal{N}, \mathcal{E})$ a graph corresponding to a power network $\mathcal{P} = (\mathcal{N}, \mathcal{L})$. Suppose bus $k = 1$ is the reference bus. If the induced subgraph $\mathcal{G} - \{1\}$ has no cycle, then STCR is equivalent to SDR.*

Proof. Consider $\mathcal{G}' = (\mathcal{N}, \mathcal{E}')$ where $\mathcal{E}' = \mathcal{E} \cup \{\{1, m\} : \{1, m\} \notin \mathcal{E}\}$. Since $\mathcal{G} - \{1\}$ has no cycle, every cycle in \mathcal{G}' contains vertex $k = 1$. Also, since for all $m \in \mathcal{N} \setminus \{1\}$, $\{1, m\} \in \mathcal{E}'$, every cycle $1 - m_1 - m_2 - m_3 - 1$ of 4 vertices has a chord $\{1, m_2\}$. Thus, \mathcal{G}' is a chordal extension of \mathcal{G} .

On the other hand, since $\mathcal{G} - \{1\}$ has no cycle, every maximal clique \mathcal{K} of \mathcal{G}' contains vertex $k = 1$ and has at most 3 vertices, i.e., $\mathcal{K} = \{1, k, m\}$ for all $\{k, m\} \in \mathcal{E}$. Then the constraint $V \succeq 0$ in SDR is equivalent to $V_{\{1,k,m\}} \succeq 0$ for all $\{k, m\} \in \mathcal{E}$. \square

4.6 Computational results

In this section, we evaluate the accuracy and the computational efficiency of TCR and STCR as compared to SOCR, CHR and SDR.

We tested the models 1, 2, 3, 5 and 6 on standard test cases available from MATPOWER [40,54,55]. *It is important to note that, unlike what was done in [41, 44–46], we did not make any modification or simplification to the data.*

We solved all the relaxations in MATLAB using CVX 2.1 [56,57] with the solver MOSEK 8.0.0.60 and default precision (tolerance $\epsilon = 1.49 \times 10^{-8}$). All the computations were carried out on an Intel Core i7-6700 CPU @ 3.40 GHz computing platform. When solving SOCR for instances with at least 1000 buses, MOSEK ended its computation with message `Mosek error: MSK_RES_TRM_STALL()`. For these test cases, we replace constraints (4.4) by equivalent ones

$$\begin{bmatrix} V_{kk} + V_{mm} & 0 & 2V_{km} \\ 0 & V_{kk} + V_{mm} & V_{kk} - V_{mm} \\ 2V_{km}^* & V_{kk} - V_{mm} & V_{kk} + V_{mm} \end{bmatrix} \succeq 0 \quad \forall (k, m) \in \mathcal{L}.$$

We considered two objective functions: the generation cost [\$/h] (4.1a) and the active loss [MW] where $c_{g2} = 0$, $c_{g1} = 1$ and $c_{g0} = 0$ for all $g \in \mathcal{G}$ in (4.1a). Both objective functions of test cases from [55] are the same. We denote \underline{v} the best lower bound which is the maximum value among \hat{v}_{SOCR} , \hat{v}_{TCR} , \hat{v}_{STCR} , \hat{v}_{CHR} , \hat{v}_{SDR} , respective optimal values of SOCR, TCR, STCR, CHR and SDR. The optimality gap is measured as $100(1 - \hat{v}_R/\bar{v})$, where \bar{v} is the upper bound provided by the MATPOWER-solver ‘‘MIPS’’ and \hat{v}_R is the relaxation optimal value. For some test cases: 1888rte, 1951rte, 2848rte, 2868rte, 6468rte, 6470rte, 6495rte and 6515rte, MIPS failed to find a local optimal solution, so we considered the upper bounds reported in [55].

Table 4.1 and Table 4.2 summarize the optimality gaps of the five relaxations for cost minimization and loss minimization, respectively. The results support the following key points:

1. CHR is equivalent to SDR as predicted by Proposition 1.
2. TCR and STCR are stronger than SOCR. When compared to SOCR, TCR reduces the optimality gap from 0.17% to 0.06% on average for large-scale instances in Table 4.2.
3. Optimality gaps of TCR and STCR are very close to CHR or SDR. We observe significant

optimality gaps of TCR and STCR when the optimality gap of CHR or SDR is not close to zero, e.g., `case5` and `case_ACTIV_SG_500` instances in Table 4.1.

4. STCR is stronger than TCR as predicted by Proposition 3. For example, STCR reduces substantially the optimality gap of TCR from 12.75% to 5.22% on `case5` instance in Table 4.1.

The computation times reported by MOSEK are shown in Table 4.1 and Table 4.2. The time CVX took to pre-compile a model is not included. For CHR, the computation time does not take into account the time of building the chordal extension of an instance’s graph. We did not solve SDR for the extra large-scale instances (those with at least 6000 buses) because of the high computational cost. In Tables 4.1 and 4.2, we note:

1. Among all relaxations, SOCR is the fastest and SDR is the slowest.
2. CHR is on average around 30 times faster than SDR for large-scale instances.
3. TCR is on average around 30 times faster than CHR for large-scale instances and 55 times for extra large-scale instances.
4. TCR is on average around 3 times faster than STCR for large-scale instances and 7 times for extra large-scale instances.

4.7 Conclusion

We proposed a new formulation of the semidefinite relaxation for the ACOPF problem. This formulation is based on a positive semidefiniteness constraint combined with reformulation-linearization technique (RLT) constraints defined on the reference (slack) bus. We proved that it is equivalent to the standard SDP relaxation. Thereafter, we derived a tight-and-cheap semidefinite relaxation (TCR) stronger than the standard SOCP relaxation. Experiments on unmodified MATPOWER instances show that the proposed relaxation offers an interesting trade-off between the standard SDP and SOCP relaxations for large-scale power systems because it is very close to the SDP relaxation in terms of optimality gap, but computationally it is much faster than the chordal relaxation (which is equivalent to the SDP relaxation).

A strong TCR (STCR) was also proposed. We showed that, under some assumption, it is tantamount to the standard SDP relaxation. Although faster than the chordal relaxation, it is not as fast as TCR.

Acknowledgment

We thank Stéphane Alarie and Laurent Lenoir, both of the Hydro-Québec Research Institute (IREQ), for helpful comments on early drafts of this paper. We also thank the anonymous reviewers for their many helpful suggestions that helped us improve this paper.

Table 4.1 Cost minimization

| Test case | \bar{v} [\$h] | \underline{v} [\$h] | Optimality gap [%] | | | | | Computation time [s] | | | | |
|------------------------------------|-----------------|-----------------------|--------------------|-------------|-------------|-------------|-------------|----------------------|--------------|---------------|-----------------|------------------|
| | | | SOCR | TCR | STCR | CHR | SDR | SOCR | TCR | STCR | CHR | SDR |
| <i>Small-scale instances</i> | | | | | | | | | | | | |
| LMBD3_50 | 5 812.64 | 5 789.91 | 1.32 | 0.74 | 0.39 | 0.39 | 0.39 | 0.08 | 0.06 | 0.06 | 0.06 | 0.06 |
| LMBD3_60 | 5 707.11 | 5 707.11 | 0.05 | 0.00 | 0.00 | 0.00 | 0.00 | 0.07 | 0.08 | 0.06 | 0.06 | 0.05 |
| case5 | 17 551.89 | 16 635.78 | 14.54 | 12.75 | 5.22 | 5.22 | 5.22 | 0.06 | 0.07 | 0.07 | 0.07 | 0.07 |
| case6ww | 3 143.97 | 3 143.97 | 0.63 | 0.00 | 0.00 | 0.00 | 0.00 | 0.09 | 0.07 | 0.07 | 0.07 | 0.06 |
| case9 | 5 296.69 | 5 296.69 | 0.00 | 0.00 | 0.00 | 0.00 | 0.00 | 0.07 | 0.07 | 0.07 | 0.07 | 0.07 |
| case14 | 8 081.53 | 8 081.52 | 0.08 | 0.00 | 0.00 | 0.00 | 0.00 | 0.07 | 0.08 | 0.07 | 0.08 | 0.07 |
| case24_ieee_rts | 63 352.21 | 63 352.20 | 0.01 | 0.00 | 0.00 | 0.00 | 0.00 | 0.09 | 0.13 | 0.14 | 0.11 | 0.13 |
| case30 | 576.89 | 576.89 | 0.57 | 0.07 | 0.00 | 0.00 | 0.00 | 0.08 | 0.14 | 0.16 | 0.13 | 0.16 |
| case_ieee30 | 8 906.14 | 8 906.14 | 0.04 | 0.00 | 0.00 | 0.00 | 0.00 | 0.08 | 0.11 | 0.11 | 0.08 | 0.10 |
| case39 | 41 864.18 | 41 862.03 | 0.02 | 0.01 | 0.01 | 0.01 | 0.01 | 0.08 | 0.19 | 0.18 | 0.11 | 0.25 |
| case57 | 41 737.79 | 41 737.78 | 0.06 | 0.01 | 0.00 | 0.00 | 0.00 | 0.08 | 0.17 | 0.19 | 0.16 | 0.25 |
| case89pegase | 5 819.81 | 5 819.65 | 0.17 | 0.04 | 0.00 | 0.00 | 0.00 | 0.16 | 0.68 | 0.83 | 0.90 | 1.08 |
| Average | | | 0.39 | 0.23 | 0.09 | 0.09 | 0.09 | 0.10 | 0.30 | 0.34 | 0.34 | 0.43 |
| <i>Medium-scale instances</i> | | | | | | | | | | | | |
| case118 | 129 660.70 | 129 654.54 | 0.25 | 0.03 | 0.02 | 0.00 | 0.00 | 0.08 | 0.33 | 0.42 | 0.32 | 1.09 |
| case_ACTIV_SG_200 | 27 557.57 | 27 557.55 | 0.00 | 0.00 | 0.00 | 0.00 | 0.00 | 0.21 | 0.56 | 0.65 | 0.72 | 4.66 |
| case_illinois200 | 36 748.39 | 36 748.33 | 0.02 | 0.00 | 0.00 | 0.00 | 0.00 | 0.22 | 0.83 | 0.92 | 0.87 | 6.28 |
| case300 | 719 725.11 | 719 710.63 | 0.15 | 0.02 | 0.01 | 0.00 | 0.00 | 0.20 | 0.97 | 1.20 | 0.95 | 10.52 |
| case_ACTIV_SG_500 | 72 578.30 | 71 048.04 | 5.38 | 4.39 | 4.20 | 2.11 | 2.11 | 0.75 | 3.21 | 4.04 | 3.14 | 103.35 |
| Average | | | 2.10 | 1.67 | 1.60 | 0.80 | 0.80 | 0.40 | 1.68 | 2.08 | 1.68 | 43.36 |
| <i>Large-scale instances</i> | | | | | | | | | | | | |
| case1354pegase | 74 069.35 | 74 061.72 | 0.08 | 0.02 | 0.02 | 0.01 | 0.01 | 5.73 | 6.34 | 13.23 | 9.72 | 1 657.85 |
| case1888rte | 59 805.1 | 59 601.29 | 0.39 | 0.36 | 0.35 | 0.34 | 0.34 | 8.88 | 10.61 | 26.64 | 17.88 | 4 629.31 |
| case1951rte | 81 737.7 | 81 725.16 | 0.08 | 0.03 | 0.03 | 0.01 | 0.02 | 11.24 | 12.49 | 31.78 | 23.31 | 5 595.59 |
| case2383wp | 1 868 511.83 | 1 861 214.70 | 1.07 | 0.50 | 0.48 | 0.40 | 0.39 | 11.55 | 11.60 | 33.76 | 216.38 | 9 420.67 |
| case2736sp | 1 307 883.13 | 1 307 695.31 | 0.31 | 0.03 | 0.01 | 0.02 | 0.02 | 10.24 | 12.28 | 36.42 | 303.63 | 10 786.69 |
| case2737sop | 777 629.30 | 777 517.52 | 0.27 | 0.03 | 0.02 | 0.02 | 0.01 | 8.90 | 11.47 | 35.68 | 242.92 | 10 601.37 |
| case2746wop | 1 208 279.81 | 1 208 182.18 | 0.40 | 0.03 | 0.02 | 0.01 | 0.01 | 9.87 | 11.51 | 35.57 | 343.90 | 10 480.83 |
| case2746wp | 1 631 775.10 | 1 631 665.81 | 0.33 | 0.03 | 0.02 | 0.01 | 0.01 | 11.34 | 13.00 | 36.68 | 340.18 | 11 654.59 |
| case2848rte | 53 021.8 | 53 005.20 | 0.08 | 0.04 | 0.04 | 0.03 | 0.04 | 12.17 | 14.36 | 44.56 | 46.64 | 14 567.98 |
| case2868rte | 79 794.7 | 79 787.67 | 0.07 | 0.02 | 0.02 | 0.01 | 0.02 | 14.05 | 17.03 | 55.08 | 47.20 | 16 933.60 |
| case2869pegase | 133 999.29 | 133 983.11 | 0.09 | 0.03 | 0.03 | 0.01 | 0.03 | 15.45 | 18.76 | 60.18 | 49.29 | 14 866.00 |
| case3012wp | 2 591 706.57 | 2 587 512.73 | 0.82 | 0.38 | 0.37 | 0.17 | 0.16 | 12.90 | 15.21 | 49.39 | 1 276.67 | 16 051.95 |
| case3120sp | 2 142 703.76 | 2 140 385.00 | 0.56 | 0.13 | 0.12 | 0.11 | 0.11 | 14.98 | 16.55 | 52.77 | 765.39 | 14 636.04 |
| case3375wp | 7 412 030.68 | 7 407 116.46 | 0.30 | 0.14 | 0.14 | 0.08 | 0.07 | 15.23 | 17.64 | 66.37 | 1 216.15 | 18 229.90 |
| Average | | | 0.36 | 0.12 | 0.12 | 0.08 | 0.08 | 12.03 | 14.02 | 43.71 | 402.09 | 12 336.09 |
| <i>Extra large-scale instances</i> | | | | | | | | | | | | |
| case6468rte | 86 860.0 | 86 808.12 | 0.27 | 0.08 | 0.08 | 0.06 | – | 35.47 | 40.79 | 314.92 | 1 990.53 | – |
| case6470rte | 98 345.5 | 98 333.90 | 0.18 | 0.06 | 0.03 | 0.01 | – | 53.34 | 51.88 | 371.42 | 2 729.29 | – |
| case6495rte | 106 283.4 | 106 072.44 | 0.46 | 0.23 | 0.23 | 0.20 | – | 50.50 | 65.15 | 431.65 | 3 592.15 | – |
| case6515rte | 109 804.2 | 109 688.71 | 0.38 | 0.16 | 0.14 | 0.11 | – | 48.02 | 59.60 | 427.22 | 3 523.01 | – |
| Average | | | 0.32 | 0.13 | 0.12 | 0.09 | – | 46.84 | 54.38 | 386.42 | 2 960.41 | – |

Table 4.2 Loss minimization

| Test case | \bar{v} [MW] | \underline{v} [MW] | Optimality gap [%] | | | | | Computation time [s] | | | | |
|------------------------------------|----------------|----------------------|--------------------|-------------|-------------|-------------|-------------|----------------------|--------------|---------------|-----------------|------------------|
| | | | SOCR | TCR | STCR | CHR | SDR | SOCR | TCR | STCR | CHR | SDR |
| <i>Small-scale instances</i> | | | | | | | | | | | | |
| LMBD3_50 | 317.38 | 317.38 | 0.00 | 0.00 | 0.00 | 0.00 | 0.00 | 0.05 | 0.06 | 0.06 | 0.05 | 0.06 |
| LMBD3_60 | 316.75 | 316.75 | 0.01 | 0.00 | 0.00 | 0.00 | 0.00 | 0.05 | 0.05 | 0.07 | 0.05 | 0.06 |
| case5 | 1 001.06 | 1 001.06 | 0.00 | 0.00 | 0.00 | 0.00 | 0.00 | 0.08 | 0.10 | 0.09 | 0.09 | 0.09 |
| case6ww | 216.84 | 216.84 | 0.16 | 0.00 | 0.00 | 0.00 | 0.00 | 0.06 | 0.07 | 0.06 | 0.08 | 0.06 |
| case9 | 317.32 | 317.32 | 0.00 | 0.00 | 0.00 | 0.00 | 0.00 | 0.07 | 0.07 | 0.07 | 0.07 | 0.07 |
| case14 | 259.55 | 259.55 | 0.00 | 0.00 | 0.00 | 0.00 | 0.00 | 0.07 | 0.07 | 0.07 | 0.06 | 0.05 |
| case24_ieee_rts | 2 875.75 | 2 875.74 | 0.01 | 0.00 | 0.00 | 0.00 | 0.00 | 0.10 | 0.14 | 0.14 | 0.12 | 0.16 |
| case30 | 191.09 | 191.09 | 0.23 | 0.01 | 0.00 | 0.00 | 0.00 | 0.08 | 0.13 | 0.15 | 0.10 | 0.18 |
| case_ieee30 | 284.77 | 284.77 | 0.05 | 0.00 | 0.00 | 0.00 | 0.00 | 0.07 | 0.09 | 0.09 | 0.08 | 0.27 |
| case39 | 6 284.15 | 6 283.90 | 0.01 | 0.00 | 0.00 | 0.00 | 0.00 | 0.09 | 0.19 | 0.18 | 0.12 | 0.22 |
| case57 | 1 262.10 | 1 262.10 | 0.03 | 0.00 | 0.00 | 0.00 | 0.00 | 0.08 | 0.14 | 0.16 | 0.15 | 0.21 |
| case89pegase | 5 819.81 | 5 819.65 | 0.17 | 0.04 | 0.00 | 0.00 | 0.00 | 0.16 | 0.68 | 0.83 | 0.90 | 1.08 |
| Average | | | 0.09 | 0.01 | 0.00 | 0.00 | 0.00 | 0.10 | 0.29 | 0.33 | 0.34 | 0.44 |
| <i>Medium-scale instances</i> | | | | | | | | | | | | |
| case118 | 4 251.23 | 4 251.03 | 0.01 | 0.01 | 0.00 | 0.00 | 0.00 | 0.09 | 0.31 | 0.35 | 0.25 | 0.83 |
| case_ACTIV_SG_200 | 1 483.92 | 1 483.92 | 0.01 | 0.00 | 0.00 | 0.00 | 0.00 | 0.19 | 0.52 | 0.65 | 0.56 | 4.07 |
| case_illinois200 | 2 246.49 | 2 246.48 | 0.01 | 0.00 | 0.00 | 0.00 | 0.00 | 0.25 | 0.79 | 0.90 | 0.83 | 5.80 |
| case300 | 23 737.72 | 23 737.55 | 0.06 | 0.01 | 0.01 | 0.00 | 0.00 | 0.19 | 0.91 | 1.05 | 0.86 | 9.93 |
| case_ACTIV_SG_500 | 7 817.46 | 7 817.41 | 0.02 | 0.00 | 0.00 | 0.00 | 0.00 | 0.75 | 4.04 | 5.03 | 3.75 | 127.07 |
| Average | | | 0.02 | 0.00 | 0.00 | 0.00 | 0.00 | 0.40 | 1.97 | 2.41 | 1.85 | 52.04 |
| <i>Large-scale instances</i> | | | | | | | | | | | | |
| case1354pegase | 74 069.35 | 74 061.72 | 0.08 | 0.02 | 0.02 | 0.01 | 0.01 | 5.73 | 6.34 | 13.23 | 9.72 | 1 657.85 |
| case1888rte | 59 805.1 | 59 601.29 | 0.39 | 0.36 | 0.35 | 0.34 | 0.34 | 8.88 | 10.61 | 26.64 | 17.88 | 4 629.31 |
| case1951rte | 81 737.7 | 81 725.16 | 0.08 | 0.03 | 0.03 | 0.01 | 0.02 | 11.24 | 12.49 | 31.78 | 23.31 | 5 595.59 |
| case2383wp | 24 991.40 | 24 979.30 | 0.21 | 0.07 | 0.07 | 0.05 | 0.05 | 10.83 | 10.88 | 32.25 | 188.90 | 7 758.35 |
| case2736sp | 18 335.95 | 18 334.71 | 0.19 | 0.03 | 0.02 | 0.01 | 0.01 | 9.27 | 11.01 | 31.96 | 290.60 | 10 768.88 |
| case2737sop | 11 397.39 | 11 396.61 | 0.18 | 0.02 | 0.01 | 0.01 | 0.01 | 8.46 | 11.38 | 29.65 | 216.13 | 9 715.82 |
| case2746wop | 19 212.35 | 19 211.42 | 0.21 | 0.03 | 0.02 | 0.01 | 0.00 | 10.15 | 11.26 | 30.92 | 320.35 | 9 093.47 |
| case2746wp | 25 269.45 | 25 268.43 | 0.19 | 0.03 | 0.01 | 0.00 | 0.01 | 10.76 | 12.34 | 33.78 | 336.99 | 11 785.35 |
| case2848rte | 53 021.8 | 53 005.20 | 0.08 | 0.04 | 0.04 | 0.03 | 0.04 | 12.17 | 14.36 | 44.56 | 46.64 | 14 567.98 |
| case2868rte | 79 794.7 | 79 787.67 | 0.07 | 0.02 | 0.02 | 0.01 | 0.02 | 14.05 | 17.03 | 55.08 | 47.20 | 16 933.60 |
| case2869pegase | 133 999.29 | 133 983.11 | 0.09 | 0.03 | 0.03 | 0.01 | 0.03 | 15.45 | 18.76 | 60.18 | 49.29 | 14 866.00 |
| case3012wp | 27 645.97 | 27 637.25 | 0.22 | 0.05 | 0.04 | 0.04 | 0.03 | 16.80 | 17.57 | 55.82 | 1 448.81 | 17 689.12 |
| case3120sp | 21 513.52 | 21 495.85 | 0.24 | 0.10 | 0.09 | 0.09 | 0.08 | 15.08 | 17.09 | 58.92 | 830.41 | 15 981.61 |
| case3375wp | 49 004.69 | 48 995.70 | 0.15 | 0.04 | 0.03 | 0.02 | 0.03 | 15.07 | 16.85 | 70.58 | 1 229.45 | 17 306.68 |
| Average | | | 0.17 | 0.06 | 0.05 | 0.04 | 0.04 | 12.17 | 13.97 | 43.70 | 416.32 | 12 230.42 |
| <i>Extra large-scale instances</i> | | | | | | | | | | | | |
| case6468rte | 86 860.0 | 86 808.12 | 0.27 | 0.08 | 0.08 | 0.06 | – | 35.47 | 40.79 | 314.92 | 1 990.53 | – |
| case6470rte | 98 345.5 | 98 333.90 | 0.18 | 0.06 | 0.03 | 0.01 | – | 53.34 | 51.88 | 371.42 | 2 729.29 | – |
| case6495rte | 106 283.4 | 106 072.44 | 0.46 | 0.23 | 0.23 | 0.20 | – | 50.50 | 65.15 | 431.65 | 3 592.15 | – |
| case6515rte | 109 804.2 | 109 688.71 | 0.38 | 0.16 | 0.14 | 0.11 | – | 48.02 | 59.60 | 427.22 | 3 523.01 | – |
| Average | | | 0.32 | 0.13 | 0.12 | 0.09 | – | 46.84 | 54.38 | 386.42 | 2 960.41 | – |

CHAPITRE 5 ARTICLE 2: TIGHT-AND-CHEAP CONIC RELAXATION FOR THE OPTIMAL REACTIVE POWER DISPATCH PROBLEM

Christian Bingane, Miguel F. Anjos, and Sébastien Le Digabel. Tight-and-cheap conic relaxation for the optimal reactive power dispatch problem. IEEE Transactions on Power Systems, 2019.

Abstract: The optimal reactive power dispatch (ORPD) problem is an alternating current optimal power flow (ACOPF) problem where discrete control devices for regulating the reactive power, such as shunt elements and tap changers, are considered. The ORPD problem is modelled as a mixed-integer nonlinear optimization problem and its complexity is increased compared to the ACOPF problem, which is highly nonconvex and generally hard to solve. Recently, convex relaxations of the ACOPF problem have attracted a significant interest since they can lead to global optimality. We propose a tight conic relaxation of the ORPD problem and show that a round-off technique applied with this relaxation leads to near-global optimal solutions with very small guaranteed optimality gaps, unlike with the nonconvex continuous relaxation. We report computational results on selected MATPOWER test cases with up to 3375 buses.

Keywords: Conic optimization, discrete variables, optimal power flow, power systems, semidefinite programming.

5.1 Nomenclature

5.1.1 Notations

| | |
|-------------------------|---|
| \mathbb{R}/\mathbb{C} | Set of real/complex numbers, |
| \mathbb{H}^n | Set of $n \times n$ Hermitian matrices, |
| j | Imaginary unit, |
| a/a | Real/complex number, |
| \mathbf{a}/\mathbf{a} | Real/complex vector, |
| A/A | Real/complex matrix. |

5.1.2 Operators

| | |
|-------------------------------------|--|
| $\text{Re}(\cdot)/\text{Im}(\cdot)$ | Real/imaginary part operator, |
| $(\cdot)^*$ | Conjugate operator, |
| $ \cdot $ | Magnitude or cardinality set operator, |

| | |
|-----------------|-------------------------------|
| $\angle(\cdot)$ | Phase operator, |
| $(\cdot)^H$ | Conjugate transpose operator. |

5.1.3 Input data

| | |
|---|---|
| $\mathcal{P} = (\mathcal{N}, \mathcal{L})$ | Power network, |
| \mathcal{N} | Set of buses, |
| $\mathcal{U} \subseteq \mathcal{N}$ | Set of buses k where a shunt element is connected, |
| $\mathcal{G} = \bigcup_{k \in \mathcal{N}} \mathcal{G}_k$ | Set of generators, |
| \mathcal{G}_k | Set of generators connected to bus k , |
| \mathcal{L} | Set of branches, |
| $\mathcal{T} \subseteq \mathcal{L}$ | Set of branches with tap changers, |
| p_{Dk}/q_{Dk} | Active/reactive power demand at bus k , |
| g'_k/b'_k | Conductance/susceptance of shunt element at bus k , |
| c_{g2}, c_{g1}, c_{g0} | Generation cost coefficients of generator g , |
| $y_\ell^{-1} = r_\ell + jx_\ell$ | Series impedance of branch ℓ , |
| b'_ℓ | Total shunt susceptance of branch ℓ . |

5.1.4 Variables

| | |
|-----------------------|---|
| p_{Gg}/q_{Gg} | Active/reactive power generation by generator g , |
| v_k | Complex (phasor) voltage at bus k , |
| u_k | Shunt variable corresponding to the shunt element connected at bus k , |
| $p_{f\ell}/q_{f\ell}$ | Active/reactive power flow injected along branch ℓ by its <i>from</i> end, |
| $p_{t\ell}/q_{t\ell}$ | Active/reactive power flow injected along branch ℓ by its <i>to</i> end, |
| t_ℓ | Turns ratio of tap changer ℓ . |

5.2 Introduction

The optimal power flow (OPF) problem, first formulated in [27], consists in finding a network operating point that optimizes an objective function subject to power flow equations and other operational constraints [15, 16, 28, 58]. The continuous version with AC power flow equations, also called AC optimal power flow (ACOPF) problem, is nonconvex and NP-hard [29, 30]. The optimal reactive power dispatch (ORPD) problem, also known as Volt/VAR optimization problem, can be seen as an ACOPF problem with discrete control devices for regulating the reactive power such as shunt elements and tap changers [59, 60]. Because of the presence of discrete variables, the ORPD problem is generally more difficult than the ACOPF.

A mixed-integer nonlinear program (MINLP) is an optimization problem which involves both continuous and integer variables and whose objective function and feasible set are described by nonlinear functions [21]. A MINLP is said to be *convex* if its continuous relaxation, i.e., the problem obtained by dropping the integrality constraints, is a convex optimization problem; otherwise, it is said to be *nonconvex*. MINLPs inherit difficulties from nonlinear programs (NLPs) and mixed-integer linear programs (MILPs) since they are a generalization of both classes. In fact, there exist simple cases of nonconvex MINLPs which are not only NP-hard, but even undecidable. See more details in [22, 23].

Recently, convex relaxations of the ACOPF problem, in particular second-order cone programming (SOCP) [17], semidefinite programming (SDP) [18], and quadratic convex (QC) [61] relaxations, have attracted a significant interest for several reasons. First, they can lead to global optimality; second, because they are relaxations, they provide a bound on the global optimal value of the ACOPF problem; and third, if one of these relaxations is infeasible, then the ACOPF problem is infeasible. Mixed-integer QC relaxations were proposed in [34] and mixed-integer SOCP relaxations in [62–64] for MINLPs in power systems. However, [58] emphasized that convex relaxations of the OPF problem are aimed at complementing nonconvex (local) solvers with the valuable information about the quality of the solution obtained, rather than at replacing them.

Moreover, several applications of OPF are multi-period problems by nature due to factors such as changing market prices, ramping limits of generation units, and demand behavior [65]. Extending a convex relaxation from a single-period OPF problem to a multi-period one may jeopardize its exactness. This is discussed in [26] where a tight convex relaxation for the multi-period case is proposed.

On the other hand, some heuristic techniques discussed in [66] have been proposed for handling discrete variables in the OPF problem. One approach works as follows: first, solve the continuous relaxation of the OPF problem, i.e., treat the discrete variables as continuous; second, round-off solutions corresponding to discrete variables to their nearest discrete values; and third, fix discrete variables to these values and then solve the corresponding OPF subproblem. This approach is called the *round-off technique* and remains the simplest to deal with discrete variables in the ORPD problem, although it may lead to poor suboptimal solutions or infeasible ones. Some deficiencies were already pointed out in [67]: for instance, since the OPF problem is in general highly nonconvex, solving its continuous relaxation with a local optimizer in the first step may lead to a poor local solution which, after round-off in the second step, may lead to a very poor solution in the third step. More discussion about the round-off strategy can be found in [58, 60].

The main contribution of this paper is to show that a round-off technique used with a tight convex continuous relaxation may lead to near-global optimal solutions of the ORPD problem. This

contribution is in two parts. First, we propose SDP-based relaxations of the ORPD problem with a new tight convex model of tap changer; second, a modified round-off technique where, in the first step, we solve a SDP-based relaxation instead of the nonconvex continuous relaxation of the ORPD problem. More details about semidefinite optimization can be found in [4]. Computational results show that the SDP-based relaxations of the ORPD problem are tight, and furthermore that applying the round-off technique with these relaxations leads to near-global solutions, even for large-scale instances. To the best of our knowledge, it is the first time that extensive computations with this approach are carried out for the ORPD problem with large-scale meshed networks.

The remainder of this paper is organized as follows. In Section 5.3, we state the mathematical model of the ORPD problem. In Section 5.4, we describe two SDP-based relaxations of the ORPD problem: a simple one already proposed in [68] and a new tighter one. In Section 5.5, we present our round-off technique, and we report computational results in Section 5.6. Section 5.7 concludes the paper.

5.3 ORPD: Formulation

Consider a typical power network $\mathcal{P} = (\mathcal{N}, \mathcal{L})$ where $\mathcal{N} = \{1, 2, \dots, n\}$ and $\mathcal{L} \subseteq \mathcal{N} \times \mathcal{N}$ denote respectively the set of buses and the set of branches (transmission lines and tap changers). We denote by $\mathcal{U} \subseteq \mathcal{N}$ the set of buses k where a shunt element is connected, and $\mathcal{T} \subseteq \mathcal{L}$ the set of branches with tap changers. Each branch $\ell \in \mathcal{L}$ has a *from* end k (on the *tap* side) and a *to* end m as modeled in [40]. We denote $\ell = (k, m)$. The ORPD problem is given as:

$$\min f(\mathbf{u}, \mathbf{t}, \mathbf{p}_G, \mathbf{q}_G, \mathbf{p}_f, \mathbf{q}_f, \mathbf{p}_t, \mathbf{q}_t, \mathbf{v}) \quad (5.1a)$$

over variables $\mathbf{u} \in \{0, 1\}^{|\mathcal{U}|}$, $\mathbf{t} \in \mathbb{R}^{|\mathcal{T}|}$, $\mathbf{p}_G, \mathbf{q}_G \in \mathbb{R}^{|\mathcal{G}|}$, $\mathbf{p}_f, \mathbf{q}_f, \mathbf{p}_t, \mathbf{q}_t \in \mathbb{R}^{|\mathcal{L}|}$, and $\mathbf{v} \in \mathbb{C}^{|\mathcal{N}|}$, subject to

— Power balance equations:

$$\sum_{g \in \mathcal{G}_k} p_{Gg} - p_{Dk} - g'_k u_k |v_k|^2 = \sum_{\ell=(k,m) \in \mathcal{L}} p_{f\ell} + \sum_{\ell=(m,k) \in \mathcal{L}} p_{t\ell} \quad \forall k \in \mathcal{U}, \quad (5.1b)$$

$$\sum_{g \in \mathcal{G}_k} q_{Gg} - q_{Dk} + b'_k u_k |v_k|^2 = \sum_{\ell=(k,m) \in \mathcal{L}} q_{f\ell} + \sum_{\ell=(m,k) \in \mathcal{L}} q_{t\ell} \quad \forall k \in \mathcal{U}, \quad (5.1c)$$

$$\sum_{g \in \mathcal{G}_k} p_{Gg} - p_{Dk} = \sum_{\ell=(k,m) \in \mathcal{L}} p_{f\ell} + \sum_{\ell=(m,k) \in \mathcal{L}} p_{t\ell} \quad \forall k \in \mathcal{N} \setminus \mathcal{U}, \quad (5.1d)$$

$$\sum_{g \in \mathcal{G}_k} q_{Gg} - q_{Dk} = \sum_{\ell=(k,m) \in \mathcal{L}} q_{f\ell} + \sum_{\ell=(m,k) \in \mathcal{L}} q_{t\ell} \quad \forall k \in \mathcal{N} \setminus \mathcal{U}, \quad (5.1e)$$

— Branch flow equations:

$$p_{f\ell} + jq_{f\ell} = \frac{v_k}{t_\ell} \left[\left(j \frac{b'_\ell}{2} + y_\ell \right) \frac{v_k}{t_\ell} - y_\ell v_m \right]^* \quad \forall \ell = (k, m) \in \mathcal{T}, \quad (5.1f)$$

$$p_{t\ell} + jq_{t\ell} = v_m \left[-y_\ell \frac{v_k}{t_\ell} + \left(j \frac{b'_\ell}{2} + y_\ell \right) v_m \right]^* \quad \forall \ell = (k, m) \in \mathcal{T}, \quad (5.1g)$$

$$p_{f\ell} + jq_{f\ell} = v_k \left[\left(j \frac{b'_\ell}{2} + y_\ell \right) v_k - y_\ell v_m \right]^* \quad \forall \ell = (k, m) \in \mathcal{L} \setminus \mathcal{T}, \quad (5.1h)$$

$$p_{t\ell} + jq_{t\ell} = v_m \left[-y_\ell v_k + \left(j \frac{b'_\ell}{2} + y_\ell \right) v_m \right]^* \quad \forall \ell = (k, m) \in \mathcal{L} \setminus \mathcal{T}, \quad (5.1i)$$

— Generator power capacities:

$$\underline{p}_{Gg} \leq p_{Gg} \leq \bar{p}_{Gg}, \quad \underline{q}_{Gg} \leq q_{Gg} \leq \bar{q}_{Gg} \quad \forall g \in \mathcal{G}, \quad (5.1j)$$

— Line thermal limits:

$$|p_{f\ell} + jq_{f\ell}| \leq \bar{s}_\ell, \quad |p_{t\ell} + jq_{t\ell}| \leq \bar{s}_\ell \quad \forall \ell \in \mathcal{L}, \quad (5.1k)$$

— Voltage magnitude limits:

$$\underline{v}_k \leq |v_k| \leq \bar{v}_k \quad \forall k \in \mathcal{N}, \quad (5.1l)$$

— Reference bus constraint:

$$\angle v_1 = 0, \quad (5.1m)$$

— Shunt variable:

$$u_k \in \{0, 1\} \quad \forall k \in \mathcal{U}, \quad (5.1n)$$

— Tap ratio constraint:

$$t_\ell \in \{\underline{t}_\ell, \dots, \bar{t}_\ell\} \quad \forall \ell \in \mathcal{T}. \quad (5.1o)$$

Constraints (5.1b)–(5.1i) derive from Kirchhoff's laws and represent power flow equations in the network. We assume $\underline{v}_k > 0$ for all $k \in \mathcal{N}$ in (5.1l) and $\underline{t}_\ell > 0$ for all $\ell \in \mathcal{T}$ in (5.1o). Constraint (5.1m) specifies bus $k = 1$ as the reference bus. In (5.1n), we assume that the shunt connected to a bus $k \in \mathcal{U}$ has an on/off switch. For all $\ell \in \mathcal{T}$, the tap ratio t_ℓ in (5.1o) is a discrete variable that typically takes on $2\bar{\eta} + 1$ values $\{\hat{t}_{-\bar{\eta}}, \dots, \hat{t}_0, \dots, \hat{t}_{\bar{\eta}}\}$, uniformly distributed around \hat{t}_0 . In this paper, we assume without loss of generality that \hat{t}_ℓ varies between 0.9 and 1.1 pu with steps of 0.0125 pu (17 different settings) for all $\ell \in \mathcal{T}$.

The objective function $f(\mathbf{u}, \mathbf{t}, \mathbf{p}_G, \mathbf{q}_G, \mathbf{p}_f, \mathbf{q}_f, \mathbf{p}_t, \mathbf{q}_t, \mathbf{v})$ in (5.1a) may represent any objective function related to the ORPD problem: power loss, voltage deviation, number of control actions,

generation cost, etc. Some of them are considered in [69]. We note that power loss is a widely used objective function for the ORPD problem. However, according to [28], just minimizing loss is inconsistent with economic principles and may result in suboptimal dispatch while minimizing cost would be the correct objective function for economically dispatching resources and would inherently meet the objective of minimizing loss. Recently, [60] considered minimizing generation cost instead of power loss in their formulation of the ORPD problem. In this work, we consider both cost minimization and loss minimization in our computational results. We also assume that (5.1a) is a convex function, and then relaxations proposed in this paper remain valid for any convex objective function related to the ORPD problem.

5.4 ORPD: Convexification

In this section, we describe two semidefinite relaxations of the ORPD problem: a simple one (SDR1) already proposed in [68] and a new tighter one (SDR2). SDR2 is obtained by combining SDR1 with a new tight convex model of tap changer and we show that SDR2 is then stronger than SDR1. Since both SDR1 and SDR2 can be expensive to solve for large-scale instances, we derive from them two relaxations that are cheaper to solve: TCR1 and TCR2 respectively.

5.4.1 Semidefinite relaxation 1 (SDR1)

Let

$$\mathbf{V} := \mathbf{v}\mathbf{v}^H, \quad (5.2a)$$

$$\mathbf{W}_{\{\ell\}} := \begin{bmatrix} V_{kk} & W_{k\ell} & V_{km} \\ W_{k\ell}^* & W_{\ell\ell} & W_{\ell m} \\ V_{km}^* & W_{\ell m}^* & V_{mm} \end{bmatrix} = \begin{bmatrix} v_k \\ w_\ell \\ v_m \end{bmatrix} \begin{bmatrix} v_k \\ w_\ell \\ v_m \end{bmatrix}^H \quad \forall \ell = (k, m) \in \mathcal{T}, \quad (5.2b)$$

$$w_\ell := \frac{v_k}{t_\ell} \quad \forall \ell = (k, m) \in \mathcal{T}. \quad (5.2c)$$

The ORPD problem (5.1) can be reformulated as follows

min (5.1a)

s. t. (5.1d), (5.1e), (5.1j), (5.1k), (5.1m), (5.1n), (5.1o),

(5.2a), (5.2b), (5.2c),

$$\sum_{g \in \mathcal{G}_k} p_{Gg} - p_{Dk} - g'_k u_k V_{kk} = \sum_{\ell=(k,m) \in \mathcal{L}} p_{f\ell} + \sum_{\ell=(m,k) \in \mathcal{L}} p_{t\ell} \quad \forall k \in \mathcal{U}, \quad (5.3a)$$

$$\sum_{g \in \mathcal{G}_k} q_{Gg} - q_{Dk} + b'_k u_k V_{kk} = \sum_{\ell=(k,m) \in \mathcal{L}} q_{f\ell} + \sum_{\ell=(m,k) \in \mathcal{L}} q_{t\ell} \quad \forall k \in \mathcal{U}, \quad (5.3b)$$

$$p_{f\ell} + jq_{f\ell} = \left(-j\frac{b'_\ell}{2} + y_\ell^*\right) W_{\ell\ell} - y_\ell^* W_{\ell m} \quad \forall \ell = (k, m) \in \mathcal{T}, \quad (5.3c)$$

$$p_{t\ell} + jq_{t\ell} = -y_\ell^* W_{\ell m}^* + \left(-j\frac{b'_\ell}{2} + y_\ell^*\right) V_{mm} \quad \forall \ell = (k, m) \in \mathcal{T}, \quad (5.3d)$$

$$p_{f\ell} + jq_{f\ell} = \left(-j\frac{b'_\ell}{2} + y_\ell^*\right) V_{kk} - y_\ell^* V_{km} \quad \forall \ell = (k, m) \in \mathcal{L} \setminus \mathcal{T}, \quad (5.3e)$$

$$p_{t\ell} + jq_{t\ell} = -y_\ell^* V_{km}^* + \left(-j\frac{b'_\ell}{2} + y_\ell^*\right) V_{mm} \quad \forall \ell = (k, m) \in \mathcal{L} \setminus \mathcal{T}, \quad (5.3f)$$

$$\underline{v}_k^2 \leq V_{kk} \leq \bar{v}_k^2 \quad \forall k \in \mathcal{N}. \quad (5.3g)$$

If we define $\xi_k := u_k V_{kk} \in \{0, V_{kk}\}$ for all $k \in \mathcal{U}$, a linear formulation of (5.3a)–(5.3b) is given as

$$\sum_{g \in \mathcal{G}_k} p_{Gg} - p_{Dk} - g'_k \xi_k = \sum_{\ell=(k,m) \in \mathcal{L}} p_{f\ell} + \sum_{\ell=(m,k) \in \mathcal{L}} p_{t\ell} \quad \forall k \in \mathcal{U}, \quad (5.4a)$$

$$\sum_{g \in \mathcal{G}_k} q_{Gg} - q_{Dk} + b'_k \xi_k = \sum_{\ell=(k,m) \in \mathcal{L}} q_{f\ell} + \sum_{\ell=(m,k) \in \mathcal{L}} q_{t\ell} \quad \forall k \in \mathcal{U}, \quad (5.4b)$$

$$0 \leq \xi_k \leq V_{kk} \quad \forall k \in \mathcal{U}. \quad (5.4c)$$

From (5.2b) and (5.2c), we have

$$W_{k\ell} = \frac{V_{kk}}{t_\ell} \quad \forall \ell = (k, m) \in \mathcal{T}, \quad (5.5a)$$

$$W_{\ell\ell} = \frac{V_{kk}}{t_\ell^2} \quad \forall \ell = (k, m) \in \mathcal{T}, \quad (5.5b)$$

which implies

$$\frac{V_{kk}}{\bar{t}_\ell} \leq W_{k\ell} \leq \frac{V_{kk}}{\underline{t}_\ell} \quad \forall \ell = (k, m) \in \mathcal{T}, \quad (5.6a)$$

$$\frac{V_{kk}}{\bar{t}_\ell^2} \leq W_{\ell\ell} \leq \frac{V_{kk}}{\underline{t}_\ell^2} \quad \forall \ell = (k, m) \in \mathcal{T}, \quad (5.6b)$$

since $0 < \underline{t}_\ell \leq t_\ell \leq \bar{t}_\ell$ for all $\ell \in \mathcal{T}$. Finally, we can show that V in (5.2a) and, for all $\ell \in \mathcal{T}$, $W_{\{\ell\}}$ in (5.2b) are rank-one positive semidefinite matrices. The *semidefinite relaxation 1* (SDR1) in Model 7 is obtained by dropping the rank constraints. For all $\ell = (k, m) \in \mathcal{T}$, since $W_{\{\ell\}} \succeq 0$ implies $W_{k\ell}^2 \leq V_{kk} W_{\ell\ell}$, (5.6) can be rewritten as

$$W_{k\ell} \geq \frac{V_{kk}}{\bar{t}_\ell} \quad \forall \ell = (k, m) \in \mathcal{T}, \quad (5.7a)$$

$$W_{\ell\ell} \leq \frac{V_{kk}}{\underline{t}_\ell^2} \quad \forall \ell = (k, m) \in \mathcal{T}. \quad (5.7b)$$

 Model 7 Semidefinite relaxation 1 (SDR1)

Variables:

$$\boldsymbol{\xi} \in \mathbb{R}^{|\mathcal{U}|}, \quad (5.8a)$$

$$\mathbf{p}_G, \mathbf{q}_G \in \mathbb{R}^{|\mathcal{G}|}, \quad (5.8b)$$

$$\mathbf{p}_f, \mathbf{q}_f, \mathbf{p}_t, \mathbf{q}_t \in \mathbb{R}^{|\mathcal{L}|}, \quad (5.8c)$$

$$\mathbf{V} \in \mathbb{H}^{|\mathcal{M}|}, \quad (5.8d)$$

$$(\mathbf{W}_{\ell\ell}, \mathbf{W}_{k\ell}, \mathbf{W}_{\ell m}) \in \mathbb{R} \times \mathbb{R} \times \mathbb{C} \quad \forall \ell = (k, m) \in \mathcal{T}. \quad (5.8e)$$

Minimize: (5.1a)

Subject to: (5.1d), (5.1e), (5.1j), (5.1k), (5.3c)–(5.3g), (5.4), (5.7), $\mathbf{V} \succeq 0$, and $\mathbf{W}_{\{\ell\}} \succeq 0 \forall \ell \in \mathcal{T}$.

We point out that the variables u_k and t_ℓ are eliminated in Model 7 for all $k \in \mathcal{U}$ and for all $\ell \in \mathcal{T}$. This approach was already proposed in [68] and was recently used in [70]. Once the solution of Model 7 is obtained, the optimal value \hat{u}_k of the shunt element connected to a bus $k \in \mathcal{U}$ and the optimal tap ratio \hat{t}_ℓ of a transformer $\ell = (k, m) \in \mathcal{T}$ can be determined respectively as follows:

$$\hat{u}_k = \frac{\xi_k}{V_{kk}} \in [0, 1], \quad (5.9a)$$

$$\hat{t}_\ell = \sqrt{\frac{V_{kk}}{W_{\ell\ell}}} \in [\underline{t}_\ell, \bar{t}_\ell]. \quad (5.9b)$$

If the optimal solutions $\hat{\mathbf{V}}$ and $\hat{\mathbf{W}}_{\{\ell\}}$ for all $\ell \in \mathcal{T}$ are rank-one matrices, $\hat{u}_k \in \{0, 1\}$ for all $k \in \mathcal{U}$, and $\hat{t}_\ell \in \{\underline{t}_\ell, \dots, \bar{t}_\ell\}$ for all $\ell \in \mathcal{T}$, then there exists a complex vector $\hat{\mathbf{v}}$ that is a global optimal solution of (5.1). We say that the relaxation SDR1 is exact.

We also consider a cheaper relaxation, called “*tight-and-cheap relaxation I*”, given in Model 8 and obtained as follows. We replace $\mathbf{V} \succeq 0$ and $\mathbf{W}_{\{\ell\}} \succeq 0$ for all $\ell \in \mathcal{T}$ in Model 7 by

$$\begin{bmatrix} 1 & \mathbf{v}_k^* & \mathbf{v}_m^* \\ \mathbf{v}_k & V_{kk} & V_{km} \\ \mathbf{v}_m & V_{km}^* & V_{mm} \end{bmatrix} \succeq 0 \quad \forall \ell = (k, m) \in \mathcal{L} \setminus \mathcal{T}, \quad (5.10a)$$

$$\begin{bmatrix} 1 & \mathbf{w}_{\{\ell\}}^H \\ \mathbf{w}_{\{\ell\}} & W_{\{\ell\}} \end{bmatrix} \succeq 0 \quad \forall \ell = (k, m) \in \mathcal{T}, \quad (5.10b)$$

where $\mathbf{w}_{\{\ell\}}^H = (v_k^*, w_\ell^*, v_m^*)$ for all $\ell = (k, m) \in \mathcal{T}$, and we add the following constraints

$$\operatorname{Re}(v_1) \geq \frac{V_{11} + v_1 \bar{v}_1}{v_1 + \bar{v}_1}, \quad (5.10c)$$

$$\operatorname{Im}(v_1) = 0, \quad (5.10d)$$

corresponding to the reference bus $k = 1$.

Model 8 Tight-and-cheap relaxation 1 (TCR1)

Variables: (5.8), $\mathbf{v} \in \mathbb{C}^{|\mathcal{N}|}$, $\mathbf{w} \in \mathbb{C}^{|\mathcal{T}|}$.

Minimize: (5.1a)

Subject to: (5.1d), (5.1e), (5.1j), (5.1k), (5.3c)–(5.3g), (5.4), (5.6), (5.10).

The tight-and-cheap relaxation (TCR) was first proposed in [24] for the ACOPF problem. It was shown in [24] that TCR is stronger than the standard SOCP relaxation and nearly as tight as the standard SDP relaxation. Moreover, computation experiments on standard test cases with up to 6515 buses showed that solving TCR for large-scale instances is much less expensive than solving the chordal relaxation, a SDP relaxation technique that exploits the sparsity of power networks.

5.4.2 Semidefinite relaxation 2 (SDR2)

For all $\ell = (k, m) \in \mathcal{T}$, variables $W_{k\ell}$ and $W_{\ell\ell}$ in (5.5) are respectively described by constraints of the form $z_n = x/y^n$, $n = 1, 2$. Consider the set

$$\mathcal{S}_1 = \{(x, y, z_1, z_2) \in \mathbb{R}^4 : \underline{x} \leq x \leq \bar{x}, \underline{y} \leq y \leq \bar{y}, z_1 = x/y, z_2 = x/y^2\},$$

where $0 < \underline{x} < \bar{x}$ and $0 < \underline{y} < \bar{y}$. We can show that \mathcal{S}_1 is equivalent to

$$\mathcal{S}_2 = \{(x, z_1, z_2) \in \mathbb{R}^3 : z_2 = z_1^2/x, (x, z_1) \in \Omega\},$$

where $\Omega = \{(x, z_1) \in \mathbb{R}^2 : \underline{x} \leq x \leq \bar{x}, x/\bar{y} \leq z_1 \leq x/\underline{y}\}$ is the convex quadrilateral with vertices $(\underline{x}, \underline{x}/\bar{y})$, $(\bar{x}, \bar{x}/\bar{y})$, $(\bar{x}, \bar{x}/\underline{y})$, and $(\underline{x}, \underline{x}/\underline{y})$.

In Section 5.4.1, the proposed convex set that contains \mathcal{S}_2 is

$$\mathcal{S}_3 = \{(x, z_1, z_2) \in \mathbb{R}^3 : \underline{x} \leq x \leq \bar{x}, z_2 \geq z_1^2/x, z_1 \geq x/\bar{y}, z_2 \leq x/\underline{y}\}.$$

In this section, we propose a tighter convex set containing \mathcal{S}_2 .

Lemma 3. Let $f(x, z_1) = z_1^2/x$ defined over $\mathbb{R}_+ \times \mathbb{R}$. Then f is convex.

Proof. For all $(x, z_1) \in \mathbb{R}_+ \times \mathbb{R}$,

$$\nabla^2 f(x, z_1) = \frac{2}{x^3} \begin{bmatrix} z_1^2 & -xz_1 \\ -xz_1 & x^2 \end{bmatrix} = \frac{2}{x^3} \begin{bmatrix} z_1 \\ -x \end{bmatrix} \begin{bmatrix} z_1 \\ -x \end{bmatrix}^T \succeq 0.$$

Then f is convex. □

Lemma 4. Let $(x, z_1) \in \Omega$. If $z_2 = z_1^2/x$, then $x + \underline{y}z_2 \leq (\underline{y} + \bar{y})z_1$.

Proof. Let $(x, z_1) \in \Omega$ and $z_2 = z_1^2/x$. We have $x/\bar{y} \leq z_1 \leq x/\underline{y}$ with $0 < \underline{y} < \bar{y}$. Therefore, $(x - \underline{y}z_1)(x - \bar{y}z_1) \leq 0$. On the other hand,

$$(x - \underline{y}z_1)(x - \bar{y}z_1) = x^2 - (\underline{y} + \bar{y})xz_1 + \underline{y}\bar{y}z_1^2 = x[x - (\underline{y} + \bar{y})z_1 + \underline{y}\bar{y}z_2] \leq 0.$$

Since $x > 0$, it follows that $x - (\underline{y} + \bar{y})z_1 + \underline{y}\bar{y}z_2 \leq 0$. □

Proposition 5. Let $f(x, z_1) = z_1^2/x$ defined over Ω . The concave envelope or the tightest concave overestimator of f on Ω is $h(x, z_1) = \frac{1}{\underline{y}\bar{y}}[(\underline{y} + \bar{y})z_1 - x]$.

Proof. The function h is affine and, from Lemma 4, overestimates f on Ω . Then h is a concave overestimator of f on Ω . We note that $h(x, z_1) = f(x, z_1)$ for all $(x, z_1) \in \Omega$ such that $z_1 = x/\bar{y}$ or $z_1 = x/\underline{y}$.

Suppose that there exists a concave overestimator \tilde{h} of f on Ω such that $f(x, z_1) \leq \tilde{h}(x, z_1) \leq h(x, z_1)$ for all $(x, z_1) \in \Omega$ and $\tilde{h}(\tilde{x}, \tilde{z}_1) < h(\tilde{x}, \tilde{z}_1)$ for some $(\tilde{x}, \tilde{z}_1) \in \Omega$. Since Ω is the convex quadrilateral with vertices $(\underline{x}, \underline{x}/\bar{y})$, $(\bar{x}, \bar{x}/\bar{y})$, $(\bar{x}, \bar{x}/\underline{y})$, and $(\underline{x}, \underline{x}/\underline{y})$, there exist nonnegative scalars $\alpha_1, \alpha_2, \alpha_3$, and α_4 such that $\alpha_1 + \alpha_2 + \alpha_3 + \alpha_4 = 1$ and $(\tilde{x}, \tilde{z}_1) = \alpha_1(\underline{x}, \underline{x}/\bar{y}) + \alpha_2(\bar{x}, \bar{x}/\bar{y}) + \alpha_3(\bar{x}, \bar{x}/\underline{y}) + \alpha_4(\underline{x}, \underline{x}/\underline{y})$. Therefore,

$$\begin{aligned} \tilde{h}(\tilde{x}, \tilde{z}_1) &= \tilde{h}(\alpha_1(\underline{x}, \underline{x}/\bar{y}) + \alpha_2(\bar{x}, \bar{x}/\bar{y}) + \alpha_3(\bar{x}, \bar{x}/\underline{y}) + \alpha_4(\underline{x}, \underline{x}/\underline{y})) \\ &\geq \alpha_1\tilde{h}(\underline{x}, \underline{x}/\bar{y}) + \alpha_2\tilde{h}(\bar{x}, \bar{x}/\bar{y}) + \alpha_3\tilde{h}(\bar{x}, \bar{x}/\underline{y}) + \alpha_4\tilde{h}(\underline{x}, \underline{x}/\underline{y}) \\ &= \alpha_1f(\underline{x}, \underline{x}/\bar{y}) + \alpha_2f(\bar{x}, \bar{x}/\bar{y}) + \alpha_3f(\bar{x}, \bar{x}/\underline{y}) + \alpha_4f(\underline{x}, \underline{x}/\underline{y}) \\ &= \alpha_1h(\underline{x}, \underline{x}/\bar{y}) + \alpha_2h(\bar{x}, \bar{x}/\bar{y}) + \alpha_3h(\bar{x}, \bar{x}/\underline{y}) + \alpha_4h(\underline{x}, \underline{x}/\underline{y}) \\ &= h(\alpha_1(\underline{x}, \underline{x}/\bar{y}) + \alpha_2(\bar{x}, \bar{x}/\bar{y}) + \alpha_3(\bar{x}, \bar{x}/\underline{y}) + \alpha_4(\underline{x}, \underline{x}/\underline{y})) \\ &= h(\tilde{x}, \tilde{z}_1). \end{aligned}$$

The inequality follows from the definition of a concave function; the two subsequent equalities from the fact that h agrees with f at the vertices of Ω and $f(x, z_1) \leq \tilde{h}(x, z_1) \leq h(x, z_1)$ for all $(x, z_1) \in \Omega$;

and the last equality from the fact that h is affine. The relation obtained $\tilde{h}(\tilde{x}, \tilde{z}_1) \geq h(\tilde{x}, \tilde{z}_1)$ contradicts $\tilde{h}(\tilde{x}, \tilde{z}_1) < h(\tilde{x}, \tilde{z}_1)$. So h is the concave envelope of f on Ω . \square

A similar proof can be found in [71] on convex and concave envelopes of functions defined on convex quadrilaterals.

Proposition 6. *The convex hull of $\mathcal{S}_2 = \{(x, z_1, z_2) \in \mathbb{R}^3 : \underline{x} \leq x \leq \bar{x}, x/\bar{y} \leq z_1 \leq x/\underline{y}, z_2 = z_1^2/x\}$, where $0 < \underline{x} < \bar{x}, 0 < \underline{y} < \bar{y}$, is $\bar{\mathcal{S}}_2 = \{(x, z_1, z_2) \in \mathbb{R}^3 : \underline{x} \leq x \leq \bar{x}, z_1^2 \leq xz_2, x + \underline{y}\bar{y}z_2 \leq (\underline{y} + \bar{y})z_1\}$.*

Proof. The result follows from Lemma 3 and Proposition 5. \square

Applying Proposition 6 to (5.5), we replace (5.7) in Model 7 by

$$V_{kk} + \underline{t}_\ell \bar{t}_\ell W_{\ell\ell} \leq (\underline{t}_\ell + \bar{t}_\ell)W_{k\ell} \quad \forall \ell = (k, m) \in \mathcal{T}, \quad (5.12)$$

and define a new formulation of SDP relaxation in Model 9. We will refer to this relaxation as “semidefinite relaxation 2” (SDR2). The “tight-and-cheap relaxation 2” is given in Model 10. From Proposition 6, $\bar{\mathcal{S}}_2 \subset \mathcal{S}_3$ and then SDR2 (respectively TCR2) is stronger than SDR1 (TCR1).

Model 9 Semidefinite relaxation 2 (SDR2)

Variables: (5.8).

Minimize: (5.1a)

Subject to: (5.1d), (5.1e), (5.1j), (5.1k), (5.3c)–(5.3g), (5.4), (5.12), $V \succeq 0$, and $W_{\{\ell\}} \succeq 0 \quad \forall \ell \in \mathcal{T}$.

Model 10 Tight-and-cheap relaxation 2 (TCR2)

Variables: (5.8), $\mathbf{v} \in \mathbb{C}^{|\mathcal{N}|}$, $\mathbf{w} \in \mathbb{C}^{|\mathcal{T}|}$.

Minimize: (5.1a)

Subject to: (5.1d), (5.1e), (5.1j), (5.1k), (5.3c)–(5.3g), (5.4), (5.12), (5.10).

5.5 ORPD: Solution approach

Following [23], a mixed-integer nonlinear program (MINLP) is an optimization problem of the form

$$\hat{v} = \text{minimize } f_0(\mathbf{x}, \mathbf{y}) \quad (5.15a)$$

$$\text{subject to } f_i(\mathbf{x}, \mathbf{y}) \leq 0, \quad i = 1, 2, \dots, m, \quad (5.15b)$$

$$\mathbf{x} \in \mathbb{R}^{n_1}, \mathbf{y} \in \mathbb{Z}^{n_2}. \quad (5.15c)$$

By fixing all integer variables, i.e., $\mathbf{y} = \tilde{\mathbf{y}} \in \mathbb{Z}^{n_2}$, we obtain the following *subproblem* (SP) of (5.15)

$$\hat{v}_{SP} = \text{minimize } f_0(\mathbf{x}, \tilde{\mathbf{y}}) \quad (5.16a)$$

$$\text{subject to } f_i(\mathbf{x}, \tilde{\mathbf{y}}) \leq 0, \quad i = 1, 2, \dots, m, \quad (5.16b)$$

$$\mathbf{x} \in \mathbb{R}^{n_1}. \quad (5.16c)$$

Then we can rewrite the MINLP (5.15) as

$$\hat{v} = \min_{\tilde{\mathbf{y}} \in \mathbb{Z}^{n_2}} \left\{ \min_{\mathbf{x} \in \mathbb{R}^{n_1}} \{f_0(\mathbf{x}, \tilde{\mathbf{y}}) : f_i(\mathbf{x}, \tilde{\mathbf{y}}) \leq 0, i = 1, 2, \dots, m\} \right\}$$

If (5.16) is feasible, its global optimal value \hat{v}_{SP} provides an upper bound for \hat{v} and the optimal solution $(\hat{\mathbf{x}}_{SP}, \tilde{\mathbf{y}})$ of (5.16) is called a *suboptimal* solution of MINLP (5.15). The subproblem (5.16) may be nonconvex and solving it to global optimality may be hard. In this case, any local optimal value \bar{v}_{SP} of (5.16) can be considered as an upper bound of \hat{v} .

Consider a relaxation (R) of (5.15) of the form

$$\hat{v}_R = \text{minimize } \underline{f}_0(\mathbf{x}, \mathbf{y}) \quad (5.17a)$$

$$\text{subject to } (\mathbf{x}, \mathbf{y}) \in \bar{\Omega} \subseteq \mathbb{R}^{n_1} \times \mathbb{R}^{n_2}, \quad (5.17b)$$

where $\bar{\Omega}$ contains the feasible set of (5.15) and \underline{f}_0 underestimates f_0 for all feasible solutions of (5.15). The global optimal value \hat{v}_R is a lower bound of \hat{v} . Since it is necessary to solve (5.17) to global optimality to obtain a lower bound on \hat{v} , it is more advantageous for the relaxation (5.17) to be convex.

Let $(\hat{\mathbf{x}}_R, \hat{\mathbf{y}}_R)$ and \hat{v}_R be respectively the global optimal solution and the global optimal value of a convex relaxation (R) of a MINLP. Now, consider the subproblem (SP) associated to $\tilde{\mathbf{y}}_R$, the closest integer solution to $\hat{\mathbf{y}}_R$. We define the optimality gap of the relaxation (R) by $100(1 - \hat{v}_R/\bar{v}_{SP})$,

where \bar{v}_{SP} is a local optimal value of the subproblem (SP). If the optimality gap is close to zero, we say that the relaxation is *tight* and the suboptimal solution $(\hat{\mathbf{x}}_{SP}, \tilde{\mathbf{y}}_R)$ is *near-global optimal* for the MINLP.

This leads to the following approach to solve the ORPD problem (5.1):

1. Solve SDR1, TCR1, SDR2 or TCR2 and find corresponding shunt solutions $\hat{\mathbf{u}} \in [0, 1]^{|\mathcal{U}|}$ and tap ratios $\hat{\mathbf{t}} \in \prod_{\ell \in \mathcal{T}} [t_\ell, \bar{t}_\ell]$ with formulas (5.9),
2. Round-off \mathbf{u} and \mathbf{t} to their respective nearest discrete values $\tilde{\mathbf{u}} \in \{0, 1\}^{|\mathcal{U}|}$ and $\tilde{\mathbf{t}} \in \prod_{\ell \in \mathcal{T}} \{t_\ell, \dots, \bar{t}_\ell\}$,
3. Fix $\mathbf{u} = \tilde{\mathbf{u}}$ and $\mathbf{t} = \tilde{\mathbf{t}}$ and solve the ACOPF subproblem with a nonlinear (local) solver.

5.6 Computational results

In this section, we evaluate the accuracy and the computational efficiency of SDR1 and TCR1 as compared to SDR2 and TCR2.

In order to increase the computational speed of solving SDR1 and SDR2, we exploited the sparsity of a power network by replacing the SDP constraint $V \succeq 0$ by small SDP constraints defined on a chordal extension of the power network. More details about exploiting the sparsity of power networks in SDP relaxations of the OPF problem can be found in [24, 31, 32, 45, 46].

Let us interpret the network $\mathcal{P} = (\mathcal{N}, \mathcal{L})$ as a connected, simple and undirected graph $\mathcal{G} = (\mathcal{N}, \mathcal{E})$ where $\mathcal{N} = \{1, \dots, n\}$ represents the set of vertices and $\mathcal{E} = \{\{k, m\} : (k, m) \text{ or } (m, k) \in \mathcal{L}\}$, the set of edges. It was proved in [20] that the SDP constraint $V \succeq 0$ in SDR1 or SDR2 is equivalent to $V_{\mathcal{K}} \succeq 0$ for every maximal clique \mathcal{K} of a chordal extension \mathcal{G}' of \mathcal{G} . $V_{\mathcal{K}}$ is the submatrix of V in which the set of row indices that remain and the set of column indices that remain are both \mathcal{K} . To compute the maximal cliques of a chordal extension of \mathcal{G} , we used the same algorithm as in [24].

We tested the models 7, 8, 9, 10, on standard test cases available from MATPOWER [40, 54, 55]. We assigned a shunt variable u_k to each shunt element connected to a bus $k \in \mathcal{U}$ and we assumed that the tap ratio t_ℓ of each transformer $\ell \in \mathcal{T}$ varies from 0.9 to 1.1 pu by steps of 0.0125 pu. Table 5.1 lists the test cases along with the number of shunt elements $|\mathcal{U}|$ and the number of transformers $|\mathcal{T}|$.

We solved SDR1, TCR1, SDR2 and TCR2 in MATLAB using CVX 2.1 [56] with the solver MOSEK 8.0.0.60 and default precision (tolerance $\epsilon = 1.49 \times 10^{-8}$). All relaxations were implemented as a MATLAB package, which is available on GitHub [72]. It requires that MATPOWER and CVX be installed and that the input instance be provided in MATPOWER format. MOSEK numerically failed to solve SDR1 for `case3120sp`.

All ACOPF subproblems were solved with the MATPOWER-solver MIPS. When MIPS numerically failed to solve subproblems for some test cases, marked with “*” in Table 5.2 and Table 5.3,

Table 5.1 Dimensions of test instances

| Test case | $ \mathcal{N} $ | $ \mathcal{L} $ | $ \mathcal{U} $ | $ \mathcal{T} $ |
|-------------------------------|-----------------|-----------------|-----------------|-----------------|
| <i>Small-scale instances</i> | | | | |
| case14 | 14 | 20 | 1 | 3 |
| case24_ieee_rts | 24 | 38 | 1 | 5 |
| case30 | 30 | 41 | 2 | 0 |
| case_ieee30 | 30 | 41 | 2 | 4 |
| case39 | 39 | 46 | 0 | 12 |
| case57 | 57 | 80 | 3 | 17 |
| case89pegase | 89 | 210 | 44 | 32 |
| <i>Medium-scale instances</i> | | | | |
| case118 | 118 | 186 | 14 | 9 |
| case_ACTIV_SG_200 | 200 | 245 | 4 | 66 |
| case_illinois200 | 200 | 245 | 4 | 66 |
| case300 | 300 | 411 | 29 | 107 |
| case_ACTIV_SG_500 | 500 | 597 | 15 | 131 |
| <i>Large-scale instances</i> | | | | |
| case1354pegase | 1 354 | 1 991 | 1 082 | 234 |
| case2383wp | 2 383 | 2 896 | 0 | 164 |
| case2736sp | 2 736 | 3 269 | 1 | 168 |
| case2737sop | 2 737 | 3 269 | 5 | 169 |
| case2746wop | 2 746 | 3 307 | 6 | 171 |
| case2746wp | 2 746 | 3 279 | 0 | 171 |
| case2869pegase | 2 869 | 4 582 | 2 197 | 493 |
| case3012wp | 3 012 | 3 572 | 9 | 201 |
| case3120sp | 3 120 | 3 693 | 9 | 206 |
| case3375wp | 3 374 | 4 161 | 9 | 381 |

we then used the solver FMINCON. Among these subproblems, FMINCON did not converge to a feasible solution after 1000 iterations for case3012wp (SDR1), case3120sp (TCR1) in cost minimization, and case3120sp (SDR1, TCR1), case3375wp (SDR1, TCR1) in loss minimization.

All the computations were carried out on an Intel Core i7-6700 CPU @ 3.40 GHz computing platform.

We report results for two different objective functions: the generation cost $\sum_{g \in \mathcal{G}} c_{g2} p_{Gg}^2 + c_{g1} p_{Gg} + c_{g0}$ [\$/h] and the active power losses $\sum_{g \in \mathcal{G}} p_{Gg}$ [MW]. Both objective functions of test cases from [55] are the same. We denote \underline{v} the best lower bound which is the maximum value among \hat{v}_{SDR1} , \hat{v}_{SDR2} , \hat{v}_{TCR1} , \hat{v}_{TCR2} , respective optimal values of SDR1, TCR1, SDR2, and TCR2. The normalized \hat{v}_R of a relaxation is measured as $\hat{v}_R / \underline{v} \leq 1$, where \hat{v}_R is the relaxation's optimal value. Table 5.2 and Table 5.3 summarize the normalized optimal values of relaxations. The results support the following key points:

1. Among all relaxations, SDR2 is the strongest.
2. SDR1 (respectively SDR2) is stronger than TCR1 (respectively TCR2).
3. SDR1 and TCR2 are comparable.

For a relaxation, the local optimal value of the ACOPF subproblem obtained from the relaxation's optimal solution after rounding-off the discrete variables \mathbf{u} and \mathbf{t} is denoted \bar{v}_{SP} . The normalized \bar{v}_{SP} in Table 5.2 and Table 5.3 is the value $\bar{v}_{SP}/\bar{v} \geq 1$, where \bar{v} the best upper bound, i.e., the minimum value among all \bar{v}_{SP} . In Table 5.2 and Table 5.3, we observe that:

1. In general, applying the round-off technique with SDR2 (respectively TCR2) provide tighter upper bounds than with SDR1 (respectively TCR1) for large-scale instances.
2. Applying the round-off technique with TCR2 is comparable to using SDR1.

Optimality gaps of the four relaxations are given in Table 5.4 and Table 5.5. The optimality gap of a relaxation is measured as $100(1 - \hat{v}_R/\bar{v}_{SP})$, where \hat{v}_R is the relaxation's optimal value and \bar{v}_{SP} is a local optimal value of the corresponding subproblem. With the optimality gap, we can guarantee the near-global optimality of the suboptimal solution obtained with MIPS. Results in Table 5.4 and Table 5.5 show that:

1. Suboptimal solutions obtained from SDR2's optimal solutions have the lowest guaranteed optimality gaps. We can say that they are near-global optimal for all but one test case: `case_ACTIV_SG_500` (cost minimization).
2. In general, suboptimal solutions obtained from SDR1's and TCR2's optimal solutions have almost the same guaranteed optimality gaps.
3. Suboptimal solutions obtained from TCR1's optimal solutions have slightly larger optimality gaps.

The computation times required to solve SDR1, TCR1, SDR2, and TCR2 as reported by MOSEK are also shown in Table 5.4 and Table 5.5. We see that

1. Solving SDR1 (respectively TCR1) is as expensive as solving SDR2 (respectively TCR2) in general.
2. Solving SDR1 (respectively SDR2) is much more expensive than solving TCR1 (respectively TCR2) for large-scale instances. The TCRs are on average 30 times faster than the SDRs.

Overall, we can see that TCR2 offers an interesting trade-off between the optimality gap and the computation time.

5.7 Conclusion

We proposed a tight SDP relaxation (SDR2) for the ORPD problem. This formulation is based on a standard SDP relaxation (SDR1) combined with a tight convex tap changer model. Experiments on

selected MATPOWER instances with up to 3375 buses show that SDR2 is stronger than SDR1, and computationally comparable. From both SDR1 and SDR2, we derived tight-and-cheap relaxations TCR1 and TCR2, respectively.

A round-off technique based on a SDP relaxation of the ORPD problem instead of the nonconvex continuous relaxation was also proposed. Computational results show that applying the round-off technique with SDR2 and TCR2 provides suboptimal solutions which are near-global optimal. Both provide almost the same guaranteed optimality gaps, but TCR2 is computationally much less expensive for large-scale instances. In summary, the proposed TCR-based approach provides the best trade-off between optimality gap and computation time compared to the SDR-based approach.

Table 5.2 Cost minimization: Normalized optimal values

| Test case | \underline{v} [\$/h] | \bar{v} [\$/h] | Normalized \hat{v}_R | | | | Normalized \bar{v}_{SP} | | | |
|-------------------------------|------------------------|------------------|------------------------|---------------|---------------|---------------|---------------------------|---------------|---------------|---------------|
| | | | SDR1 | SDR2 | TCR1 | TCR2 | SDR1 | SDR2 | TCR1 | TCR2 |
| <i>Small-scale instances</i> | | | | | | | | | | |
| case14 | 8 078.62 | 8 078.75 | 1.0000 | 1.0000 | 1.0000 | 1.0000 | 1.0000 | 1.0000 | 1.0000 | 1.0000 |
| case24_ieee_rts | 63 333.39 | 63 335.67 | 1.0000 | 1.0000 | 0.9999 | 1.0000 | 1.0000 | 1.0000 | 1.0000 | 1.0000 |
| case30 | 576.89 | 576.89 | 1.0000 | 1.0000 | 0.9993 | 0.9993 | 1.0000 | 1.0000 | 1.0000 | 1.0000 |
| case_ieee30 | 8 902.67 | 8 902.75 | 1.0000 | 1.0000 | 1.0000 | 1.0000 | 1.0000 | 1.0000 | 1.0000 | 1.0000 |
| case39 | 41 850.24 | 41 852.45 | 1.0000 | 1.0000 | 1.0000 | 1.0000 | 1.0000 | 1.0000 | 1.0000 | 1.0000 |
| case57 | 41 682.14 | 41 688.61 | 0.9997 | 1.0000 | 0.9996 | 0.9999 | 1.0000 | 1.0000 | 1.0000 | 1.0000 |
| case89pegase | 5 803.58 | 5 804.23 | 0.9996 | 1.0000 | 0.9992 | 0.9999 | 1.0001 | 1.0000 | 1.0001 | 1.0001 |
| Average | | | 0.9998 | 1.0000 | 0.9996 | 0.9999 | 1.0000 | 1.0000 | 1.0000 | 1.0000 |
| <i>Medium-scale instances</i> | | | | | | | | | | |
| case118 | 129 526.00 | 129 662.15 | 0.9987 | 1.0000 | 0.9987 | 0.9997 | 1.0003 | 1.0000 | 1.0003 | 1.0000 |
| case_ACTIV_SG_200 | 27 552.84 | 27 553.52 | 1.0000 | 1.0000 | 1.0000 | 1.0000 | *1.0000 | 1.0000 | *1.0000 | 1.0000 |
| case_illinois200 | 36 738.07 | 36 743.37 | 1.0000 | 1.0000 | 0.9998 | 0.9998 | *1.0000 | 1.0000 | 1.0000 | 1.0000 |
| case300 | 718 938.90 | 719 154.24 | 0.9994 | 1.0000 | 0.9989 | 0.9992 | 1.0002 | 1.0000 | 1.0002 | 1.0002 |
| case_ACTIV_SG_500 | 70 316.47 | 72 454.07 | 0.9875 | 1.0000 | 0.9751 | 0.9792 | 1.0016 | 1.0033 | 1.0000 | 1.0018 |
| Average | | | 0.9950 | 1.0000 | 0.9902 | 0.9919 | 1.0007 | 1.0013 | 1.0001 | 1.0007 |
| <i>Large-scale instances</i> | | | | | | | | | | |
| case1354pegase | 73 999.72 | 74 005.77 | 0.9998 | 1.0000 | 0.9995 | 0.9998 | 1.0000 | 1.0000 | 1.0000 | 1.0000 |
| case2383wp | 1 856 849.35 | 1 862 626.70 | 0.9996 | 1.0000 | 0.9981 | 0.9992 | 1.0039 | 1.0000 | 1.0068 | 1.0033 |
| case2736sp | 1 306 771.84 | 1 307 134.47 | 0.9997 | 1.0000 | 0.9988 | 0.9998 | 1.0001 | 1.0000 | 1.0002 | 1.0001 |
| case2737sop | 777 020.01 | 777 337.82 | 0.9997 | 1.0000 | 0.9990 | 0.9997 | 1.0001 | 1.0000 | 1.0001 | 1.0001 |
| case2746wop | 1 206 874.60 | 1 207 872.71 | 0.9994 | 1.0000 | 0.9983 | 0.9994 | 1.0001 | 1.0000 | 1.0002 | 1.0001 |
| case2746wp | 1 630 617.28 | 1 631 018.94 | 0.9997 | 1.0000 | 0.9988 | 0.9996 | 1.0001 | 1.0000 | 1.0002 | 1.0000 |
| case2869pegase | 133 867.21 | 133 877.91 | 0.9998 | 1.0000 | 0.9994 | 0.9997 | 1.0000 | 1.0000 | 1.0000 | 1.0000 |
| case3012wp | 2 578 533.79 | 2 590 254.80 | 0.9987 | 1.0000 | 0.9968 | 0.9985 | – | 1.0000 | 1.0009 | 1.0013 |
| case3120sp | 2 135 933.93 | 2 143 654.67 | – | 1.0000 | 0.9975 | 0.9988 | – | 1.0002 | – | 1.0000 |
| case3375wp | 7 397 491.46 | *7 409 223.47 | 0.9998 | 1.0000 | 0.9988 | 0.9994 | *1.0002 | *1.0000 | *1.0002 | *1.0004 |
| Average | | | – | 1.0000 | 0.9985 | 0.9994 | – | 1.0000 | – | 1.0005 |

Table 5.3 Loss minimization: Normalized optimal values

| Test case | \underline{v} [MW] | \bar{v} [MW] | Normalized \hat{v}_R | | | | Normalized \bar{v}_{SP} | | | |
|-------------------------------|----------------------|----------------|------------------------|---------------|---------------|---------------|---------------------------|---------------|---------------|---------------|
| | | | SDR1 | SDR2 | TCR1 | TCR2 | SDR1 | SDR2 | TCR1 | TCR2 |
| <i>Small-scale instances</i> | | | | | | | | | | |
| case14 | 259.49 | 259.49 | 1.0000 | 1.0000 | 1.0000 | 1.0000 | 1.0000 | 1.0000 | 1.0000 | 1.0000 |
| case24_ieee_rts | 2 875.33 | 2 875.37 | 1.0000 | 1.0000 | 0.9999 | 1.0000 | 1.0000 | 1.0000 | 1.0000 | 1.0000 |
| case30 | 191.09 | 191.09 | 1.0000 | 1.0000 | 0.9999 | 0.9999 | 1.0000 | 1.0000 | 1.0000 | 1.0000 |
| case_ieee30 | 284.68 | 284.71 | 0.9997 | 1.0000 | 0.9997 | 1.0000 | 1.0000 | 1.0000 | 1.0000 | 1.0000 |
| case39 | 6 283.20 | 6 283.44 | 1.0000 | 1.0000 | 1.0000 | 1.0000 | 1.0000 | 1.0000 | 1.0000 | 1.0000 |
| case57 | 1 260.83 | 1 260.98 | 0.9998 | 1.0000 | 0.9998 | 1.0000 | 1.0000 | 1.0000 | 1.0000 | 1.0000 |
| case89pegase | 5 803.58 | 5 804.23 | 0.9996 | 1.0000 | 0.9992 | 0.9999 | 1.0001 | 1.0000 | 1.0001 | 1.0001 |
| Average | | | 0.9998 | 1.0000 | 0.9997 | 1.0000 | 1.0000 | 1.0000 | 1.0000 | 1.0000 |
| <i>Medium-scale instances</i> | | | | | | | | | | |
| case118 | 4 250.75 | 4 251.17 | 1.0000 | 1.0000 | 1.0000 | 1.0000 | 1.0000 | 1.0000 | 1.0000 | 1.0000 |
| case_ACTIV_SG_200 | 1 483.23 | 1 483.32 | 1.0000 | 1.0000 | 0.9999 | 0.9999 | 1.0000 | 1.0000 | *1.0000 | 1.0000 |
| case_illinois200 | 2 245.96 | 2 246.22 | 1.0000 | 1.0000 | 0.9999 | 0.9999 | *1.0000 | 1.0000 | 1.0000 | 1.0000 |
| case300 | 23 723.13 | 23 725.42 | 0.9999 | 1.0000 | 0.9996 | 0.9997 | 1.0000 | 1.0001 | 1.0001 | 1.0001 |
| case_ACTIV_SG_500 | 7 815.64 | 7 817.25 | 1.0000 | 1.0000 | 0.9998 | 0.9998 | 1.0000 | 1.0000 | 1.0000 | 1.0000 |
| Average | | | 1.0000 | 1.0000 | 0.9998 | 0.9999 | 1.0000 | 1.0000 | 1.0000 | 1.0000 |
| <i>Large-scale instances</i> | | | | | | | | | | |
| case1354pegase | 73 999.72 | 74 005.77 | 0.9998 | 1.0000 | 0.9995 | 0.9998 | 1.0000 | 1.0000 | 1.0000 | 1.0000 |
| case2383wp | 24 967.98 | 24 983.29 | 1.0000 | 1.0000 | 0.9992 | 0.9997 | 1.0000 | 1.0000 | 1.0001 | 1.0001 |
| case2736sp | 18 324.27 | 18 329.28 | 0.9999 | 1.0000 | 0.9993 | 0.9998 | 1.0001 | 1.0000 | 1.0001 | 1.0000 |
| case2737sop | 11 391.09 | 11 394.38 | 0.9997 | 1.0000 | 0.9992 | 0.9997 | 1.0001 | 1.0000 | 1.0001 | 1.0001 |
| case2746wop | 19 197.71 | 19 209.58 | 0.9996 | 1.0000 | 0.9989 | 0.9996 | 1.0001 | 1.0000 | 1.0001 | 1.0001 |
| case2746wp | 25 255.49 | 25 260.72 | 0.9999 | 1.0000 | 0.9992 | 0.9997 | 1.0001 | 1.0000 | 1.0001 | 1.0000 |
| case2869pegase | 133 867.21 | 133 877.91 | 0.9998 | 1.0000 | 0.9994 | 0.9997 | 1.0000 | 1.0000 | 1.0000 | 1.0000 |
| case3012wp | 27 611.41 | 27 648.22 | 0.9995 | 1.0000 | 0.9986 | 0.9994 | 1.0001 | 1.0000 | 1.0001 | 1.0003 |
| case3120sp | 21 463.22 | 21 524.52 | 0.9998 | 1.0000 | 0.9991 | 0.9997 | – | 1.0000 | – | 1.0000 |
| case3375wp | 48 950.55 | 49 002.59 | 0.9997 | 1.0000 | 0.9993 | 0.9995 | – | 1.0027 | – | 1.0000 |
| Average | | | 0.9998 | 1.0000 | 0.9992 | 0.9996 | – | 1.0003 | – | 1.0001 |

Table 5.4 Cost minimization: Optimality gaps and computation times

| Test case | Optimality gap [%] | | | | Computation time [s] | | | |
|-------------------------------|--------------------|-------------|-------------|-------------|----------------------|---------------|--------------|--------------|
| | SDR1 | SDR2 | TCR1 | TCR2 | SDR1 | SDR2 | TCR1 | TCR2 |
| <i>Small-scale instances</i> | | | | | | | | |
| case14 | 0.00 | 0.00 | 0.00 | 0.00 | 0.15 | 0.13 | 0.12 | 0.36 |
| case24_ieee_rts | 0.01 | 0.00 | 0.01 | 0.00 | 0.19 | 0.55 | 0.54 | 0.28 |
| case30 | 0.00 | 0.00 | 0.07 | 0.07 | 0.12 | 0.12 | 0.20 | 0.20 |
| case_ieee30 | 0.00 | 0.00 | 0.00 | 0.00 | 0.12 | 0.11 | 0.13 | 0.14 |
| case39 | 0.01 | 0.01 | 0.01 | 0.01 | 0.43 | 0.41 | 0.61 | 0.52 |
| case57 | 0.05 | 0.02 | 0.05 | 0.03 | 0.47 | 0.21 | 0.20 | 0.24 |
| case89pegase | 0.06 | 0.01 | 0.10 | 0.03 | 2.26 | 1.64 | 0.76 | 0.72 |
| Average | 0.03 | 0.01 | 0.05 | 0.02 | 0.91 | 0.69 | 0.45 | 0.42 |
| <i>Medium-scale instances</i> | | | | | | | | |
| case118 | 0.27 | 0.11 | 0.27 | 0.13 | 0.30 | 0.36 | 0.38 | 0.40 |
| case_ACTIV_SG_200 | *0.00 | 0.00 | *0.01 | 0.01 | 0.82 | 0.79 | 0.57 | 0.55 |
| case_illinois200 | *0.02 | 0.01 | 0.03 | 0.03 | 0.94 | 1.41 | 0.73 | 0.75 |
| case300 | 0.11 | 0.03 | 0.16 | 0.13 | 1.23 | 2.25 | 0.99 | 0.89 |
| case_ACTIV_SG_500 | 4.31 | 3.27 | 5.36 | 5.14 | 4.37 | 4.53 | 3.85 | 3.14 |
| Average | 1.69 | 1.26 | 2.10 | 2.00 | 2.23 | 2.60 | 1.92 | 1.63 |
| <i>Large-scale instances</i> | | | | | | | | |
| case1354pegase | 0.03 | 0.01 | 0.06 | 0.03 | 13.35 | 11.95 | 7.53 | 6.66 |
| case2383wp | 0.74 | 0.31 | 1.17 | 0.71 | 307.06 | 325.67 | 14.19 | 12.97 |
| case2736sp | 0.07 | 0.03 | 0.16 | 0.07 | 426.85 | 398.85 | 13.84 | 12.05 |
| case2737sop | 0.08 | 0.04 | 0.16 | 0.08 | 381.34 | 372.61 | 11.23 | 12.75 |
| case2746wop | 0.15 | 0.08 | 0.27 | 0.15 | 477.80 | 425.23 | 10.96 | 11.68 |
| case2746wp | 0.06 | 0.02 | 0.16 | 0.07 | 418.71 | 414.08 | 11.27 | 11.19 |
| case2869pegase | 0.03 | 0.01 | 0.07 | 0.04 | 55.71 | 80.07 | 21.27 | 19.78 |
| case3012wp | - | 0.45 | 0.87 | 0.73 | 1 670.60 | 1 618.99 | 12.27 | 12.17 |
| case3120sp | - | 0.38 | - | 0.48 | 763.19 | 672.87 | 13.64 | 13.22 |
| case3375wp | *0.20 | *0.16 | *0.29 | *0.24 | 1 638.91 | 1 763.90 | 20.47 | 18.89 |
| Average | - | 0.16 | - | 0.27 | 684.22 | 678.29 | 14.15 | 13.63 |

Table 5.5 Loss minimization: Optimality gaps and computation times

| Test case | Optimality gap [%] | | | | Computation time [s] | | | |
|-------------------------------|--------------------|-------------|-------------|-------------|----------------------|---------------|--------------|--------------|
| | SDR1 | SDR2 | TCR1 | TCR2 | SDR1 | SDR2 | TCR1 | TCR2 |
| <i>Small-scale instances</i> | | | | | | | | |
| case14 | 0.00 | 0.00 | 0.00 | 0.00 | 0.12 | 0.12 | 0.12 | 0.12 |
| case24_ieee_rts | 0.00 | 0.00 | 0.00 | 0.00 | 0.16 | 0.18 | 0.39 | 0.20 |
| case30 | 0.00 | 0.00 | 0.01 | 0.01 | 0.13 | 0.13 | 0.17 | 0.17 |
| case_ieee30 | 0.04 | 0.01 | 0.05 | 0.02 | 0.16 | 0.34 | 0.49 | 0.28 |
| case39 | 0.00 | 0.00 | 0.00 | 0.00 | 0.17 | 0.19 | 0.22 | 0.22 |
| case57 | 0.03 | 0.01 | 0.03 | 0.01 | 0.19 | 0.23 | 0.18 | 0.49 |
| case89pegase | 0.06 | 0.01 | 0.10 | 0.03 | 2.26 | 1.64 | 0.76 | 0.72 |
| Average | 0.03 | 0.01 | 0.04 | 0.02 | 0.82 | 0.66 | 0.41 | 0.43 |
| <i>Medium-scale instances</i> | | | | | | | | |
| case118 | 0.01 | 0.01 | 0.01 | 0.01 | 0.29 | 0.27 | 0.30 | 0.30 |
| case_ACTIV_SG_200 | 0.01 | 0.01 | *0.01 | 0.01 | 0.73 | 0.74 | 0.48 | 1.06 |
| case_illinois200 | *0.01 | 0.01 | 0.02 | 0.02 | 1.83 | 0.92 | 1.70 | 0.74 |
| case300 | 0.02 | 0.02 | 0.06 | 0.05 | 1.02 | 0.91 | 0.98 | 0.88 |
| case_ACTIV_SG_500 | 0.03 | 0.02 | 0.04 | 0.04 | 5.82 | 4.56 | 4.59 | 3.95 |
| Average | 0.02 | 0.02 | 0.04 | 0.03 | 2.85 | 2.21 | 2.32 | 2.00 |
| <i>Large-scale instances</i> | | | | | | | | |
| case1354pegase | 0.03 | 0.01 | 0.06 | 0.03 | 13.35 | 11.95 | 7.53 | 6.66 |
| case2383wp | 0.07 | 0.06 | 0.15 | 0.10 | 252.55 | 271.06 | 13.94 | 12.56 |
| case2736sp | 0.05 | 0.03 | 0.11 | 0.05 | 434.61 | 280.45 | 10.52 | 9.58 |
| case2737sop | 0.06 | 0.03 | 0.12 | 0.06 | 210.99 | 215.05 | 8.67 | 8.55 |
| case2746wop | 0.10 | 0.06 | 0.18 | 0.12 | 394.81 | 444.52 | 9.88 | 11.20 |
| case2746wp | 0.04 | 0.02 | 0.11 | 0.05 | 431.06 | 403.43 | 9.70 | 9.72 |
| case2869pegase | 0.03 | 0.01 | 0.07 | 0.04 | 55.71 | 80.07 | 21.27 | 19.78 |
| case3012wp | 0.19 | 0.13 | 0.28 | 0.22 | 2 354.15 | 2 426.65 | 16.82 | 17.45 |
| case3120sp | - | 0.28 | - | 0.32 | 1 193.18 | 973.71 | 16.66 | 19.16 |
| case3375wp | - | 0.38 | - | 0.15 | 1 415.74 | 1 588.19 | 28.25 | 39.33 |
| Average | - | 0.12 | - | 0.12 | 753.59 | 749.07 | 15.09 | 16.54 |

CHAPITRE 6 ARTICLE 3: CONICOPF: A TIGHT-AND-CHEAP CONIC RELAXATION WITH ACCURACY METRICS FOR SINGLE-PERIOD AND MULTI-PERIOD ACOPF PROBLEMS

Christian Bingane, Miguel F. Anjos, and Sébastien Le Digabel. CONICOPF: A tight-and-cheap conic relaxation with accuracy metrics for single-period and multi-period ACOPF problems. Submitted for publication to Mathematical Programming Computation.

Abstract: Computational speed and global optimality are a key need for practical algorithms of the OPF problem. Recently, we proposed a tight-and-cheap conic relaxation for the ACOPF problem that offers a favourable trade-off between the standard second-order cone and the standard semidefinite relaxations for large-scale meshed networks in terms of optimality gap and computation time. In this paper, we show theoretically and numerically that this relaxation can be exact and can provide a global optimal solution for the ACOPF problem. Thereafter, we propose a multi-period tight-and-cheap relaxation for the multi-period ACOPF problem. Computational experiments using MATPOWER test cases with up to 500 buses show that this new relaxation is promising for real-life applications.

Keywords: Global optimization, multi-period optimal power flow, power systems, semidefinite programming.

6.1 Nomenclature

6.1.1 Notations

| | |
|-------------------------|---|
| \mathbb{R}/\mathbb{C} | Set of real/complex numbers, |
| \mathbb{H}^n | Set of $n \times n$ Hermitian matrices, |
| j | Imaginary unit, |
| a/a | Real/complex number, |
| \mathbf{a}/\mathbf{a} | Real/complex vector, |
| A/A | Real/complex matrix. |

6.1.2 Operators

| | |
|-------------------------------------|-------------------------------|
| $\text{Re}(\cdot)/\text{Im}(\cdot)$ | Real/imaginary part operator, |
| $(\cdot)^*$ | Conjugate operator, |

| | |
|----------------------|--|
| $ \cdot $ | Magnitude or cardinality set operator, |
| $\angle(\cdot)$ | Phase operator, |
| $(\cdot)^T$ | Transpose operator, |
| $(\cdot)^H$ | Conjugate transpose operator, |
| $\text{rank}(\cdot)$ | Rank operator. |

6.1.3 Input data

| | |
|---|--|
| $\mathcal{P} = (\mathcal{N}, \mathcal{L})$ | Power network, |
| \mathcal{N} | Set of buses, |
| $\mathcal{G} = \bigcup_{k \in \mathcal{N}} \mathcal{G}_k$ | Set of generators, |
| \mathcal{G}_k | Set of generators connected to bus k , |
| \mathcal{L} | Set of branches, |
| $p_{Dk}^\tau / q_{Dk}^\tau$ | Active/reactive power demand at bus k at period τ , |
| g'_k / b'_k | Conductance/susceptance of shunt element at bus k , |
| c_{g2}, c_{g1}, c_{g0} | Generation cost coefficients of generator g , |
| $y_\ell^{-1} = r_\ell + jx_\ell$ | Series impedance of branch ℓ , |
| b'_ℓ | Total shunt susceptance of branch ℓ , |
| t_ℓ | Turns ratio of branch ℓ . |

6.1.4 Variables

| | |
|-----------------------------------|---|
| $p_{Gg}^\tau / q_{Gg}^\tau$ | Active/reactive power generation by generator g at period τ , |
| v_k^τ | Complex (phasor) voltage at bus k at period τ , |
| $p_{f\ell}^\tau / q_{f\ell}^\tau$ | Active/reactive power flow injected along branch ℓ by its <i>from</i> end at period τ , |
| $p_{t\ell}^\tau / q_{t\ell}^\tau$ | Active/reactive power flow injected along branch ℓ by its <i>to</i> end at period τ . |

6.2 Introduction

The optimal power flow (OPF) problem, first formulated in [27], seeks to find a network operating point that optimizes an objective function subject to power flow equations and other operational constraints [15, 16, 28, 58]. The continuous classical version with AC power flow equations, which is nonconvex and NP-hard [30], is generally also called AC optimal power flow (ACOPF) problem.

In recent years, convex relaxations of the ACOPF problem, such as the second-order cone relaxation (SOCP) [17], the semidefinite relaxation (SDR) [18], the quadratic convex relaxation [61], and others [34–38], have attracted a significant interest for several reasons. First, they can lead to global optimality. Second, because they are relaxations, they provide a bound on the global optimal

value of the ACOPF problem. Third, if one of them is infeasible, then the ACOPF problem is infeasible. We should note that, according to [58], convex relaxations of the OPF problem are aimed at complementing nonlinear (local) solvers with valuable information about the quality of the solution obtained, rather than at replacing them.

For general meshed networks, SDR is stronger than SOCR but requires heavier computation. Therefore, the chordal relaxation (CHR) was proposed in [31] in order to exploit the fact that power networks are not densely connected, thus reducing data storage and increasing computation speed. However, even CHR remains expensive to solve compared to SOCR for large-scale power systems. On the other hand, for radial networks, SOCR is tantamount to SDR. In this case, one would normally solve the first one rather than the second one due to the difference in computation time. A full literature review on these three relaxations can be found in [32,33].

According to [15], high computational speed is a key need for practical OPF algorithms, especially in real-time applications and when dealing with large-scale power systems. In fact, in real-time applications, an OPF problem is run every few minutes to update device and resource settings in response to the constantly changing conditions of power systems [6]. This need motivated the choice of the tight-and-cheap conic relaxation (TCR), first proposed in [24], that offers a favourable trade-off between SOCR and SDR for large-scale meshed instances of ACOPF in terms of optimality gap and computation time. Indeed, TCR was proven to be stronger than SOCR and nearly as tight as SDR. Moreover, computational experiments on standard test cases with up to 6515 buses showed that solving TCR for large-scale instances is much less expensive than solving CHR.

Convex relaxations can lead to global optimality of the original ACOPF problem when they are exact, i.e., the optimality gap is null. For instance, [41] provided numerical examples on several IEEE benchmarks systems where SDR is exact. On the other hand, when a convex relaxation is not exact, it only provides a lower bound on the objective value, and its solution is not even feasible for the original problem [73,74]. In this case, different methods, discussed in [75], have been proposed in the literature to obtain a feasible solution of the ACOPF problem from an inexact convex relaxation.

SDR or CHR is exact when its optimal solution fulfills the rank-one condition. In this paper, we show that TCR is exact when its optimal solution also fulfills a similar condition. Unlike SOCR, an additional cycle condition is not necessary for meshed networks [33]. We should note that, for many test cases, convex relaxations of the ACOPF problem are inexact even though optimality gaps are close to zero [24,61,76]. The optimality gap is thus insufficient as metric of the exactness of a convex relaxation [75]. To assess the exactness of TCR, we consider two other metrics: the exactness error and the optimality distance. With these metrics, we show that TCR is exact and provides a global optimal solution to the ACOPF problem for some MATPOWER test cases.

Thereafter, we propose a multi-period TCR for the multi-period ACOPF problem. A multi-period OPF problem is a sequence of ordinary OPF problems strung together by dynamic costs and constraints [6]. We consider a 24-period ACOPF problem and computational experiments using MATPOWER test cases with up to 118 buses show that this new relaxation is promising for real-life applications.

The remainder of this paper is organized as follows. In Section 6.3, we recall TCR and we show that it can be exact. In Section 6.4, we formulate the mathematical model of the multi-period ACOPF problem (without loss of generality) and we derive the multi-period TCR. We report in Section 6.5 computational results on the exactness of TCR and the efficiency of the multi-period TCR. Section 6.6 concludes the paper.

6.3 ACOPF: Tight-and-cheap relaxation

Consider a typical power network $\mathcal{P} = (\mathcal{N}, \mathcal{L})$ where $\mathcal{N} = \{1, 2, \dots, n\}$ and $\mathcal{L} \subseteq \mathcal{N} \times \mathcal{N}$ denote respectively the set of buses and the set of branches (transmission lines, transformers and phase shifters). Each branch $\ell \in \mathcal{L}$ has a *from* end k (on the *tap side*) and a *to* end m as modeled in [40]. We note $\ell = (k, m)$. The ACOPF problem is given as:

$$\min \sum_{g \in \mathcal{G}} c_{g2} p_{Gg}^2 + c_{g1} p_{Gg} + c_{g0} \quad (6.1a)$$

over variables $\mathbf{p}_G, \mathbf{q}_G \in \mathbb{R}^{|\mathcal{G}|}$, $\mathbf{p}_f, \mathbf{q}_f, \mathbf{p}_t, \mathbf{q}_t \in \mathbb{R}^{|\mathcal{L}|}$, and $\mathbf{v} \in \mathbb{C}^{|\mathcal{N}|}$, subject to

— Power balance equations:

$$\sum_{g \in \mathcal{G}_k} p_{Gg} - p_{Dk} - g'_k |v_k|^2 = \sum_{\ell=(k,m) \in \mathcal{L}} p_{f\ell} + \sum_{\ell=(m,k) \in \mathcal{L}} p_{t\ell} \quad \forall k \in \mathcal{N}, \quad (6.1b)$$

$$\sum_{g \in \mathcal{G}_k} q_{Gg} - q_{Dk} + b'_k |v_k|^2 = \sum_{\ell=(k,m) \in \mathcal{L}} q_{f\ell} + \sum_{\ell=(m,k) \in \mathcal{L}} q_{t\ell} \quad \forall k \in \mathcal{N}, \quad (6.1c)$$

— Line flow equations:

$$p_{f\ell} + jq_{f\ell} = \frac{v_k}{t_\ell} \left[\left(j \frac{b'_\ell}{2} + y_\ell \right) \frac{v_k}{t_\ell} - y_\ell v_m \right]^* \quad \forall \ell = (k, m) \in \mathcal{L}, \quad (6.1d)$$

$$p_{t\ell} + jq_{t\ell} = v_m \left[-y_\ell \frac{v_k}{t_\ell} + \left(j \frac{b'_\ell}{2} + y_\ell \right) v_m \right]^* \quad \forall \ell = (k, m) \in \mathcal{L}, \quad (6.1e)$$

— Generator power capacities:

$$\underline{p}_{Gg} \leq p_{Gg} \leq \bar{p}_{Gg}, \quad \underline{q}_{Gg} \leq q_{Gg} \leq \bar{q}_{Gg} \quad \forall g \in \mathcal{G}, \quad (6.1f)$$

— Line thermal limits:

$$|p_{f\ell} + jq_{f\ell}| \leq \bar{s}_\ell, |p_{t\ell} + jq_{t\ell}| \leq \bar{s}_\ell \quad \forall \ell \in \mathcal{L}, \quad (6.1g)$$

— Voltage magnitude limits:

$$\underline{v}_k \leq |v_k| \leq \bar{v}_k \quad \forall k \in \mathcal{N}, \quad (6.1h)$$

— Reference bus constraint:

$$\angle v_1 = 0. \quad (6.1i)$$

The objective function (6.1a) is the cost of conventional generation commonly used in the literature. Constraints (6.1b)–(6.1e) are derived from Kirchhoff's laws and represent power flows in the network. Constraint (6.1i) specifies bus $k = 1$ as the reference bus. We assume that $\underline{v}_k > 0$ for all $k \in \mathcal{N}$ in (6.1h), and that the generation cost $c_{g2}p_{Gg}^2 + c_{g1}p_{Gg} + c_{g0}$ is a convex function for all $g \in \mathcal{G}$.

Problem (6.1) is highly nonconvex and NP-hard [30] due to the nonconvex constraints (6.1d)–(6.1e). Applying local methods to this problem provides no guarantee about the optimality of any solution found. Moreover, it is intractable to solve to global optimality for large-scale instances.

With $V := \mathbf{v}\mathbf{v}^H$, the ACOPF problem (6.1) can be reformulated as follows

minimize (6.1a)

subject to (6.1f), (6.1g), (6.1i),

$$\sum_{g \in \mathcal{G}_k} p_{Gg} - p_{Dk} - g'_k V_{kk} = \sum_{\ell=(k,m) \in \mathcal{L}} p_{f\ell} + \sum_{\ell=(m,k) \in \mathcal{L}} p_{t\ell} \quad \forall k \in \mathcal{N}, \quad (6.2a)$$

$$\sum_{g \in \mathcal{G}_k} q_{Gg} - q_{Dk} + b'_k V_{kk} = \sum_{\ell=(k,m) \in \mathcal{L}} q_{f\ell} + \sum_{\ell=(m,k) \in \mathcal{L}} q_{t\ell} \quad \forall k \in \mathcal{N}, \quad (6.2b)$$

$$p_{f\ell} + jq_{f\ell} = \frac{1}{|t_\ell|^2} \left(-j\frac{b'_\ell}{2} + y_\ell^* \right) V_{kk} - \frac{y_\ell^*}{t_\ell} V_{km} \quad \forall \ell = (k, m) \in \mathcal{L}, \quad (6.2c)$$

$$p_{t\ell} + jq_{t\ell} = -\frac{y_\ell^*}{t_\ell^*} V_{km} + \left(-j\frac{b'_\ell}{2} + y_\ell^* \right) V_{mm} \quad \forall \ell = (k, m) \in \mathcal{L}, \quad (6.2d)$$

$$\underline{v}_k^2 \leq V_{kk} \leq \bar{v}_k^2 \quad \forall k \in \mathcal{N}, \quad (6.2e)$$

$$V = \mathbf{v}\mathbf{v}^H. \quad (6.2f)$$

The nonconvexity of (6.2) is captured by the constraint (6.2f). We can show that $V = \mathbf{v}\mathbf{v}^H$ if and only if $V \succeq 0$ and $\text{rank}(V) = 1$. The standard semidefinite relaxation (SDR), first introduced in [18], is obtained by dropping the rank constraint. If we relax the constraint $V \succeq 0$ in SDR by $|\mathcal{L}|$

constraints of the form

$$V_{\{k,m\}} := \begin{bmatrix} V_{kk} & V_{km} \\ V_{km}^* & V_{mm} \end{bmatrix} \succeq 0 \quad \forall (k,m) \in \mathcal{L}, \quad (6.3)$$

we obtain the standard second-order cone relaxation (SOCR) [17], which is equivalent to SDR for radial networks.

SDR can be very expensive to solve for large-scale instances and SOCR remains weaker than SDR for meshed networks. We then consider a cheaper relaxation, called *tight-and-cheap relaxation* (TCR), given in Model 11 and obtained as follows. We replace (6.2f) by

$$\begin{bmatrix} 1 & v_k^* & v_m^* \\ v_k & V_{kk} & V_{km} \\ v_m & V_{km}^* & V_{mm} \end{bmatrix} \succeq 0 \quad \forall \ell = (k,m) \in \mathcal{L}, \quad (6.4a)$$

and we add the following constraints

$$\operatorname{Re}(v_1) \geq \frac{V_{11} + \underline{v}_1 \bar{v}_1}{\underline{v}_1 + \bar{v}_1}, \quad (6.4b)$$

$$\operatorname{Im}(v_1) = 0, \quad (6.4c)$$

corresponding to the reference bus $k = 1$.

Model 11 Tight-and-cheap relaxation (TCR)

Variables:

$$\begin{aligned} \mathbf{p}_G, \mathbf{q}_G &\in \mathbb{R}^{|\mathcal{G}|}, \\ \mathbf{p}_f, \mathbf{q}_f, \mathbf{p}_t, \mathbf{q}_t &\in \mathbb{R}^{|\mathcal{L}|}, \\ \mathbf{v} &\in \mathbb{C}^{|\mathcal{N}|}, \\ V &\in \mathbb{H}^{|\mathcal{N}|}. \end{aligned}$$

Minimize: (6.1a)

Subject to: (6.1f), (6.1g), (6.2a)–(6.2e), (6.4).

TCR was first proposed in [24] for the ACOPF problem. It was shown in [24] that TCR is stronger than SOCR and nearly as tight as SDR. Moreover, computational experiments on standard test cases with up to 6515 buses showed that solving TCR for large-scale instances is much less expensive than solving the chordal relaxation, a SDP relaxation technique that exploits the sparsity of power networks.

Lemma 5. Let $(\mathbf{x}, X) \in \mathbb{C}^n \times \mathbb{H}^n$ and let

$$Y = \begin{bmatrix} 1 & \mathbf{x}^H \\ \mathbf{x} & X \end{bmatrix} \in \mathbb{H}^{n+1}.$$

Then Y is a rank-one matrix if and only if $X = \mathbf{x}\mathbf{x}^H$.

Proof. Consider the Schur complement $X - \mathbf{x}\mathbf{x}^H$ of 1 in Y . By the Guttman rank additivity formula, $\text{rank}(Y) = 1 + \text{rank}(X - \mathbf{x}\mathbf{x}^H)$. Then $\text{rank}(Y) = 1$ iff $X = \mathbf{x}\mathbf{x}^H$. \square

Proposition 7. If the optimal solution (\mathbf{v}, V) of TCR in Model 11 is such that $V_{kk} = |\mathbf{v}_k|^2$ for all $k \in \mathcal{N}$, then TCR is exact. Moreover, the TCR solution $\mathbf{v} \in \mathbb{C}^n$ is a global optimal solution for the ACOPF problem (6.1).

Proof. Let (\mathbf{v}, V) be the optimal solution of TCR in Model 11. We show that if $V_{kk} = |\mathbf{v}_k|^2$ for all $k \in \mathcal{N}$, then $V_{km} = \mathbf{v}_k \mathbf{v}_m^*$ for all $(k, m) \in \mathcal{L}$.

For all $\ell = (k, m) \in \mathcal{L}$, the semidefinite constraint (6.4a) is equivalent to

$$\begin{bmatrix} V_{kk} - |\mathbf{v}_k|^2 & V_{km} - \mathbf{v}_k \mathbf{v}_m^* \\ V_{km}^* - \mathbf{v}_k^* \mathbf{v}_m & V_{mm} - |\mathbf{v}_m|^2 \end{bmatrix} \succeq 0.$$

If $V_{kk} = |\mathbf{v}_k|^2$ or $V_{mm} = |\mathbf{v}_m|^2$, then $V_{km} = \mathbf{v}_k \mathbf{v}_m^*$. Therefore, if $V_{kk} = |\mathbf{v}_k|^2$ for all $k \in \mathcal{N}$, then $V_{km} = \mathbf{v}_k \mathbf{v}_m^*$ for all $(k, m) \in \mathcal{L}$. It follows that the TCR solution $\mathbf{v} \in \mathbb{C}^n$ is a global optimal solution of the ACOPF problem (6.1) since it is feasible for (6.2), which is equivalent to (6.1). \square

Lemma 5 and Proposition 7 prove that the TCR optimal solution \mathbf{v} is a global optimal solution for the ACOPF problem (6.1) if the positive semidefinite matrix in (6.4a) is rank-one at optimality for all branches $\ell = (k, m) \in \mathcal{L}$. We note that, when TCR is exact, global optimal voltages of the ACOPF problem are directly given by the TCR optimal solution \mathbf{v} , unlike SDR or SOCR where we have to recover them from the optimal solution V .

6.4 MP-ACOPF: Multi-period TCR

Many power system applications that require solving an OPF problem are multi-period because of the evolution of market prices, of the ramping limits of generation units and of the behavior of the demand [65]. An OPF problem is run to meet the requirements of a time horizon optimally in every period. Then, the multi-period model must be adjusted to ensure that decisions in one period are consistent with the next one [77].

Consider a set $\{1, 2, \dots, \bar{\tau}\}$ of time periods τ . All parameters in the ACOPF problem (6.1) remain the same for all periods except demand which varies in each period. Without loss of generality, the MP-ACOPF problem is given as:

$$\min \sum_{\tau=1}^{\bar{\tau}} \sum_{g \in \mathcal{G}} c_{g2} p_{Gg}^{\tau 2} + c_{g1} p_{Gg}^{\tau} + c_{g0} \quad (6.5a)$$

over variables $\mathbf{p}_G^{\tau}, \mathbf{q}_G^{\tau} \in \mathbb{R}^{|\mathcal{G}|}$, $\mathbf{p}_f^{\tau}, \mathbf{q}_f^{\tau}, \mathbf{p}_t^{\tau}, \mathbf{q}_t^{\tau} \in \mathbb{R}^{|\mathcal{L}|}$, and $\mathbf{v}^{\tau} \in \mathbb{C}^{|\mathcal{N}|}$ for all $\tau = 1, \dots, \bar{\tau}$, subject to

— Power balance equations:

$$\sum_{g \in \mathcal{G}_k} p_{Gg}^{\tau} - p_{Dk}^{\tau} - g'_k |\mathbf{v}_k^{\tau}|^2 = \sum_{\ell=(k,m) \in \mathcal{L}} p_{f\ell}^{\tau} + \sum_{\ell=(m,k) \in \mathcal{L}} p_{t\ell}^{\tau} \quad \forall k \in \mathcal{N}, \forall \tau = 1, \dots, \bar{\tau}, \quad (6.5b)$$

$$\sum_{g \in \mathcal{G}_k} q_{Gg}^{\tau} - q_{Dk}^{\tau} + b'_k |\mathbf{v}_k^{\tau}|^2 = \sum_{\ell=(k,m) \in \mathcal{L}} q_{f\ell}^{\tau} + \sum_{\ell=(m,k) \in \mathcal{L}} q_{t\ell}^{\tau} \quad \forall k \in \mathcal{N}, \forall \tau = 1, \dots, \bar{\tau}, \quad (6.5c)$$

— Line flow equations:

$$p_{f\ell}^{\tau} + j q_{f\ell}^{\tau} = \frac{\mathbf{v}_k^{\tau}}{t_{\ell}} \left[\left(j \frac{b'_{\ell}}{2} + y_{\ell} \right) \frac{\mathbf{v}_k^{\tau}}{t_{\ell}} - y_{\ell} \mathbf{v}_m^{\tau} \right]^* \quad \forall \ell = (k, m) \in \mathcal{L}, \forall \tau = 1, \dots, \bar{\tau}, \quad (6.5d)$$

$$p_{t\ell}^{\tau} + j q_{t\ell}^{\tau} = \mathbf{v}_m^{\tau} \left[-y_{\ell} \frac{\mathbf{v}_k^{\tau}}{t_{\ell}} + \left(j \frac{b'_{\ell}}{2} + y_{\ell} \right) \mathbf{v}_m^{\tau} \right]^* \quad \forall \ell = (k, m) \in \mathcal{L}, \forall \tau = 1, \dots, \bar{\tau}, \quad (6.5e)$$

— Generator power capacities:

$$\underline{p}_{Gg} \leq p_{Gg}^{\tau} \leq \bar{p}_{Gg}, \underline{q}_{Gg} \leq q_{Gg}^{\tau} \leq \bar{q}_{Gg} \quad \forall g \in \mathcal{G}, \forall \tau = 1, \dots, \bar{\tau}, \quad (6.5f)$$

— Line thermal limits:

$$|p_{f\ell}^{\tau} + j q_{f\ell}^{\tau}| \leq \bar{s}_{\ell}, |p_{t\ell}^{\tau} + j q_{t\ell}^{\tau}| \leq \bar{s}_{\ell} \quad \forall \ell \in \mathcal{L}, \forall \tau = 1, \dots, \bar{\tau}, \quad (6.5g)$$

— Voltage magnitude limits:

$$\underline{v}_k \leq |\mathbf{v}_k^{\tau}| \leq \bar{v}_k \quad \forall k \in \mathcal{N}, \forall \tau = 1, \dots, \bar{\tau}, \quad (6.5h)$$

— Reference bus constraints:

$$\angle \mathbf{v}_1^{\tau} = 0 \quad \forall \tau = 1, \dots, \bar{\tau}, \quad (6.5i)$$

— Ramp constraints:

$$\underline{\Delta}_g^{\tau} \leq p_{Gg}^{\tau+1} - p_{Gg}^{\tau} \leq \bar{\Delta}_g^{\tau} \quad \forall g \in \mathcal{G}, \forall \tau = 1, \dots, \bar{\tau} - 1. \quad (6.5j)$$

In (6.5), the ACOPF problem (6.1) was replicated in each period $\tau = 1, \dots, \bar{\tau}$, and coupled sequentially by the ramp constraints (6.5j). These constraints enforce the generation limits when the demand increases or falls sharply between two consecutive periods. Note that one can also consider other time-coupled constraints such as storage ones [6, 78]. Beyond the constraints that can be taken into account, the major concern of the MP-ACOPF problem (6.5) is the computational scalability because the number of variables and constraints in the ACOPF problem (6.1) has been multiplied by the number of periods [6].

We now propose a convex relaxation of the MP-ACOPF problem (6.5). For all $\tau = 1, \dots, \bar{\tau}$, let $V^\tau := \mathbf{v}^\tau \mathbf{v}^{\tau H}$. With the same reasoning as for the single-period ACOPF problem (6.1), we define in Model 12 a tight-and-cheap relaxation for the MP-ACOPF problem (6.5). We call this relaxation “*multi-period tight-and-cheap relaxation*” (MP-TCR). We should note that other convex relaxations of the MP-ACOPF problem were already considered in the literature, e.g., SDR in [78], SOCR in [79].

Proposition 8. *For all $\tau = 1, \dots, \bar{\tau}$, if the optimal solution $(\mathbf{v}^\tau, V^\tau)$ of MP-TCR in Model 12 is such that $V_{kk}^\tau = |\mathbf{v}_k^\tau|^2$ for all $k \in \mathcal{N}$, then MP-TCR is exact. Moreover, for each time period $\tau = 1, \dots, \bar{\tau}$, the MP-TCR solution $\mathbf{v}^\tau \in \mathbb{C}^n$ is a global optimal solution for the MP-ACOPF problem (6.5).*

Proof. The result follows from Proposition 7. □

6.5 Computational results

6.5.1 Exactness of TCR

In this section, we evaluate the exactness of TCR. We tested Model 11 on standard test cases available from MATPOWER [40, 54, 55].

We solved TCR in MATLAB using CVX 2.1 [56] with the solver MOSEK 8.0.0.60 and default precision (tolerance $\epsilon = 1.49 \times 10^{-8}$). All the computations were carried out on an Intel Core i7-6700 CPU @ 3.40 GHz computing platform. TCR and others relaxations defined in [24, 25] were implemented as a MATLAB package, which is available on GitHub [72]. It requires that MATPOWER and CVX be installed and the input test case be in MATPOWER format.

We considered two different objective functions: the generation cost [\$/h] (6.1a) and the active loss [MW] where $c_{g2} = 0$, $c_{g1} = 1$ and $c_{g0} = 0$ for all $g \in \mathcal{G}$ in (6.1a). Both objective functions of test cases from [55] are the same.

We assess the exactness of TCR using three metrics:

 Model 12 Multi-period tight-and-cheap relaxation (MP-TCR)

Variables:

$$\begin{aligned} \mathbf{p}_G^\tau, \mathbf{q}_G^\tau &\in \mathbb{R}^{|\mathcal{G}|}, \\ \mathbf{p}_f^\tau, \mathbf{q}_f^\tau, \mathbf{p}_t^\tau, \mathbf{q}_t^\tau &\in \mathbb{R}^{|\mathcal{L}|}, \\ \mathbf{v}^\tau &\in \mathbb{C}^{|\mathcal{N}|}, \\ \mathbf{V}^\tau &\in \mathbb{H}^{|\mathcal{N}|} \end{aligned}$$

 for all $\tau = 1, \dots, \bar{\tau}$.

Minimize: (6.5a)

 Subject to: (6.5f), (6.5g), (6.5j), and for all $\tau = 1, \dots, \bar{\tau}$,

$$\begin{aligned} \sum_{g \in \mathcal{G}_k} p_{Gg}^\tau - p_{Dk}^\tau - g'_k V_{kk}^\tau &= \sum_{\ell=(k,m) \in \mathcal{L}} p_{f\ell}^\tau + \sum_{\ell=(m,k) \in \mathcal{L}} p_{t\ell}^\tau & \forall k \in \mathcal{N}, \\ \sum_{g \in \mathcal{G}_k} q_{Gg}^\tau - q_{Dk}^\tau + b'_k V_{kk}^\tau &= \sum_{\ell=(k,m) \in \mathcal{L}} q_{f\ell}^\tau + \sum_{\ell=(m,k) \in \mathcal{L}} q_{t\ell}^\tau & \forall k \in \mathcal{N}, \\ p_{f\ell}^\tau + j q_{f\ell}^\tau &= \frac{1}{|t_\ell|^2} \left(-j \frac{b'_\ell}{2} + y_\ell^* \right) V_{kk}^\tau - \frac{y_\ell^*}{t_\ell} V_{km}^\tau & \forall \ell = (k, m) \in \mathcal{L}, \\ p_{t\ell}^\tau + j q_{t\ell}^\tau &= -\frac{y_\ell^*}{t_\ell^*} V_{mk}^\tau + \left(-j \frac{b'_\ell}{2} + y_\ell^* \right) V_{mm}^\tau & \forall \ell = (k, m) \in \mathcal{L}, \\ \underline{v}_k^2 &\leq V_{kk}^\tau \leq \bar{v}_k^2 & \forall k \in \mathcal{N}, \\ \begin{bmatrix} 1 & \mathbf{v}_k^{\tau*} & \mathbf{v}_m^{\tau*} \\ \mathbf{v}_k^\tau & V_{kk}^\tau & V_{km}^\tau \\ \mathbf{v}_m^\tau & V_{km}^{\tau*} & V_{mm}^\tau \end{bmatrix} &\succeq 0 & \forall \ell = (k, m) \in \mathcal{L}, \\ \operatorname{Re}(\mathbf{v}_1^\tau) &\geq \frac{V_{11}^\tau + \underline{v}_1 \bar{v}_1}{\underline{v}_1 + \bar{v}_1}, \\ \operatorname{Im}(\mathbf{v}_1^\tau) &= 0. \end{aligned}$$

 1. the *exactness error* (which derives from Proposition 7) measured as

$$\varepsilon := \max_{k \in \mathcal{N}} \left(1 - \frac{|\mathbf{v}_k^{\text{TCR}}|}{\sqrt{V_{kk}^{\text{TCR}}}} \right) \times 100\%,$$

 where $(\mathbf{v}^{\text{TCR}}, \mathbf{V}^{\text{TCR}})$ is the optimal solution of TCR;

 2. the *optimality gap*

$$\gamma := \left(1 - \frac{v^{\text{TCR}}}{v^{\text{MAT}}} \right) \times 100\%,$$

 where v^{MAT} is the upper bound provided by the MATPOWER-solver (MIPS) and v^{TCR} is the TCR optimal value; and

3. the *optimality distance* defined as

$$\rho := \frac{\|\mathbf{v}^{\text{MAT}} - \mathbf{v}^{\text{TCR}}\|}{\|\mathbf{v}^{\text{MAT}}\|} \times 100\%,$$

where \mathbf{v}^{MAT} and \mathbf{v}^{TCR} represent the optimal bus voltages provided by MIPS and TCR, respectively.

Table 6.1 and Table 6.2 summarize these three metrics for cost minimization and loss minimization respectively. The results highlight the following key points:

1. TCR is exact for the `case6ww` instance in both cost and loss minimizations, and for the `case14` instance in cost minimization. TCR optimal voltages correspond exactly to optimal voltages provided by MIPS.
2. TCR is exact for the `LMBD3_60` instance in loss minimization, even though TCR optimal voltages do not match to optimal voltages provided by MIPS.
3. TCR is near-exact (i.e., $\varepsilon < 0.1\%$ and $\rho < 0.1\%$) for the `case24_ieee_rts` and `case_illinois200` instances in both cost and loss minimizations, for the `case_ieee30` instance in cost minimization and for the `case5` and `case_ACTIV_SG_500` instances in loss minimization.
4. TCR is on average more accurate in loss minimization than in cost minimization.

Table 6.1 Exactness of TCR: Cost minimization

| Test case | v^{MAT} [\$ / h] | v^{TCR} [\$ / h] | ε [%] | γ [%] | ρ [%] |
|-------------------------------|---------------------------|---------------------------|-------------------|--------------|-------------|
| <i>Small-scale instances</i> | | | | | |
| LMBD3_50 | 5 812.64 | 5 769.87 | 3.52 | 0.74 | 6.05 |
| LMBD3_60 | 5 707.11 | 5 707.01 | 0.26 | 0.00 | 0.16 |
| case5 | 17 551.89 | 15 313.38 | 1.04 | 12.75 | 6.55 |
| case6ww | 3 143.97 | 3 143.97 | 0.00 | 0.00 | 0.00 |
| case9 | 5 296.69 | 5 296.69 | 0.82 | 0.00 | 0.00 |
| case14 | 8 081.53 | 8 081.52 | 0.00 | 0.00 | 0.00 |
| case24_ieee_rts | 63 352.21 | 63 352.15 | 0.07 | 0.00 | 0.07 |
| case30 | 576.89 | 576.50 | 0.65 | 0.07 | 0.65 |
| case_ieee30 | 8 906.15 | 8 906.02 | 0.01 | 0.00 | 0.01 |
| case39 | 41 864.18 | 41 861.91 | 1.83 | 0.01 | 0.32 |
| case57 | 41 737.79 | 41 735.28 | 0.21 | 0.01 | 0.23 |
| case89pegase | 5 819.81 | 5 817.66 | 0.50 | 0.04 | 1.47 |
| Average | | | 0.58 | 0.23 | 0.74 |
| <i>Medium-scale instances</i> | | | | | |
| case118 | 129 660.70 | 129 618.42 | 2.28 | 0.03 | 0.81 |
| case_ACTIV_SG_200 | 27 557.57 | 27 557.33 | 0.16 | 0.00 | 0.17 |
| case_illinois200 | 36 748.39 | 36 747.94 | 0.01 | 0.00 | 0.02 |
| case300 | 719 725.11 | 719 547.51 | 6.46 | 0.02 | 3.16 |
| case_ACTIV_SG_500 | 72 578.30 | 69 391.48 | 11.81 | 4.39 | 7.80 |
| Average | | | 6.18 | 1.67 | 3.78 |

Table 6.2 Exactness of TCR: Loss minimization

| Test case | v^{MAT} [MW] | v^{TCR} [MW] | ε [%] | γ [%] | ρ [%] |
|-------------------------------|-----------------------|-----------------------|-------------------|--------------|-------------|
| <i>Small-scale instances</i> | | | | | |
| LMBD3_50 | 317.38 | 317.38 | 0.06 | 0.00 | 0.51 |
| LMBD3_60 | 316.75 | 316.75 | 0.00 | 0.00 | 0.09 |
| case5 | 1 001.06 | 1 001.06 | 0.01 | 0.00 | 0.01 |
| case6ww | 216.84 | 216.84 | 0.00 | 0.00 | 0.00 |
| case9 | 317.32 | 317.32 | 0.77 | 0.00 | 0.00 |
| case14 | 259.55 | 259.55 | 0.17 | 0.00 | 0.29 |
| case24_ieee_rts | 2 875.75 | 2 875.74 | 0.05 | 0.00 | 0.05 |
| case30 | 191.09 | 191.07 | 0.49 | 0.01 | 0.21 |
| case_ieee30 | 284.77 | 284.77 | 0.13 | 0.00 | 0.29 |
| case39 | 6 284.15 | 6 283.90 | 1.57 | 0.00 | 0.50 |
| case57 | 1 262.10 | 1 262.07 | 0.20 | 0.00 | 0.15 |
| case89pegase | 5 819.81 | 5 817.66 | 0.50 | 0.04 | 1.47 |
| Average | | | 0.48 | 0.01 | 0.58 |
| <i>Medium-scale instances</i> | | | | | |
| case118 | 4 251.23 | 4 250.99 | 0.98 | 0.01 | 0.47 |
| case_ACTIV_SG_200 | 1 483.92 | 1 483.91 | 0.19 | 0.00 | 0.19 |
| case_illinois200 | 2 246.49 | 2 246.43 | 0.03 | 0.00 | 0.07 |
| case300 | 23 737.72 | 23 735.69 | 9.64 | 0.01 | 2.47 |
| case_ACTIV_SG_500 | 7 817.46 | 7 817.31 | 0.04 | 0.00 | 0.06 |
| Average | | | 2.33 | 0.00 | 0.67 |

6.5.2 MP-TCR

Next we assess the accuracy and the computational efficiency of MP-TCR. We considered a 24-period ACOPF problem, i.e., $\bar{\tau} = 24$ in the MP-ACOPF problem (6.5). Experimental settings are the same as in the previous section. We tested Model 12 on MATPOWER instances. All instances' parameters remain the same for all periods except demand which varies in each period.

For each node $k \in \mathcal{N}$, demand $p_{Dk} + jq_{Dk}$ for an ACOPF problem was multiplied by a factor given in Figure 6.1, to obtain demand $p_{Dk}^\tau + jq_{Dk}^\tau$ in each period $\tau = 1, \dots, \bar{\tau}$ for an MP-ACOPF problem. The time varying multiplier factor was estimated based on a real power demand curve for a typical winter day provided by Hydro-Quebec [77].

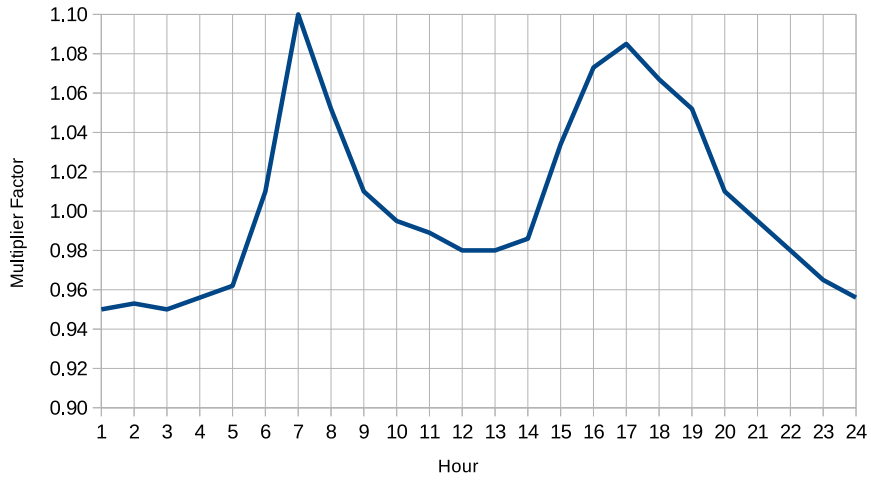


Figure 6.1 Time varying demand profile

For all $\tau = 1, \dots, \bar{\tau} - 1$ and for all $g \in \mathcal{G}$, bounds $\bar{\Delta}_g^\tau$ and $\underline{\Delta}_g^\tau$ on ramp constraints (6.5j) were estimated as $\Delta^\tau \pm 0.1|\Delta^\tau|$, where

$$\Delta^\tau = \frac{1}{|\mathcal{G}|} \sum_{k \in \mathcal{N}} p_{Dk}^{\tau+1} - p_{Dk}^\tau.$$

Table 6.3 and Table 6.4 summarize the optimal values $v^{\text{MP-TCR}}$ of MP-TCR for cost minimization and loss minimization, respectively. MP-TCR was infeasible for following instances: LMBD3_50, LMBD3_60, case6ww, case24_ieee_rts, case89pegase, and all medium-scale instances except case118. The infeasibility of MP-TCR for these instances is explained by the fact that the demand varies at each period (hour) while the generation bounds remain unchanged for all periods. For some instances marked with “*” in Table 6.3, MOSEK ended its computation with message `Mosek error: MSK_RES_TRM_STALL()`.

For each feasible instance, and for each period $\tau = 1, \dots, \bar{\tau}$, we calculated the exactness error ε^τ , and we report the minimum, the average, and the maximum values in Table 6.3 and Table 6.4. The results support the following key points:

1. MP-TCR is exact for the `case14` instance in cost minimization. Optimal active and reactive outputs of each generator and optimal voltage magnitudes of each bus are given in Figure 6.2 and Figure 6.3, respectively.
2. MP-TCR is near-exact for the `case5` instance in loss minimization.
3. MP-TCR is on average more accurate in loss minimization than in cost minimization.

We solved MP-TCR without any decomposition and computation times reported by MOSEK are shown in Table 6.3 and Table 6.4. We note that, for a 24-period problem, MP-TCR is computationally cheap and may be promising for large-scale instances with a decomposition technique.

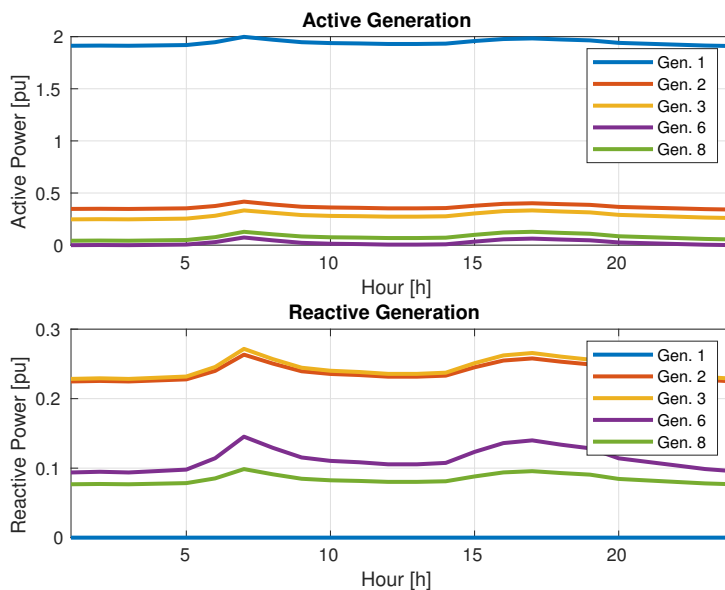


Figure 6.2 Cost minimization of `case14` instance: Optimal active and reactive outputs of each generator

6.6 Conclusion

In this paper, we showed theoretically that the tight-and-cheap conic relaxation (TCR) of the ACOPF problem can be exact. To assess the exactness of TCR, we used three metrics: the exactness error, the optimality gap and the optimality distance. In a new result, TCR provided a global optimal solution for 2 test cases: `case6ww` for both cost and loss minimization, `case14` for cost minimization and

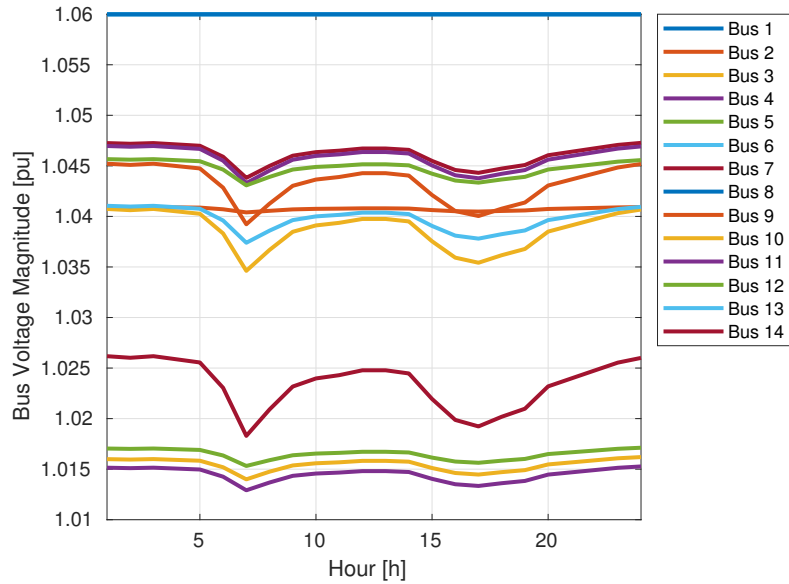


Figure 6.3 Cost minimization of `case14` instance: Voltage magnitudes of each bus

LMBD3_60 for loss minimization. Experiments on other MATPOWER instances show that TCR optimal solutions are near-global optimal.

Thereafter, we defined the multi-period TCR (MP-TCR) for the multi-period ACOPF (MP-ACOPF) problem. MP-TCR was also shown to be exact for the `case14` instance in cost minimization. Experiments on MATPOWER instances with up to 118 buses show that, without any sophisticated decomposition algorithm, MP-TCR is computationally cheap and is promising for large-scale power systems in real-life applications.

Table 6.3 MP-TCR: Cost minimization

| Test case | $v^{\text{MP-TCR}}$ [\$/h] | Exactness error [%] | | | Time [s] |
|------------------------------|----------------------------|---------------------|-------------|-------------|-------------|
| | | Min | Avg | Max | |
| <i>Small-scale instances</i> | | | | | |
| <code>case5</code> | 391 803.23 | 0.56 | 0.77 | 1.03 | 0.26 |
| <code>case9</code> | 128 004.73 | 0.64 | 0.83 | 0.97 | 0.27 |
| <code>case14</code> | 194 952.01 | 0.00 | 0.00 | 0.00 | 0.43 |
| <code>case30</code> | 14 747.65 | 3.71 | 5.51 | 6.52 | 2.23 |
| <code>case_ieee30</code> | *214 819.16 | 0.03 | 0.04 | 0.05 | 1.34 |
| <code>case39</code> | 1 039 085.79 | 4.93 | 5.35 | 5.82 | 2.36 |
| <code>case57</code> | *1 007 169.75 | 0.20 | 0.24 | 0.25 | 3.94 |
| Average | | 1.76 | 2.17 | 2.46 | 2.36 |
| <i>Medium-scale instance</i> | | | | | |
| <code>case118</code> | *3 128 441.17 | 2.27 | 2.32 | 2.35 | 7.56 |

Table 6.4 MP-TCR: Loss minimization

| Test case | $v^{\text{MP-TCR}}$ [MW] | Exactness error [%] | | | Time [s] |
|------------------------------|--------------------------|---------------------|-------------|-------------|-------------|
| | | Min | Avg | Max | |
| <i>Small-scale instances</i> | | | | | |
| <code>case5</code> | 24 118.98 | 0.02 | 0.02 | 0.02 | 0.15 |
| <code>case9</code> | 7 644.56 | 0.59 | 0.75 | 0.84 | 0.26 |
| <code>case14</code> | 6 252.62 | 0.16 | 0.17 | 0.18 | 0.40 |
| <code>case30</code> | 4 771.54 | 3.02 | 5.02 | 6.03 | 2.04 |
| <code>case_ieee30</code> | 6 860.80 | 0.13 | 0.14 | 0.15 | 0.84 |
| <code>case39</code> | 151 478.20 | 1.94 | 3.10 | 5.14 | 1.82 |
| <code>case57</code> | 30 431.56 | 0.18 | 0.20 | 0.30 | 1.93 |
| Average | | 1.02 | 1.61 | 2.24 | 1.50 |
| <i>Medium-scale instance</i> | | | | | |
| <code>case118</code> | 102 418.57 | 0.98 | 0.99 | 1.05 | 5.42 |

CHAPITRE 7 DISCUSSION GÉNÉRALE

7.1 Synthèse des travaux

La principale contribution de cette thèse est d'avoir développé une nouvelle relaxation conique pour le problème d'écoulement de puissance optimal, qui s'avère être prometteuse pour des applications réelles dans la gestion de réseaux électriques.

Dans le chapitre 4, nous avons montré que cette relaxation est un bon compromis en termes de gap d'optimalité et de temps de résolution entre deux principales relaxations coniques du problème classique d'écoulement de puissance optimal développées ces dernières années : la relaxation conique du second ordre et la relaxation semidéfinie. En effet, nous avons prouvé que la nouvelle relaxation est théoriquement plus forte que la relaxation conique du second ordre et les résultats numériques sur des réseaux avec jusqu'à 6515 nœuds ont montré que la résoudre est beaucoup moins coûteuse que la relaxation semidéfinie.

Ensuite, dans le chapitre 5, nous avons combiné cette même relaxation à la technique de l'arrondi pour résoudre le problème de répartition optimale de puissance réactive, qui est un problème d'optimisation non linéaire mixte en nombres entiers. Les résultats numériques sur des réseaux ayant jusqu'à 3375 nœuds montrent que les solutions optimales obtenues avec cette approche sont quasi globales, alors qu'on obtient généralement des solutions de mauvaise qualité lorsque l'on combine la technique de l'arrondi avec la relaxation continue et non convexe du problème. Nous avons donc montré que l'efficacité de la technique de l'arrondi dépend de la relaxation considérée.

Dans le chapitre 6, nous avons commencé par prouver théoriquement que la nouvelle relaxation peut être exacte et permettre d'obtenir une solution optimale globale au problème classique d'écoulement de puissance optimal. Des résultats numériques sur quelques réseaux confirment cette assertion. Par la suite, nous l'avons extrapolée au problème multi-période d'écoulement de puissance optimal et les résultats numériques montrent que la nouvelle relaxation peut être un outil complémentaire pour des applications réelles. En effet, la relaxation sur un horizon de 24 heures s'est avérée exacte pour un réseau à 14 nœuds et sa résolution sur celui à 118 nœuds, sans technique de décomposition, a pris environ 5 secondes.

7.2 Limitations de la solution proposée

Bien que nous ayons montré que la nouvelle relaxation peut être exacte, c'est-à-dire fournir une solution optimale globale au problème d'écoulement de puissance optimal, ceci n'est pas géné-

ralement le cas. Cependant, dans le cas où elle n'est pas exacte, sa solution optimale peut être utilisée comme point initial d'un solveur local. D'où la complémentarité de la relaxation pour des applications réelles avec les outils existants.

La relaxation proposée ne peut être directement appliquée que pour les réseaux triphasés équilibrés. En effet, en pratique, un réseau électrique est triphasé, c'est-à-dire composé de trois fils en parallèle qui interconnectent une source triphasée à une charge triphasée. Dans cette thèse, nous avons modélisé un réseau électrique par un schéma unifilaire, qui est utilisé pour simplifier la représentation des réseaux triphasés équilibrés. Le modèle unifilaire n'est plus valide lorsque le réseau est déséquilibré et dans ce cas, la relaxation devrait être adaptée.

Le modèle de réseau considéré dans ce travail ne prend pas en compte d'autres composants ou d'autres considérations qui complexifieraient encore plus le problème d'écoulement de puissance optimal : les systèmes de transmission flexible en courant alternatif, les batteries, l'intégration des sources d'énergie renouvelable, etc.

CHAPITRE 8 CONCLUSION ET RECOMMANDATIONS

Dans cette thèse, nous avons proposé un modèle efficace et fiable pour résoudre le problème d'écoulement de puissance optimal. Ce modèle répond à la problématique posée par l'Institut de recherche d'Hydro-Québec sur la réduction des pertes actives dans un réseau de transport sur un horizon de 24 heures. Le modèle proposé prend en compte les équations d'écoulement de puissance, les limites des moyens de contrôle, les limites en régime permanent des quantités électriques et les contraintes opérationnelles.

Ce nouveau modèle est prometteur pour des applications réelles dans le sens qu'il peut être un outil complémentaire pour les opérateurs de réseaux électriques. En effet, sa résolution numérique est relativement faible : environ quelques secondes pour des réseaux ayant jusqu'à 6000 nœuds, et sa solution optimale est quasi globale pour le problème d'écoulement de puissance optimal.

À la lumière des limitations mentionnées dans le chapitre précédent, voici quelques améliorations qui pourraient être faites :

1. Adapter le modèle proposé aux réseaux triphasés déséquilibrés, ce qui est généralement le cas des réseaux de distribution.
2. Explorer en profondeur les cas où le modèle est exact, c'est-à-dire que sa solution optimale l'est aussi pour le problème d'écoulement de puissance optimal.
3. Dans la résolution du modèle, appliquer une technique de Branch-and-Bound, Cutting-Plane ou une autre pour obtenir la solution optimale globale au problème d'écoulement de puissance optimal.
4. Adapter les méthodes proposées dans ce travail à d'autres considérations liées au problème d'écoulement de puissance optimal qui n'ont pas été prises en compte.
5. Appliquer une technique de décomposition pour la résolution du problème multi-période.

RÉFÉRENCES

- [1] Jean-Claude Rizzi and Stéphane Alarie. Réduction des pertes actives d'un réseau de transport d'énergie. 2013.
- [2] Stephen Boyd and Lieven Vandenbergh. *Convex Optimization*. Cambridge University Press, 2004.
- [3] Christoph Helmberg. *Semidefinite Programming for Combinatorial Optimization*. Konrad-Zuse-Zentrum für Informationstechnik Berlin, 2000.
- [4] Miguel F. Anjos and Jean B. Lasserre. Introduction to semidefinite, conic and polynomial optimization. In *Handbook on Semidefinite, Conic and Polynomial Optimization*, pages 1–22. Springer, 2012.
- [5] James A. Momoh. *Electric Power System Applications of Optimization*. CRC Press, 2008.
- [6] Joshua Adam Taylor. *Convex Optimization of Power Systems*. Cambridge University Press, 2015.
- [7] Mohit Tawarmalani and Nikolaos V. Sahinidis. *Convexification and Global Optimization in Continuous and Mixed-Integer Nonlinear Programming : Theory, Algorithms, Software, and Applications*, volume 65. Springer Science & Business Media, 2002.
- [8] Michel X Goemans and David P Williamson. Improved approximation algorithms for maximum cut and satisfiability problems using semidefinite programming. *Journal of the ACM (JACM)*, 42(6) :1115–1145, 1995.
- [9] Yurii Nesterov and Arkadii Nemirovskii. *Interior-Point Polynomial Algorithms in Convex Programming*, volume 13. SIAM, 1994.
- [10] Alexandre d'Aspremont. Quelques applications de la programmation semidefinie, 2013.
- [11] Robert M. Freund. Introduction to semidefinite programming (SDP). *Massachusetts Institute of Technology*, 2004.
- [12] François Glineur. Étude des méthodes de point intérieur appliquées à la programmation linéaire et à la programmation semidéfinie. 1997.
- [13] Frédéric Roupin. L'approche par programmation semidéfinie en optimisation combinatoire. *Bulletin de la Société française de recherche opérationnelle et d'aide à la décision*, 13 :7–11, 2004.
- [14] J. Duncan Glover, Mulukutla S. Sarma, and Thomas J. Overbye. *Power System Analysis and Design*. Cengage Learning, 5th edition, 2012.

- [15] Stephen Frank, Ingrida Steponavice, and Steffen Rebennack. Optimal power flow : A bibliographic survey I. *Energy Systems*, 3(3) :221–258, 2012.
- [16] Stephen Frank, Ingrida Steponavice, and Steffen Rebennack. Optimal power flow : A bibliographic survey II. *Energy Systems*, 3(3) :259–289, 2012.
- [17] R. A. Jabr. Radial distribution load flow using conic programming. *IEEE Transactions on Power Systems*, 21(3) :1458–1459, Aug 2006.
- [18] Xiaoqing Bai, Hua Wei, Katsuki Fujisawa, and Yong Wang. Semidefinite programming for optimal power flow problems. *International Journal of Electrical Power & Energy Systems*, 30(6) :383–392, 2008.
- [19] R. A. Jabr. Optimal power flow using an extended conic quadratic formulation. *IEEE Transactions on Power Systems*, 23(3) :1000–1008, Aug 2008.
- [20] Robert Grone, Charles R. Johnson, Eduardo M. Sá, and Henry Wolkowicz. Positive definite completions of partial Hermitian matrices. *Linear algebra and its applications*, 58 :109–124, 1984.
- [21] Pierre Bonami, Mustafa Kiliç, and Jeff Linderoth. Algorithms and software for convex mixed integer nonlinear programs. In *Mixed integer nonlinear programming*, pages 1–39. Springer, 2012.
- [22] Jon Lee and Sven Leyffer. *Mixed Integer Nonlinear Programming*, volume 154. Springer Science & Business Media, 2011.
- [23] Samuel Burer and Adam N. Letchford. Non-convex mixed-integer nonlinear programming : A survey. *Surveys in Operations Research and Management Science*, 17(2) :97–106, 2012.
- [24] Christian Bingane, Miguel F. Anjos, and Sébastien Le Digabel. Tight-and-cheap conic relaxation for the AC optimal power flow problem. *IEEE Transactions on Power Systems*, 33(6) :7181–7188, 2018.
- [25] Christian Bingane, Miguel F. Anjos, and Sébastien Le Digabel. Tight-and-cheap conic relaxation for the optimal reactive power dispatch problem. *IEEE Transactions on Power Systems*, 2019.
- [26] Christian Bingane, Miguel F. Anjos, and Sébastien Le Digabel. CONICOPF : A tight-and-cheap conic relaxation with accuracy metrics for single-period and multi-period ACOPF problems. Technical Report G-2019-19, Les cahiers du GERAD, 2019.
- [27] J. Carpentier. Contribution to the economic dispatch problem. *Bulletin de la Société française des électriciens*, 3(8) :431–447, 1962.
- [28] Mary B. Cain, Richard P. O’Neill, and Anya Castillo. History of optimal power flow and formulations. *Federal Energy Regulatory Commission*, pages 1–36, 2012.

- [29] Abhinav Verma. *Power grid security analysis : An optimization approach*. Columbia University, 2010.
- [30] Karsten Lehmann, Alban Grastien, and Pascal Van Hentenryck. AC-feasibility on tree networks is NP-hard. *IEEE Transactions on Power Systems*, 31(1) :798–801, 2016.
- [31] R. A. Jabr. Exploiting sparsity in SDP relaxations of the OPF problem. *IEEE Transactions on Power Systems*, 27(2) :1138–1139, May 2012.
- [32] S. H. Low. Convex relaxation of optimal power flow–Part I : Formulations and equivalence. *IEEE Transactions on Control of Network Systems*, 1(1) :15–27, March 2014.
- [33] S. H. Low. Convex relaxation of optimal power flow–Part II : Exactness. *IEEE Transactions on Control of Network Systems*, 1(2) :177–189, June 2014.
- [34] Hassan Hijazi, Carleton Coffrin, and Pascal Van Hentenryck. Convex quadratic relaxations for mixed-integer nonlinear programs in power systems. *Mathematical Programming Computation*, pages 1–47, 2014.
- [35] Hassan Hijazi, Carleton Coffrin, and Pascal Van Hentenryck. Polynomial SDP cuts for optimal power flow. In *Power Systems Computation Conference (PSCC), 2016*, pages 1–7. IEEE, 2016.
- [36] Cédric Jozz, Jean Maeght, Patrick Panciatici, and Jean Charles Gilbert. Application of the moment-SOS approach to global optimization of the OPF problem. *IEEE Transactions on Power Systems*, 30(1) :463–470, 2015.
- [37] Carleton Coffrin, Hassan Hijazi, and Pascal Van Hentenryck. Network flow and copper plate relaxations for AC transmission systems. In *Power Systems Computation Conference (PSCC), 2016*, pages 1–8. IEEE, 2016.
- [38] Sleiman Mhanna, Gregor Verbič, and Archie C. Chapman. Tight LP approximations for the optimal power flow problem. In *Power Systems Computation Conference (PSCC), 2016*, pages 1–7. IEEE, 2016.
- [39] Burak Kocuk, Santanu S. Dey, and X. Andy Sun. Strong SOCP relaxations for the optimal power flow problem. *Operations Research*, 64(6) :1177–1196, 2016.
- [40] R. D. Zimmerman, C. E. Murillo-Sanchez, and R. J. Thomas. MATPOWER : Steady-state operations, planning, and analysis tools for power systems research and education. *IEEE Transactions on Power Systems*, 26(1) :12–19, Feb 2011.
- [41] Javad Lavaei and Steven H. Low. Zero duality gap in optimal power flow problem. *IEEE Transactions on Power Systems*, 27(1) :92–107, 2012.
- [42] Mitsuhiro Fukuda, Masakazu Kojima, Kazuo Murota, and Kazuhide Nakata. Exploiting sparsity in semidefinite programming via matrix completion I : General framework. *SIAM Journal on Optimization*, 11(3) :647–674, 2001.

- [43] Kazuhide Nakata, Katsuki Fujisawa, Mitsuhiro Fukuda, Masakazu Kojima, and Kazuo Murota. Exploiting sparsity in semidefinite programming via matrix completion II : Implementation and numerical results. *Mathematical Programming*, 95(2) :303–327, 2003.
- [44] Daniel K. Molzahn, Jesse T. Holzer, Bernard C. Lesieutre, and Christopher L. DeMarco. Implementation of a large-scale optimal power flow solver based on semidefinite programming. *IEEE Transactions on Power Systems*, 28(4) :3987–3998, 2013.
- [45] Martin S. Andersen, Anders Hansson, and Lieven Vandenbergh. Reduced-complexity semi-definite relaxations of optimal power flow problems. *IEEE Transactions on Power Systems*, 29(4) :1855–1863, 2014.
- [46] R. Madani, M. Ashraphijuo, and J. Lavaei. OPF solver, 2014.
- [47] R. A. Jabr. A conic quadratic format for the load flow equations of meshed networks. *IEEE Transactions on Power Systems*, 22(4) :2285–2286, Nov 2007.
- [48] Garth P. McCormick. Computability of global solutions to factorable nonconvex programs—Part I : Convex underestimating problems. *Mathematical Programming*, 10(1) :147–175, 1976.
- [49] Kurt M. Anstreicher. Semidefinite programming versus the reformulation-linearization technique for nonconvex quadratically constrained quadratic programming. *Journal of Global Optimization*, 43(2-3) :471–484, 2009.
- [50] Kurt M. Anstreicher and Samuel Burer. Computable representations for convex hulls of low-dimensional quadratic forms. *Mathematical programming*, 124(1) :33–43, 2010.
- [51] Chen Chen, Alper Atamtürk, and Shmuel S. Oren. A spatial branch-and-cut method for nonconvex QCQP with bounded complex variables. *Mathematical Programming*, pages 1–29, 2017.
- [52] Cédric Josz and Daniel K. Molzahn. Moment/sum-of-squares hierarchy for complex polynomial optimization. *arXiv preprint arXiv :1508.02068*, 2015.
- [53] Carleton Coffrin, Hassan L. Hijazi, and Pascal Van Hentenryck. Strengthening the SDP relaxation of AC power flows with convex envelopes, bound tightening, and valid inequalities. *IEEE Transactions on Power Systems*, 32(5) :3549–3558, 2017.
- [54] A. B. Birchfield, T. Xu, K. M. Gegner, K. S. Shetye, and T. J. Overbye. Grid structural characteristics as validation criteria for synthetic networks. *IEEE Transactions on Power Systems*, 32(4) :3258–3265, July 2017.
- [55] Cédric Josz, Stéphane Fliscounakis, Jean Maeght, and Patrick Panciatici. AC power flow data in MATPOWER and QCQP format : iTesla, RTE snapshots, and PEGASE. *arXiv preprint arXiv :1603.01533*, 2016.

- [56] CVX Research, Inc. CVX : MATLAB software for disciplined convex programming, version 2.1. <http://cvxr.com/cvx>, August 2012.
- [57] M. Grant and S. Boyd. Graph implementations for nonsmooth convex programs. In V. Blondel, S. Boyd, and H. Kimura, editors, *Recent Advances in Learning and Control*, Lecture Notes in Control and Information Sciences, pages 95–110. Springer-Verlag Limited, 2008. http://stanford.edu/~boyd/graph_dcp.html.
- [58] Florin Capitanescu. Critical review of recent advances and further developments needed in AC optimal power flow. *Electric Power Systems Research*, 136 :57–68, 2016.
- [59] Zhifang Yang, Haiwang Zhong, Qing Xia, and Chongqing Kang. Fundamental review of the OPF problem : challenges, solutions, and state-of-the-art algorithms. *Journal of Energy Engineering*, 144(1) :04017075, 2017.
- [60] Zhifang Yang, Anjan Bose, Haiwang Zhong, Ning Zhang, Qing Xia, and Chongqing Kang. Optimal reactive power dispatch with accurately modeled discrete control devices : A successive linear approximation approach. *IEEE Transactions on Power Systems*, 32(3) :2435–2444, 2017.
- [61] Carleton Coffrin, Hassan L. Hijazi, and Pascal Van Hentenryck. The QC relaxation : A theoretical and computational study on optimal power flow. *IEEE Transactions on Power Systems*, 31(4) :3008–3018, 2016.
- [62] Tao Ding, Shiyu Liu, Wei Yuan, Zhaohong Bie, and Bo Zeng. A two-stage robust reactive power optimization considering uncertain wind power integration in active distribution networks. *IEEE Transactions on Sustainable Energy*, 7(1) :301–311, 2016.
- [63] Wenchuan Wu, Zhuang Tian, and Boming Zhang. An exact linearization method for OLTC of transformer in branch flow model. *IEEE Transactions on Power Systems*, 32(3) :2475–2476, 2017.
- [64] Burak Kocuk, Santanu S. Dey, and Xu Sun. New formulation and strong MISOCP relaxations for AC optimal transmission switching problem. *IEEE Transactions on Power Systems*, 32(6) :4161–4170, 2017.
- [65] Quentin Gemine, Damien Ernst, Quentin Louveaux, and Bertrand Cornélusse. Relaxations for multi-period optimal power flow problems with discrete decision variables. In *2014 Power Systems Computation Conference*, pages 1–7. IEEE, 2014.
- [66] Florin Capitanescu and Louis Wehenkel. Sensitivity-based approaches for handling discrete variables in optimal power flow computations. *IEEE Transactions on Power Systems*, 25(4) :1780–1789, 2010.
- [67] W.F. Tinney, J.M. Bright, K.D. Demaree, and B.A. Hughes. Some deficiencies in optimal power flow. *IEEE Transactions on Power Systems*, 3(2) :676–683, 1988.

- [68] Javad Lavaei. Zero duality gap for classical OPF problem convexifies fundamental nonlinear power problems. In *Proceedings of the 2011 American Control Conference*, pages 4566–4573. IEEE, 2011.
- [69] Xinda Ke, Nader Samaan, Jesse Holzer, Renke Huang, Bharat Vyakaranam, Mallikarjuna Vallem, Marcelo Elizondo, Ning Lu, Xiangqi Zhu, Brant Werts, et al. Coordinative real-time sub-transmission volt–var control for reactive power regulation between transmission and distribution systems. *IET Generation, Transmission & Distribution*, 2018.
- [70] Brett A. Robbins, Hao Zhu, and Alejandro D. Domínguez-García. Optimal tap setting of voltage regulation transformers in unbalanced distribution systems. *IEEE Transactions on Power Systems*, 31(1) :256–267, 2016.
- [71] Harold P. Benson. On the construction of convex and concave envelope formulas for bilinear and fractional functions on quadrilaterals. *Computational Optimization and Applications*, 27(1) :5–22, 2004.
- [72] Christian Bingane, Miguel F. Anjos, and Sébastien Le Digabel. CONICOPF : Conic relaxations of the optimal power flow problem. <https://github.com/cbingane/conicopf>, March 2019.
- [73] Bernard C Lesieutre, Daniel K Molzahn, Alex R Borden, and Christopher L DeMarco. Examining the limits of the application of semidefinite programming to power flow problems. In *2011 49th Annual Allerton Conference on Communication, Control, and Computing (Allerton)*, pages 1492–1499. IEEE, 2011.
- [74] B. Kocuk, S. S. Dey, and X. A. Sun. Inexactness of SDP relaxation and valid inequalities for optimal power flow. *IEEE Transactions on Power Systems*, 31(1) :642–651, Jan 2016.
- [75] Andreas Venzke, Spyros Chatzivasileiadis, and Daniel K Molzahn. Inexact convex relaxations for AC optimal power flow : Towards AC feasibility. *arXiv preprint arXiv :1902.04815*, 2019.
- [76] Anders Eltvéd, Joachim Dahl, and Martin S. Andersen. On the robustness and scalability of semidefinite relaxation for optimal power flow problems. *Optimization and Engineering*, pages 1–18, 2018.
- [77] Rachel Stephenson. Improving the Performance of Large-Scale Power Grids. Master’s thesis, The University of Edinburgh, 2017.
- [78] Ajit Gopalakrishnan, Arvind U Raghunathan, Daniel Nikovski, and Lorenz T Biegler. Global optimization of multi-period optimal power flow. In *2013 American Control Conference*, pages 1157–1164. IEEE, 2013.
- [79] Alvaro Lorca and Xu Andy Sun. The adaptive robust multi-period alternating current optimal power flow problem. *IEEE Transactions on Power Systems*, 33(2) :1993–2003, 2018.